

Aspects of inflammation in acute lung injury

Experimental and clinical
explorations

Niklas Larsson



UMEÅ UNIVERSITY

This work is protected by the Swedish Copyright Act (Act 1960:729)

© 2026 Niklas Larsson

ISBN: 978-91-8070-955-2 (print)

ISBN: 978-91-8070-956-9 (pdf)

ISSN: 0346-6612

Umeå University Medical Dissertations New Series no. 2413

Cover design by the author

Cover reproduced with permission

Electronic version available at: <http://umu.diva-portal.org/>

Printed by: Scandinavian Print Group, Skarpnäck, 2026

Good things take time, as they should.
John Wooden

Till Linn, Hugo, Ture och Maja

Contents

Abstract	iii
Enkel svensk sammanfattning	v
List of original papers	vii
Abbreviations	viii
Acknowledgements	xi
Introduction	1
Background	3
Inflammation	3
<i>Innate immune response</i>	3
<i>Adaptive immune response</i>	4
<i>Resolution of inflammation</i>	5
<i>Neuroendocrine and metabolic regulatory functions</i>	6
<i>Oxylipins</i>	7
<i>Cyclooxygenase products</i>	7
<i>Lipoxygenase products</i>	9
<i>Cytochrome P450 products</i>	9
<i>Pro-inflammatory mediators</i>	10
<i>Anti-inflammatory mediators</i>	12
<i>Extracellular vesicles</i>	13
ARDS.....	16
<i>Definition</i>	16
<i>Epidemiology</i>	16
<i>Pathogenesis</i>	17
<i>Ventilator induced lung injury</i>	18
<i>Treatment</i>	20
<i>Animal models</i>	22
Aims	24
Materials and methods	25
Ethical considerations	25
Animals	25
Experimental preparation	26
Research participants, human.....	28

Protocol.....	28
<i>Paper I</i>	28
<i>Paper II</i>	29
<i>Paper III</i>	30
<i>Paper IV</i>	30
<i>Paper V</i>	31
<i>t-TUCB pharmacokinetics</i>	31
<i>Methodological considerations</i>	32
Analyses	34
Statistics.....	34
Results	36
Paper I.....	36
<i>Oxylipins in bronchoalveolar lavage fluid and plasma</i>	37
<i>Oxylipins in exhaled breath condensate</i>	47
Paper II	51
<i>BALF EVs</i>	51
<i>Plasma EVs</i>	54
Paper III.....	56
<i>Oxylipins during the first day of mechanical ventilation</i>	57
<i>Oxylipins in sepsis</i>	58
Paper IV	67
<i>Catheter insertion times</i>	67
Paper V.....	68
Pharmacokinetic parameters of t-TUCB.....	71
<i>Breach of protocol</i>	71
<i>Clinical observations</i>	71
<i>t-TUCB concentrations in blood</i>	71
Discussion.....	74
Oxylipins	74
Extracellular vesicles	77
Long-term catheterization of pigs	78
Soluble epoxide hydrolase inhibitor pharmacokinetics	79
Soluble epoxide hydrolase inhibition in acute lung injury	80
Conclusions.....	82
Final remarks and future perspectives	83
References	85

Abstract

Background

Acute respiratory distress syndrome (ARDS) represents a syndrome of acutely failing lung function that, by definition, requires intensive care efforts to maintain adequate oxygenation of the patient's blood. In established ARDS, treatment options are severely limited, although previous work in rodents have shown positive effects of pharmacological treatment with soluble epoxide hydrolase inhibitors (sEH) in an experimental model of acute lung injury. Clinically, the most important treatment for ARDS is reduction of harm or complications, primarily in the form of ventilator-induced lung injury (VILI). Mechanical ventilation has positive and negative effects, where avoidance of VILI induction may necessitate ventilatory settings that lead to significant patient discomfort. We do not currently have biomarkers that identify patients with inappropriate or suboptimal positive pressure ventilatory support settings.

Aims

This thesis mainly aims to describe lung injury biomarker patterns and effects of pharmacological treatment with soluble epoxide hydrolase inhibitors (sEH) in acute lung injury.

Methods

A pig model of VILI was used to identify biomarkers among oxylipins and extracellular vesicles (EVs) in plasma and in bronchoalveolar lavage fluid (BALF), and also in exhaled breath condensate (EBC). Plasma samples from a cohort of intensive care unit (ICU) subjects were used to describe the kinetics of oxylipins after intubation and in sepsis compared to non-septic cases. We also established a pig model of long-term venous access to allow for determination of pharmacokinetic properties of a potential new anti-inflammatory medication in the form of an inhibitor of sEH. Finally, sEH inhibition was tested in a lipopolysaccharide (LPS) model of lung injury in pigs.

Results

Several oxylipins increased in BALF in response to VILI induction. Some of these were also noted to increase in plasma. As a preliminary finding, a number of oxylipins could also be detected in EBC. Regarding EVs, those containing nucleic acids increased over time in response to VILI in BALF but not in plasma. In humans, lower levels of some oxylipins were

observed after one day of mechanical ventilation and in septic patients compared to non-septic controls. Long-term cannulation of pigs was performed with satisfactory vascular access. Inhibition of sEH did not attenuate lung injury development after LPS challenge in pigs.

Conclusions

Some oxylipins and EVs may be markers of experimental lung injury, most clearly seen in BALF. In ICU patients, oxylipins in plasma seem to decrease after intubation and were lower among sepsis cases compared to non-septic cases in this cohort. Finally, sEH inhibition does not appear to attenuate lung injury in pigs.

Enkel svensk sammanfattning

Akut svår lungsvikt är vanligt vid kritisk sjukdom och är ett tillstånd med okontrollerad inflammation där effektiv behandling mot åkomman saknas. Hörnstenen i behandlingen är i stället att ge livsuppehållande stöd med respiratorbehandling och samtidigt undvika att orsaka ytterligare skada i lungan med respiratorbehandlingen. Det har visat sig att respiratorbehandling med stora andetag kan orsaka ytterligare lungskada och kraftigt öka dödligheten vid svår lungsvikt. Trots detta ges många patienter behandling med stora andetag eftersom små andetagsvolymmer i respirator är förknippade med svåra biverkningar. Laboratorieprover som påvisar skadlig respiratorbehandling saknas idag men skulle potentiellt kunna hjälpa vårdpersonal att individualisera respiratorbehandlingen så att varje patient får det den behöver och skadliga andetag undviks till de patienter som faktiskt är känsliga för dem. Dessutom finns en hypotes att man med antiinflammatorisk läkemedelsbehandling skulle kunna positivt påverka förloppet vid akut lungsvikt. Inflammation regleras av ett antal olika enzymssystem som styr kroppens produktion av reglerande ämnen. Så kallade antiinflammatoriska mediciner kan verka genom att hämma effekten av enzym i dessa system. Enzymet lösligt epoxidhydrolas är en del av reglersystemet för inflammation och hämning av detta enzym har testats i olika forskningmodeller av inflammation. Tidigare har hämning av lösligt epoxidhydrolas visats minska utvecklingen av lungsvikt hos gnagare som utsätts för svår inflammation orsakad av bakterieprodukter.

Sövda grisar användes här för försök där ett antal djur fick en svår lungskada genom att lungorna först sköljdes med stora mängder koksaltlösning och sedan utsattes för respiratorbehandling med mycket stora andetagsvolymmer. En kontrollgrupp utsattes för koksaltsköljningen men fick sedan lungskyddande respiratorbehandling med små andetagsvolymmer. Vid upprepade tillfällen under försökets gång samlades prover både från blod och från sköljvätska från luftvägarna in med en flexibel fiberkamera. Ånga från utandningsluften samlades även in för analys genom att kondenseras med ett kylt rör kopplat till utandningsdelen av respiratorn. I de tillvaratagna proverna mättes en typ av fettsyrametaboliter som är viktiga för reglering av inflammation som kallas oxylipiner samt små celldelar som kan knoppas av från kroppens celler som kallas extracellulärvesikler. Dessa arbeten syftade till att hitta avvikelser i tillvaratagna prover som skulle kunna användas

för att identifiera individer som skadas av pågående respiratorbehandling. Därutöver syftade försöken till att kartlägga vilka substanser som styr inflammationen vid akut lungsvikt. Oxylipiner mättes även i blod från intensivvårdspatienter som lämnat prover till en studie vid intensivvårdsavdelningen i Östersund. Detta arbete syftade till att öka förståelsen för hur inflammation regleras vid kritisk sjukdom och till att hitta blodprover som påverkas av respiratorbehandling. Experiment utfördes även där grisar behandlades med antingen en hämmare av enzymet lösligt epoxidhydrolas eller med icke aktiv koksaltlösning i dropp. Djuren fick sedan ett bakterieproducerat ämne som startar en svår inflammation i kroppen som även orsakar akut lungsvikt. Gruppen med och utan epoxidhydrolashämmarebehandling jämfördes för att se om behandlingen kunde minska utvecklingen av lungskada. Dessa experiment föregicks av försök för att hitta rätt dos av läkemedlet i gris där en metod utvecklades för att förse grisar med intravenösa katetrar med så liten negativ påverkan som möjligt för grisarna.

Resultaten visade att ett antal oxylipiner ökade över tid i vätska från luftvägarna hos grisar som fick skadlig respiratorbehandling jämfört med dem som inte fick det. Samtidigt sågs en motsvarande ökning av ett mindre antal oxylipiner i blodprover från samma grisar. Man kunde även se förekomst av vissa oxylipiner i kondensvätska från utandningsluft, men dessa observationer var för få för att ytterligare analyser skulle kunna göras. Även vissa extracellulärvesikler ökade i skölvätskan från luftvägarna, men inte i blod. Hos intensivvårdspatienterna sågs i stället sjunkande halter av vissa oxylipiner efter att de påbörjat respiratorbehandling och hos patienter med blodförgiftning var det vanligt att ett stort antal oxylipiner fanns i lägre halter i blodet än hos patienter utan blodförgiftning. När behandlingen med epoxidhydrolashämmare utvärderades sågs ingen effekt alls på lungskadeutveckling jämfört med om läkemedlet inte gavs.

De huvudsakliga fynden i detta arbete var att vissa oxylipiner och extracellulärvesikler skulle kunna påvisa skador av respiratorbehandling, åtminstone om man kan mäta deras förekomst direkt i luftvägarna. Detta kunde dock inte ses hos intensivvårdspatienter som fick respiratorbehandling, där man tvärtom såg sjunkande halter av vissa oxylipiner. Behandling med epoxidhydrolashämmare tycktes inte skydda grisar mot utveckling av akut lungskada vid svår generell inflammation, vilket talar emot att sådan behandling skulle kunna skydda människor mot att drabbas av inflammatoriskt betingad akut lungsvikt.

List of original papers

- Paper I Larsson N, Lehtipalo S, Gouveia-Figueira S, Claesson J, Pourazar J, Isaksson Mettävainio M, Haney M, Nording ML. Plasma and bronchoalveolar lavage fluid oxylipin levels in experimental porcine lung injury. Prostaglandins Other Lipid Mediat. 2022 Jun;160:106636.
- Paper II Larsson N, Claesson J, Lehtipalo S, Behndig A, Mobarrez F, Haney M. Extracellular vesicle release in an experimental ventilator-induced lung injury porcine model. PLoS One. 2025 Apr 9;20(4):e0320144.
- Paper III Larsson N, Nording ML, Tydén J, Johansson J, Lindberg R, Haney M. Oxylipin Profiles During the First Day of Mechanical Ventilation in an Intensive Care Unit Cohort: Research Letter. Anesthesiology. 2023 May 1;138(5):561-563.
- Paper IV Larsson N, Claesson Lingehall H, Al Zaidi N, Claesson J, Jensen-Waern M, Lehtipalo S. Percutaneously inserted long-term central venous catheters in pigs of different sizes. Lab Anim. 2015 Jul;49(3):215-9.
- Paper V Larsson N, McReynolds C B, Hwang S H, Wan D, Yang J, Lindberg R, Lehtipalo S, Claesson J, Irgum Liljeström A, Lind A, Brolin A, Isaksson Mettävainio M, Hammock B D, Morriseau C, Nording M L. Inhibition of soluble epoxide hydrolase in endotoxin induced pig lung injury. Frontiers in Pharmacology. 2025 September 10; 16:1652349.

Abbreviations

AA	Arachidonic acid
AEPU	Adamantanyl-ethylethoxy-ethoxy-pentylurea
ALA	Alpha-linoleic acid
a-ox	Autooxidation
ARDS	Acute respiratory distress syndrome
ASA	Acetylsalicylic acid
AUC	Area under the curve
BAL	Bronchoalveolar lavage
BALF	Bronchoalveolar lavage fluid
BCR	B-cell receptor
CD	Cluster of differentiation
COX	Cyclooxygenase
CPAP	Continuous positive airway pressure
CRP	C-reactive protein
CYP	Cytochrome P 450
DAMP	Damage-associated molecular pattern
DF	Detection frequency
DGLA	Dihomo- γ -linolenic acid
DHA	Docosahexaenoic acid
DHET	Dihydroxy-eicosatrienoic acid (now DiHETrE)
DiHDPE	Dihydroxy-epoxy-docosahexaenoic acid
DiHETE	Dihydroxy-eicosatetraenoic acid
DiHETrE	Dihydroxy-eicosatrienoic acid
DiHODE	Dihydroxy-octadecadienoic Acid
DiHOME	Dihydroxy-octadecenoic acid
DMSO	Dimethyl sulfoxide
EBC	Exhaled breath condensate
ECMO	Extracorporeal membrane oxygenation
EET	Epoxy-eicosatrienoic acid (now EpETrE)
EKODE	Epoxy-ketooctadecenoic acid
EPA	Eicosapentaenoic acid
EpDPE	Epoxy-docosahexaenoic acid
EpETE	Epoxy-eicosatetraenoic acid
EpETrE	Epoxy-eicosatrienoic acid
EpODE	Epoxy-eicosatrienoic acid
EpOME	Epoxy-octadecenoic acid
EV	Extracellular vesicle
GI	Gastrointestinal
HDoHE	Hydroxy-docosahexaenoic acid

HEPE	Hydroxy-eicosapentaenoic acid
HETE	Hydroxy-eicosatetraenoic acid
HETrE	Hydroperoxy-eicosatetraenoic acid
HODE	Hydroxy-octadecadienoic acid
HOTrE	Hydroxy-octadecatrienoic acid
HPETE	Hydroperoxy-eicosatetraenoic acid
HTV	High tidal volume ventilation
IC ₅₀	Inhibitory concentration 50%
ICU	Intensive care unit
IL	Interleukin
IL-1ra	Interleukin 1 receptor antagonist
INF- γ	Interferon γ
LA	Linoleic acid
LOD	Limit of detection
LOQ	Limit of quantification
LOS	Length of stay
LOX	Lipoxygenase
LPS	Lipopolysaccharide
LTA ₄	Leukotriene A ₄
LTB ₄	Leukotriene B ₄
LTV	Low tidal volume ventilation
MAPK	Mitogen-activated protein kinase
MHC	Major histocompatibility complex
MODS	Multiple organ dysfunction syndrome
NaCl	Sodium chloride
NET	Neutrophil extracellular trap
NF- κ B	Nuclear factor kappa-B
NSAID	Non-steroidal anti-inflammatory drug
oxo-EETE	Oxo-eicosatetraenoic acid
oxo-ODE	Oxo-octadecadienoic acid
PAF	Platelet activating factor
PAMP	Pathogen-associated molecular pattern
PCA	Principal component analysis
PEEP	Positive end-expiratory pressure
PGD ₂	Prostaglandin D ₂
PGE ₂	Prostaglandin E ₂
PGH ₂	Prostaglandin H ₂
PGI ₂	Prostacyclin
PRR	Pattern recognition receptor
P-SILI	Patient self-inflicted lung injury
PUFA	Polyunsaturated fatty acid
ROS	Reactive oxygen species
SAPS	Simplified acute Physiology score

sEH	Soluble epoxide hydrolase
SOFA	Sequential organ failure assessment
TCR	T-cell receptor
TGF- β	Transforming growth factor beta
TLR	Toll-like receptor
TNF	Tumor necrosis factor, formerly known as TNF- α
Treg	Regulatory T cell
TriHOME	Trihydroxy-octadecenoic acid
t-TUCB	Trans-trifluoromethoxy-phenylureido-cyclohexyloxy- benzoic acid
TXA ₂	Thromboxane A ₂
TXB ₂	Thromboxane B ₂
VILI	Ventilator induced lung injury

Acknowledgements

Even if the name – and actually also the lungs – on the cover of this book are mine, I could never have done this on my own. A number of people should receive credit for their contributions that in many cases go beyond what I have managed to acknowledge here:

My wife **Linn** for loving support and for nudging me towards actually getting this work done. You are the love of my life and you know me better than me. You did see this thesis coming two decades before its completion!

My wonderful kids **Hugo, Ture** and **Maja** for making it all worthwhile.

Professor **Michael Haney**, my principal supervisor, for pushing me forward with never-ending support and also for always excellent general advice on life, work and research.

Malin Nording, my principal co-supervisor (new title!) for chemical wizardry and for opening my eyes for a whole new field of knowledge and for being a good friend along the way.

Jonas Claesson for starting it all and for suggesting that I shouldn't waste my time not getting a PhD – advise given 18 years ago.

Stefan Lehtipalo for leading the project for many years and always adding curiosity and enthusiasm.

Annelie Behndig for support whenever needed and for guiding me into the world of invasive sampling of lung fluids.

Anders Larsson, former professor of Hedenstierna Laboratory, for super-professional advice on experimental modelling.

Jamshid Pourazar for being a science pro and for making all the experiments possible.

Sandra Gouveia-Figueira for being a tireless expert.

Rui Pinto and **Christopher Fowler**, for statistical expertise and mostly for actually making me understand what we were doing.

All my co-authors at **Hammock Laboratory** in Davis, the world's leading experts on sEH, for all your expertise and also for welcoming me into your cooperative network.

Fariborz Mobarrez, for making our work with EVs possible, and for not giving up even though I disappeared for almost a decade.

Monica Palmén for every-day enthusiasm and being the best co-boss anyone could wish for.

Johan Ölvebro for always keeping me on my toes and always providing a challenge along with a great working day.

All **co-authors** involved the different papers for all your expertise, efforts and for letting me have a really good time doing research. I'd mention you all but there is a limit to how many pages this thesis can be...

Friends and colleagues at **AnOpIVA** for laughs, support, friendship, development, and everything else that comes with a great workplace. I would also like to thank all our clinical staff for all the hard work taking care of patients. Without your efforts, there would be no place for research!

Finally, the positive influence of **Islay** products on late night productivity should not go unrecognized.

Introduction

Inflammation is a physiologic response to infection or injury in which the body defends itself against unwanted invaders, such as microbes or cancer cells. Acute inflammation is a cornerstone of the body's homeostasis and is needed to render threats harmless before recovery and healing ensues. Yet, chronic inflammation is part of the pathogenesis of a very large number of diseases. Inflammation, both chronic and acute, may also be local or systemic. This thesis explores aspects of the inflammatory response and how it contributes to acute lung injury. Specifically, the aim here is to investigate preclinical questions that may help infer answers to clinical problems in regard to acute lung injury in humans.

Acute lung injury refers to the concept of acute and usually diffuse inflammatory response manifest in lung tissue (though it can be occurring at the same time in other vital organs), and which leads to impairment of lung function, often in an intensive care setting. First specifically presented in a scientific report in 1967(1), human acute respiratory distress syndrome (ARDS) is a term specific for lung failure meeting certain diagnostic criteria including timing of onset, bilateral engagement and severity of oxygenation impairment(2, 3). Although inflammation – or markers thereof – is not part of the ARDS criteria, inflammation is a hallmark of the syndrome(4-7).

ARDS is a heterogeneous syndrome of acutely impaired lung function that is characterized by an uncontrolled inflammatory reaction in the lungs. This causes diffuse alveolar damage with markedly impaired gas exchange, including hypoxemia and clinical respiratory failure(8-11). Histopathologically, and beyond interstitial oedema and inflammation, the alveolar damage demonstrates prominent neutrophil infiltration, loss of epithelial integrity and capillary damage, along with a proteinaceous alveolar oedema and hyaline membrane formation(8, 9, 12-14).

Although human ARDS is heterogeneous by nature and is associated with many different inciting aetiologies and different phenotypes, it represents a subset of patients with respiratory failure meeting the defining diagnostic criteria(2, 3, 15). The term acute lung injury has been recently revisited with a recommendation that it be applied to describe acute impairment of lung function without meeting strict ARDS

diagnostic criteria in both humans and experimental animal models(3, 16). Clinically indistinguishable from ARDS is ventilator-induced lung injury (VILI), a term referring to the damage lungs sustained from positive-pressure mechanical ventilation(17-19).

Today, there are no clinically useful biomarkers for ARDS or VILI. Furthermore, pharmacological treatment options are extremely limited in ARDS, despite decades of research. Those two shortcomings are the main knowledge gaps that this work attempts to address.

Background

Inflammation

The inflammatory response is tightly controlled to ensure that the inflammatory reaction is sufficiently strong to adequately combat threats and yet controlled enough to avoid inappropriate or unnecessary own tissue damage(20). The regulatory process consists of an elaborate interplay between different redundant systems of mediators, both up-modulating/activating and down-modulating/deactivating(21). As inflammation is a key part of many disease processes(22) where either the body's responses to injury are over-exuberant and injurious of themselves, or where the body's immune system attacks own tissue, called auto-immune illnesses, knowledge of specific steps in inflammatory regulation may give insight into ways of diagnosing disease and possibilities to intervene by pharmacological modification of inflammatory regulatory systems(22).

Innate immune response

The first line of microbial defence consists of a fast-acting response system known as the innate immune system(23, 24). This descriptive term encompasses cells such as macrophages, dendritic cells, mast cells and neutrophils that identifies foreign microorganisms or tissue damage by pattern-recognition receptors (PRRs)(24), which are preprogramed and inherited. PRRs recognize microbes or tissue damage by binding to essential microbial components known as pathogen-associated molecular patterns (PAMPs) or endogenous substances resulting from tissue damage collectively known as damage-associated molecular patterns (DAMPs)(25). Generally, PAMPs and DAMPs are components of fundamental importance to microorganisms (PAMPs) or tissues and cells (DAMPs) that have been conserved through evolution(25, 26). Therefore, these signals remain detectable by a limited number of receptors, regardless of, for example, evolutionary attempts by microbes to avoid detection by our immune system(27, 28).

Activation of PRRs lead to subsequent intracellular activation of signalling pathways such as nuclear factor kappa-B (NF- κ B) and mitogen-activated protein kinases (MAPKs)(29, 30). This induces transcription of genes coding for pro-inflammatory mediators such as cytokines, chemokines and eicosanoid-producing enzymes(29-31).

Toll-like receptors (TLR) are important examples of PRRs(25). For example, TLR4 on macrophages recognizes and binds to bacterial lipopolysaccharide (LPS) and induces, among other responses, NF- κ B-mediated secretion of tumour necrosis factor (TNF) and interleukin 1 (IL-1)(32). Along with other mediators, these two cytokines locally induce and maintain inflammation. They have both autocrine and paracrine effects, with activation of adjacent endothelial cells and leukocytes, as well as upregulation of endothelial adhesion molecules that recruit more immune cells and enhance the production of inflammatory mediators(20, 33, 34). Likewise, LPS also activates TLR4 on dendritic cells, neutrophils, endothelial cells and type II alveolar pneumocytes(35). The integrated response includes activation of the adaptive immune system, which is acquired, targeted defence against specific pathogens. These two sides of immune response lead to local action from different types of activated leucocytes, but prominently neutrophil-mediated inflammation with production of reactive oxygen species, ROS, increased vascular permeability with vascular damages and pulmonary inflammation, possibly with development of ARDS or acute lung injury(36, 37).

TLR4 is also expressed on mast cells, and LPS is therefore one mechanism by which mast cells may be activated(38). Mast cell activation leads to degranulation which includes immediate release of histamine that leads to vasodilation and increased vascular permeability(39). Activation of mast cells also induces synthesis and release of several cytokines (TNF, IL-4, IL-5 and IL-6), chemokines and eicosanoids (including both leukotrienes and prostaglandins)(39, 40). This is a major contributor to the classical inflammatory symptoms of heat, redness, pain and swelling that were described over two thousand years ago.

Adaptive immune response

Many aspects of the innate immune response are initiated within a very short period of time from the activating insult(24, 41). A more sensitive and specific defence against damaging microorganisms or cancer cells may be activated later in the process(24). This response is characterized by specificity, memory and clonal expansion(42). The adaptive response is also an integral part of the process initiated by the innate response, as dendritic cells (and other antigen presenting cells) present foreign antigens to T-lymphocytes that, after differentiation into different subtypes, activate the cell-mediated inflammatory response(42).

After presentation of antigens on major histocompatibility complex (MHC) molecules, individual lymphocytes are activated by recognition and binding of their specific antigen(42). In the case of T-cells, their activation is dependent on the cell-specific T-cell receptor, TCR, interacting with the antigen, a process dependent on co-stimulation of other receptors(43, 44). B-cells may recognize free antigens with their specific B-cell receptor (BCR). Complete activation of B-cells is, however, often dependent on stimulation from cluster of differentiation 4 (CD4)-positive T-cells, also called T helper cells(44).

Lymphocytes with receptors that bind to a specific antigen may undergo clonal expansion, creating a large population of cells with the same specificity for binding to this antigen(45). Dependent on local cytokine environments, lymphocytes differentiate into different effector cells(46). CD4 positive T helper cells control the inflammatory response by secretion of cytokines(46, 47). Different sub-forms include Th1 cells that produce interferon- γ (IFN- γ) that further activates macrophages and reinforces cell-mediated immunity(48). The Th1-mediated effects are important pro-inflammatory stimuli. Th17 cells secrete IL-17 and other cytokines important for neutrophil recruitment(49). These cells contribute to prolonged inflammatory processes, while other T-cells, such as regulatory T cells (Tregs) suppress the inflammatory response to avoid overactivation and prevent autoimmune inflammation(50).

Resolution of inflammation

Inflammation ends when pro-inflammatory cells are eliminated or turned off, or even shift phenotype to a more anti-inflammatory or down-regulating type of action. Neutrophils have a short life span and will undergo apoptosis within hours or days(51). As dying neutrophils are phagocytosed by macrophages, the macrophages are stimulated to switch from a pro-inflammatory state to a more anti-inflammatory state where they secrete IL-10 (an anti-inflammatory cytokine), transforming growth factor beta (TGF- β) and other factors that stimulate tissue repair(52). In parallel, specialized lipid mediators with potent anti-inflammatory actions, such as lipoxins, resolvins and protectins, are produced by metabolization of arachidonic acid (AA) and related polyunsaturated fatty acids (PUFAs)(51, 53). As these mediators are produced in response to an inflammatory stimulus, this results in reduced neutrophil recruitment, dampened inflammatory response and stimulated tissue repair, forming an immunological break that prevent uncontrolled inflammation(53).

Neuroendocrine and metabolic regulatory functions

Neural input as well as hormones have major regulatory functions on the immune system. Also, the reverse is true as well. Perhaps the most obvious example is fever, resulting from hypothalamic production of prostaglandin E₂ (PGE₂) (54) in response to circulating cytokines such as IL-1, IL-6 and TNF. IL-1 and other cytokines also stimulate the hypothalamus to release corticotrophin-releasing hormone (CRH). CRH in turn stimulates release of adrenocorticotrophic hormone (ACTH) in the pituitary gland. ACTH stimulates the production and release of cortisol in the adrenal cortex. Cortisol, in turn, is a potent anti-inflammatory hormone that limits the inflammatory response by a feedback loop that terminates in down-regulation of several transcription factors, including NF- κ B(55). Cortisol also inhibits inflammation by directly stimulating production of multiple anti-inflammatory mediators, including the cytokine IL-10 and the enzyme annexin-1(56).

The autonomic nervous system is also involved in inflammatory regulation. Lymphoid tissues may have direct sympathetic innervation and noradrenaline as well as adrenaline act on adrenergic receptors on immune cells. β_2 -adrenergic receptors dominate and act mainly with anti-inflammatory effect, leading to a tendency for sympathetic attenuation of the inflammatory response, although pro-inflammatory effects of β_2 -adrenergic stimulation can also occur(57). α_1 -adrenergic receptors may have other effects but are more sparsely distributed in the immune system(58).

Vagal tone may also fine-tune inflammatory processes by the cholinergic anti-inflammatory reflex, where acetylcholine release in lymphoid tissue, such as the spleen, results in reduced production of pro-inflammatory cytokines, including TNF by macrophages(59). This swift response helps limit systemic immune overreaction in conditions such as sepsis.

Metabolic processes may also contribute to regulation of inflammation, both in regard to intensity and duration. Generally, energy surplus contributes to chronic inflammation, while caloric restriction in fasting states is associated with anti-inflammatory effects(60, 61). Surplus fat tissue may have potent endocrine effects with impact on immune function. Fat tissue will contain macrophages producing pro-inflammatory mediators such as IL-6, IL-18 and TNF(62, 63). The result is chronic inflammation, which is generally observed in association with obesity, where this group can often have increased resting C-reactive

protein (CRP) levels as well as increased plasma concentrations of a number of cytokines(64, 65).

Oxylipins

Oxylipins are bioactive lipids, or signalling molecules, derived from a limited number of PUFAs(66). These precursors are arachidonic acid (AA) (20 carbon, ω -6), dihomo- γ -linoleic acid (DGLA) (20 carbon, ω -6), eicosapentaenoic acid (EPA) (20 carbon, ω -3), docosahexaenoic acid (DHA) (22 carbon, ω -3), linoleic acid (LA) (18 carbon, ω -6) and alpha-linoleic acid (ALA) (18 carbon, ω -3) and may all be cleaved from cell membrane phospholipids by mainly phospholipase A₂(67). Specific oxylipin synthesis is thus dependent on precursor PUFA as well as enzymatic metabolic path and factors such as dietary intake may influence the actual oxylipin environment(68). Oxylipins derived from AA are called eicosanoids.

After liberation of precursor PUFA by phospholipase A₂ or other lipases, the precursor may undergo metabolism through three main enzymatic pathways: cyclooxygenase (COX), lipoxygenase (LOX) or cytochrome P450 (CYP)(66, 69). There is considerable overlap between the different pathways and metabolites may be produced by different enzymes. The specific metabolites may also have effects that in certain conditions differ from their respective main effect(68). Any overview of oxylipin biology that is not solely dedicated to these details will need to be somewhat simplified, as is the case with the current thesis. An overview of oxylipins detected in this work is presented in Figure 1.

Cyclooxygenase products

COX denotes both the enzyme COX-1, which is constitutively expressed in many tissues, and COX-2, which is not expressed under resting conditions but is induced in inflammatory states(69). COX enzymes metabolize AA to prostaglandin H₂ (PGH₂), an unstable intermediate metabolite that is further converted to highly pro-inflammatory prostaglandins or thromboxane A₂ (TXA₂) by tissue-specific synthases(69). In parallel to PGH₂ production, COX metabolizes small amounts of AA to 15-hydroxy-eicosatetraenoic acid (15-HETE) and very small amounts of AA to 11-HETE(70, 71). The HETEs have intrinsic activities but can also be further metabolized to the anti-inflammatory lipoxins(71). Notably, acetylsalicylic acid (ASA) can change COX-2 activity to increase HETE production and thereby also lipoxin production(72, 73).

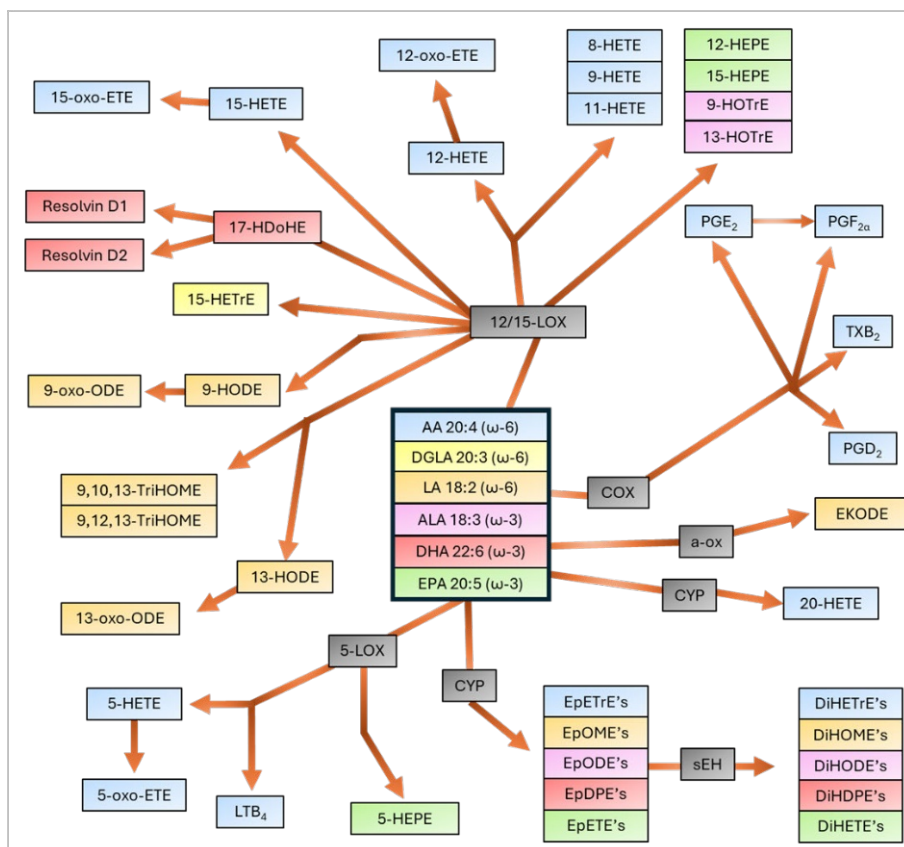


Figure 1. Investigated oxylipins. A simplified pathway map of oxylipins investigated in any of the included papers. Intermediate metabolites not investigated are not shown. Arrows indicate main metabolic pathways but alternate metabolic pathways are also possible.

COX enzymes also metabolize EPA, which is a substrate for ω -3-metabolites corresponding to the AA lipids(74). These EPA metabolites include PGE_3 and TXA_3 and generally have less potent effects than their respective AA counterparts(69).

The main pro-inflammatory effects of COX-products are described in the section below on pro-inflammatory mediators. A very large number of pharmacological agents, including non-steroidal anti-inflammatory drugs (NSAIDs) act by inhibiting COX enzymes, some non-selectively and some specifically on COX-2(75).

Lipoxygenase products

LOX enzymes catalyse di-oxygenation (insertion of molecular oxygen) of PUFAs on specific carbon positions in the fatty acid, with the number in the enzyme name denoting the carbon to receive the oxygen addition(76, 77). Further tissue- and cell-specific metabolism will then yield specific end products and there is overlap with other enzymatic and non-enzymatic pathways.

5-LOX is primarily found in myeloid cells and metabolises AA to the intermediate metabolite 5-hydroperoxy-eicosatetraenoic acid (5-HPETE), which is further metabolised to leukotriene A₄ (LTA₄). LTA₄ can be modified in different directions(69, 78). Hydrolysis by LTA₄ hydrolase will convert LTA₄ to the chemotactic factor leukotriene B₄ (LTB₄)(67). In other instances, LTA₄ will be conjugated with glutathione by the enzyme glutathione-S-transferase to leukotriene C₄ and then further to leukotriene D₄ and leukotriene E₄(69, 79). These substances induce bronchoconstriction and oedema and are important in the pathogenesis of asthma(67). 12/15-LOX will convert AA to 12-HPETE and 15-HPETE that are further converted to pro-resolving lipoxins in cooperation with other enzymes(69, 79).

The important contribution of LOX signalling in asthma is the mechanism by which LOX inhibition has become an established target for pharmacological treatment of this disease(69).

Cytochrome P450 products

CYP enzymes may hydroxylate AA to 20-HETE, but they will also metabolise many PUFAs to epoxides. AA-derived epoxides include the epoxy-eicosatrienoic acids (EpETrEs or EETs by older nomenclature)(80). EpETrEs mediate vasodilation and lowers blood pressure in addition to their anti-inflammatory modulating effect. They are, however, short lived due to rapid metabolism by soluble epoxide hydrolase, sEH. Hydrolysis by sEH convert the EpETrE epoxides to their corresponding diols, dihydroxy-eicosatrienoic acids (DiHETrEs or DHETs in older publications)(79-81). DiHETrEs are without activity or less potent than their epoxide precursors, and in some cases acting in opposite direction to the epoxides(82).

The possible stabilisation of upstream anti-inflammatory and vasodilatory substrates and simultaneous inhibition of downstream detrimental products make inhibition of sEH a pharmacological candidate target to reduce inflammation and also possibly to lower blood

pressure. sEH inhibitors have shown promise in many animal models, especially regarding inflammation. There are currently no pharmacological agents approved for use in humans that are known to inhibit sEH, although several sEH inhibitors are commercially available(83). In an LPS model of acute lung injury, sEH inhibitor treatment attenuated lung injury development(84).

Pro-inflammatory mediators

Proinflammatory cytokines are small proteins, or peptides, important for cell signalling and regulation of inflammation. TNF is primarily (but not exclusively) produced by activated macrophages and binds to specific receptors on target cells, leading to activation of leucocytes, secretion of other cytokines and induction of fever(85, 86). IFN- γ has important functions in both the innate and the adaptive immune responses. IFN- γ activates macrophages and induces MHC class II expression(86, 87). IL-1 (which encompasses a family of substances) is produced by many different immune cells and epithelial cells, as well as supporting cells in different tissues. The effects of IL-1 include increased adhesion factors on endothelial cells that attract immune cells in the blood stream, induction of fever, vasodilation, hypotension and hyperalgesia(86, 88, 89). IL-6 is a pro-inflammatory cytokine that also has anti-inflammatory effects when secreted by muscle cells as well as other effects outside the immune system. In response to PAMPs, macrophages secrete IL-6 to mediate fever and initiation of the acute phase protein synthesis. IL-6 also stimulates growth of B-cells and inhibits the function of Tregs(90-92). IL-12 is secreted by dendritic cells, neutrophils, macrophages and other cells when stimulated by antigens. IL-12 stimulates growth, differentiation and function of certain T-cells as well as the production of other cytokines such as IFN- γ and TNF(93). IL-16 primarily acts as a chemoattractant for CD4 positive T-cells as well as other CD4-positive cells(94, 95). Several additional cytokines also have pro-inflammatory effects(86).

Chemokines are a subgroup of cytokines with primarily chemoattractant effects. They induce leukocytes to migrate towards a higher concentration gradient into an area of inflammation(96). The chemokine family contains four subgroups of substances named from their N-terminal cysteine residues: CC ligand with two adjacent N-terminal cysteine residues, CXC ligand with the two cysteine residues separated by a single amino acid, XC ligand with only one N-terminal cysteine residue and finally CX₃C ligand with three amino acids separating the two cysteine residues(96). Chemokines are often pro-inflammatory and

are rapidly produced in response to cytokine stimulation. Different chemokines attract different immune cells(96, 97).

Vasoactive amines is a collective name for histamine and serotonin. Histamine is stored in granules of mast cells and basophils and can be instantly released in response to tissue injury (DAMP stimulation), detection of PAMPs or allergic reactions(98). Effects of histamine include vasodilation and increased vascular permeability mediated by the H₁-receptor (a G protein-coupled receptor) but are short-lived as histamine is degraded within minutes(98, 99). Serotonin is an amine with many different effects in different contexts, but when stored in thrombocytes, it is released upon activation of the thrombocyte. The effect on vascular tone depends on location and context, while the serotonin release from thrombocyte activation promotes thrombocyte aggregation(100).

Many of the above-mentioned oxylipins are pro-inflammatory mediators. (67, 69, 101). Prostaglandins are implicated in much of the classical presentation of inflammation; PGD₂ and PGE₂ increase vascular permeability and vasodilation as well as increased sensitization of pain nerves(69, 102). Furthermore, as mentioned above, PGE₂ induces fever(54). Prostacyclin (PGI₂) is formed in endothelial cells and is a powerful vasodilator as well as an inhibitor of thrombocyte aggregation(103). TXA₂ is synthesized in activated thrombocytes and has opposing effects to PGI₂; it induces vasoconstriction and promotes thrombocyte aggregation(69). LTB₄, primarily released from neutrophils and macrophages, is a potent chemoattractant for neutrophils and macrophages and increase activation of these cells(104). Other leukotrienes are released mostly from mast cells and eosinophils, and cause powerful bronchoconstriction, increased vascular permeability and increased airway secretions. These mediators are important in the pathogenesis of asthma and anaphylaxis(104, 105).

The complement system is part of the innate humoral immune system, but may also be activated by antibodies from the adaptive immune system(106). Activation of the complement cascade has important implications for bacterial killing, but parts of the system also actively participate in regulation of inflammation. C3a and C5a, protein fragments cleaved from plasma proteins C3 and C5, bind to receptors on mast cells and phagocytes and promote degranulation and histamine release(107). C5a is also a prominent neutrophil chemoattractant and activator of leukocytes(108).

Kinins, such as bradykinin and kallidin, are peptides cleaved from plasma kininogens by kallikreins. This leads to activation of the kinin fragment which then causes vasodilation, increased vascular permeability and initiates pain sensation through a G protein-coupled receptor(109, 110). Kinin action is of very short duration due to rapid plasma degradation(109).

Anti-inflammatory mediators

IL-10 is produced by different cells, including Tregs, certain B-cells and some macrophages. IL-10 binds to its specific receptor on immune cells and confers inhibition of pro-inflammatory gene expression (including TNF, IL-1 and IL-12). It is one of the major local feedback signals that limit inflammation and prevents uncontrolled hyperinflammation(52, 111).

TGF- β is a cytokine in three isoforms with potent inhibitory effects on inflammation that is produced by several different cell types. It inhibits proliferation of T-cells, especially Th1 and Th2, and induces naïve T-cells to differentiate into Tregs(112). TGF- β also suppresses activity in neutrophils and macrophages, and it stimulates collagen production by fibroblasts. TGF- β is important in resolution of inflammation, but overproduction is implicated in development of fibrosis(113).

Cortisol, one of the primary stress hormones, binds intracellular receptors and modulates gene expression(55, 114). Among its effects are increased synthesis of annexin-1, an inhibitor of phospholipase A₂ that inhibit formation of eicosanoids(55). As previously alluded to, cortisol also upregulates production of an NF- κ B inhibitor, leading to reduced production of pro-inflammatory cytokines such as TNF, IFN- γ , IL-1 and IL-6(55, 114). Furthermore, cortisol limits inflammation by inducing cell such as macrophages and monocytes to differentiate into subtypes that promote resolution of inflammation(115). Cortisol synthesis is tightly controlled and has a central function in limiting inflammation to avoid damage from excessive inflammation.

IL-1 receptor antagonist (IL-1ra) is produced by macrophages, monocytes, fibroblasts and others. It blocks the effects of IL-1 by competitively binding to the IL-1 receptor site, while not activating it(116). IL-1ra serves as a negative feedback loop limiting excessive inflammation by decreasing the fever response and other effects of IL-1(89).

Anti-inflammatory mediators include several oxylipins derived from AA and related PUFAs(117). Lipoxin A₄ and Lipoxin B₄ are synthesized from AA by LOX enzymes, in some cases after a process involving interplay between leucocytes and thrombocytes(118). Lipoxins inhibit neutrophil chemotaxis and adhesion and limits their activation(118). Resolvins, protectins and maresins are formed from metabolism of omega 3 fatty acids and induce anti-inflammatory effects by binding to specific receptors on immune cells(117, 119). Their effects include reduction in neutrophil recruitment, apoptosis of present neutrophils and stimulation of macrophages to increase phagocytosis of dead cells and debris(120).

Neuromediators and metabolic products may also act to reduce inflammation. As described above, acetylcholine may confer vagal signalling to limit inflammation(59). Increased metabolic demand, hypoxia, tissue damage and intense inflammation are associated with release of extracellular adenosine that binds to receptors on immune cells and inhibit cytokine release and neutrophil activity(121).

Extracellular vesicles

Extracellular vesicles (EVs) are small particles of cellular origin covered by a lipid bilayer(122). These vesicles can be formed during different circumstances and are roughly divided into different classes based on their size and origin(122). Exosomes (30 – 150 nm in diameter) are derived from endocellular organelles and are formed within cells(123). Microvesicles, also known as ectosomes or microparticles, are vesicles shed from the parent cell's cell membrane and contain cytosol engulfed in the particle(123-125). Microparticles are normally 100 – 1000 nm in diameter(123). Finally, apoptotic bodies are cell fragments produced by cellular collapse during apoptosis(124). They may be as small as 50 nm but are generally larger than 1000 nm(123).

Virtually all cell types may produce EVs under both physiological and pathological conditions, and the ability to produce EVs seems to be an evolutionary well-preserved trait(123). Immune cells use EVs in communication, both in the innate and adaptive response systems. Immune cells may release EVs containing inflammatory mediators, such as cytokines, chemokines or eicosanoids, that amplify or modulate immunological responses(126). EVs can also be used to transmit precursor molecules between cells(124). EVs are also released by thrombocytes to contribute to the coagulation cascade and to help mediate the interplay between coagulation and inflammation(127).

EVs contain both components of cell membranes, including receptor proteins and other cell surface antigens and intracellular substances(124). The cargo of EVs may include enzymes or growth factors that affect functions of target cells(124). Lipids in the covering bilayer of EVs may include substances important for physical properties as well as signalling substances or substrates for metabolic processes in other cells(128). Nucleic acids may also be included in the cargo of EVs. Primarily mRNA can be transferred from one cell to another to facilitate expression of specific proteins(124). Some EVs contain DNA in different forms. One of the mechanisms of this DNA transfer may be to act as DAMPs(129).

EVs are considered a third mechanism of communication between cells apart from direct cell to cell contact and secretion of soluble factors. In fact, EVs can facilitate communication in both distant and near range. Locally released EVs may confer communication with neighbouring cells, while EVs that enter the blood stream or lymphatics may exert effect on distant cells. EV communication can occur both by transfer of content or by interaction with surface antigens(124).

EV communication is also used in the immune system where, for example, antigen presenting cells may produce exosomes containing MHC II – antigen complexes that may stimulate T-cells from a distance(126). EVs may also carry pro-inflammatory mediators that help initiate or amplify an immune response(124). Moreover, cytotoxic T-cells may deploy EVs containing factors that induce apoptosis in distant cells. It is thus clear that EVs may participate in both pro- and anti-inflammatory modulation(126).

Given the many different functions EVs possess in different conditions, and how their production is acutely influenced by diseases and physiological processes, they may have great value as biomarkers as they are found in virtually all bodily fluids(130). EVs are readily detected by flow cytometry and are characterized by recognition of antigens that may indicate specific cellular origins(122, 124, 130). A complete overview of EV antigens is beyond the scope of this thesis but known EV markers that are employed in thesis are introduced here.

Most EV's will be positive for lactadherin, a protein that binds to phosphatidylserine, a phospholipid normally found in the cytoplasmic leaflet of lipid bilayer of cell membranes(124). Phosphatidylserine serves as a trigger of phagocytosis and also as a pro-coagulant by offering a

catalytic surface facilitating the effects of the enzymes in the coagulation cascade(131, 132).

EVs derived from thrombocytes constitutes the majority of EVs under normal resting conditions(127). Thrombocyte EVs express CD61(133), also known as integrin β 3, a thrombocyte cell surface protein shown to participate in cell adhesion(134). Activated thrombocytes will also express CD62P, or P-selectin. P-selectin is stored in granules of thrombocytes and translocated to the surface after activation(135). CD62P on EVs is thus a marker of vesicles derived from activated thrombocytes. Endothelial cells express E-selectin, or CD62E, after cytokine activation, for example in acute inflammation(135). A combined marker of EV's with CD62P/E will thus capture EVs derived from activated thrombocytes or activated endothelial cells and is suggestive of an inflammatory process or tissue injury(136).

Most leukocytes express protein tyrosine phosphatase receptor type C, also known as CD45(137). CD45-positive EVs are thus considered to be leukocyte-derived. Increases in CD45-positive EVs are often noted in inflammatory states. CD45 is a family of transmembrane proteins with important regulatory functions for immune cells(137).

Monocytes and many tissue macrophages express the LPS receptor CD14 and EVs positive for CD14 originate from monocytes or tissue macrophages(138). Upon activation, macrophages and monocytes shed EVs. CD14-positive EVs have been associated with impaired outcomes in ARDS(139).

EVs that have been isolated can be stained with SYTO 13, a fluorescent dye that binds to nucleic acids(140, 141). SYTO 13-positive EVs are thus demonstrated to contain DNA or RNA and may therefore be markers of apoptosis/necrosis, severe cellular stress or NETosis, which is release from activated neutrophils in neutrophil extracellular traps, or NETs(129). EVs positive for SYTO 13 may thus indicate cellular injury, tissue damage or active inflammation(141). EVs can also contain high mobility group box 1 (HMGB1), a nuclear protein involved in regulation of DNA transcription(129). The presence of HMGB1 together with nucleic acids, is a further sign of cellular damage or severe NETosis(129, 142).

ARDS

Definition

ARDS was first described in 1967 by Ashbaugh and colleagues(1). In 1994, a joint American-European consensus committee was formed and published an agreed upon definition of ARDS to facilitate further research(15). The definition was revised in 2012 by a consensus process endorsed by the European Society of Intensive Care Medicine, the American Thoracic Society and the Society of Critical Care Medicine called the Berlin definition(2). The Berlin definition stated that onset of ARDS was acute within a week, exhibited oedema that was not fully explained by cardiac failure or fluid overload, included a need for mechanical respiratory support, exhibited bilateral typical opacities on chest x-ray. By definition, oxygenation was also significantly impaired and the degree of oxygenation impairment was the basis for categorization of severity. Specifically, oxygenation defined by P/F ratio (ratio of partial pressure of oxygen in arterial blood to fraction of inspired oxygen) was defined as 26.4 – 39.5 kPa for mild ARDS, 13.3 – 26.3 kPa for moderate ARDS and ≤ 13.2 kPa for severe ARDS(2). In 2024, the Berlin definition was updated in a new consensus document and allow for the use of high flow nasal canula instead of continuous positive airway pressure (CPAP) as mechanical support, the use of arterial oxygen saturation by pulse oximetry instead of arterial blood gas measurements, the use of ultrasound instead of x-rays as imaging modality and finally to allow for the complete of lack of respiratory support measures in resource-limited areas(3).

Epidemiology

From a very large observational prospective study on mechanical ventilation, ARDS is estimated to affect approximately 10% of all patients in intensive care units, ICUs, and about 23% of patients receiving mechanical ventilation in the ICU(143). Estimates of incidence varies greatly, from under 4 up to 80 cases per 100 000 inhabitants per year(144, 145). During pandemic conditions, ARDS incidence may greatly increase, as was the case during the COVID-19 pandemic(144).

ARDS remains a significant cause of mortality. Historically, mortality estimates have often ranged from 40 to 50% of cases(146). Modern ARDS studies used to test the predictive capability of the Berlin definition showed that mortality increased with increasing severity and was 27% in mild, 35% in moderate and 45% in severe ARDS(2). Notably, only a minority of ARDS patients who die succumb to hypoxia. The most

common cause of death related to ARDS is multiple organ dysfunction syndrome, MODS(147), and specific pulmonary interventions, such as low tidal volume ventilation, can decrease systemic inflammatory response(144).

Pathogenesis

ARDS is an acute inflammatory condition in the lungs characterized by diffuse alveolar injury, markedly increased vascular permeability with alveolar flooding and severe gas exchange abnormalities(144, 148). Neutrophils and thrombocytes are activated and concentrated in the pulmonary microvasculature. This causes damage to the endothelium with microthrombi as well as injury to the alveolar epithelium(144). The inflammatory process leads to breakdown of the alveolocapillary barrier. Flooding of the alveoli occurs along with deposition of proteins and debris. Injury to pneumocytes in addition to alveolar oedema also leads to loss of surfactant function(144). Microscopically, there is visible diffuse alveolar damage along with deposition along the alveolar walls of hyaline membranes, consisting of fibrin residue and cell debris(148). There is a profuse neutrophil infiltration of the lung tissue along with significant increases in number of macrophages(148).

The inflammatory process in ARDS includes aspects of both innate and adaptive immune responses. Alveolar macrophages respond to PAMPs or DAMPs and release pro-inflammatory cytokines such as IL-1, IL-6, IL-8 and TNF(149, 150). Neutrophils are attracted by these mediators, adhere to the endothelium and migrates into the lung tissue where they release several toxic and damaging substances into the tissue(151). Among these are proteases, reactive oxygen species, leukotrienes and platelet activating factor (PAF)(149-152).

Activation of the complement cascade contributes both to inflammation and to damage to the endothelium as membrane attack complexes are formed while complement fragments such as C5a recruit additional leukocytes(153).

The combined effects of diminished surfactant function, alveolar oedema and tissue damage lead to the formation of atelectasis and severely reduce pulmonary compliance(144). Functionally, this leaves only a small remaining volume of aerated lung volume that receives all of the tidal ventilation, a concept known as the 'baby lung'(154, 155). Apart from ventilation/perfusion mismatch and shunts due to atelectasis, the oedema and alveolar debris can also impair diffusion of gases. The

resulting clinical phenotype is thus severely impaired pulmonary mechanics coupled with severe gas exchange abnormalities(156).

During the initial phase, often lasting the first week of ARDS, the condition is characterized by inflammation, oedema and formation of alveolar hyaline membranes. This has been described as an exudative phase(11). After this phase, the condition often evolves into a proliferative phase characterized by decreasing inflammation and type II pneumocytes proliferating to restore alveolar integrity along with infiltration of fibroblasts where normal lung architecture may not be recoverable(11). In some cases, this leads to a fibrotic phase with development of significant pulmonary fibrosis after 2-3 weeks(157).

Ventilator induced lung injury

Mechanical ventilation is often lifesaving in ARDS. Apart from the obvious positive effects of facilitating short term survival, mechanical ventilation has been described as a double-edged sword. Although it may facilitate short term survival, the treatment is inherently damaging to the lungs and may cause lung injury indistinguishable from ARDS called ventilator-induced lung injury (VILI)(17, 158). VILI seems to preferentially harm already diseased lungs, whereas healthy lungs seem to be protected from the harmful effects of mechanical ventilation and limited overdistension. One major explanatory model for this phenomenon is the previously mentioned concept of the 'baby lung', where a very small functional lung volume is massively overstretched by receiving the tidal ventilation meant to be distributed in the whole lungs(155, 159).

There are four classical mechanisms of VILI:

- Volutrauma, where alveoli are overstretched by tidal ventilation with volumes larger than the functional alveoli can safely accommodate. Volutrauma may lead to alveolar rupture or to an inflammatory response secondary to the alveolar overdistension. Volutrauma is avoided by limiting the tidal volumes(158, 160).
- Barotrauma refers to pressure-induced damage to the lung tissue, often in the form of alveolar ruptures with air leaks causing pneumothorax leading to pneumomediastinum or subcutaneous emphysema. The term may be a misnomer as the damage induced by high pressures really seem to be an effect of the overdistension caused by high pressures(160, 161). High pressures with overdistension may cause capillary stress failure with increased

permeability, capillary leakage and oedema. Barotrauma is traditionally avoided by keeping plateau pressures low and by avoiding very large pressure swings during tidal ventilation, described as repeated stretching(162, 163). It should, however, be noted that the pressure with potential to harm the lung tissue is the pressure gradient between the distal airways and the pleural space, and this pressure correlates closely to lung volume(161).

- Atelectotrauma occurs when alveoli cyclically collapse and reopen during ventilation. This is thought to inflict additional shear forces onto the lung tissue with alveolar damage as the result. Moreover, the collapsed alveoli in an atelectasis will deform the architecture of the lung tissue surrounding the atelectasis. This is thought to also add stress to the walls of the ventilated alveoli closest to an atelectasis, causing inflammation and tissue damage(160, 161).
- Biotrauma refers to the detrimental effects of inflammation that occur when the stressors of volume, pressure and atelectasis are driving inflammation, both locally and systemically(160, 161).

Potentially, the injurious effects of both overdistension and repetitive opening and closing of the airways may be correlated to local dissipation of energy intensity mediating the damages induced by ventilation(164). The concept of mechanical power describes this phenomenon and is used to quantify the degree of injurious energy delivered to the tissues(164).

There has also been considerable focus on limiting driving pressure, the difference between the peak alveolar pressure during inspiration and the pressure during expiration, positive end-expiratory pressure (PEEP). Retrospective analysis of data from clinical trials shows that driving pressure is more closely associated with mortality than any other ventilatory parameter(163). This may, however, simply be an observation that compliance – and therefore driving pressure – is more impaired in sicker patients.

In parallel to the concept of VILI, attention has been paid to patient self-inflicted lung injury (P-SILI)(165, 166). P-SILI has been proposed to arise both from even unassisted spontaneous breathing where dyspnoea-driven overly intensive breathing efforts are causing stress damage to a small and stiff “baby lung” and from patient-ventilator dyssynchrony from breathing efforts that oppose the flow of the ventilator(165, 166).

Treatment

There is no definitive pathology-reversing treatment for ARDS. The main treatment goal is to refrain from doing further harm by otherwise avoidable induction of VILI(167). Low tidal volume ventilation, or lung-protective ventilation, is the most important intervention against ARDS(167). Low tidal volume ventilation is universally considered protective against VILI, although the exact limits to safe tidal volumes are not well defined. Generally, tidal volumes are set to around 6 ml/kg ideal body weight(144, 168). In cases where compliance is low and plateau pressures high, further reduction of the tidal volumes may be warranted(168). Conversely, if compliance is high and plateau pressures low and the patient is dyspnoeic, somewhat larger tidal volumes (still below 8 ml/kg) may be acceptable(169). Interestingly, observational data suggest that tidal volumes in clinical practice may be considerably higher than those applied as lung-protective ventilation in studies(143). Notably, the relation of tidal volumes, oxygenation, and lung compliance in COVID-19 cases did not always follow expected ARDS patterns(170).

PEEP is a generally accepted part of ventilatory praxis, but the optimal PEEP level remains an elusive concept. High PEEP will recruit collapsed lung tissue and prevent further collapse(171). At the same time, excessive PEEP may over-distend healthy lung tissue and cause hemodynamic instability(171). PEEP is often titrated to severity of ARDS or to physiological effect, but an unequivocal mortality benefit remains to be proven(171, 172).

Prone positioning has several significant physiological effects that may be associated with benefit. Oxygenation is often clearly improved after proning and studies imply that prone positioning during 16 hours per day may confer survival benefit in patients with severe ARDS(173). Prone positioning was also widely adopted during the COVID-19 pandemic(174, 175).

Extracorporeal membrane oxygenation, ECMO, is a technique where blood is circulated and oxygenated in a machine circuit outside the body, along with simultaneous carbon dioxide removal. Studies are not conclusive but consensus-based guidelines conclude that ECMO can be used for selected extreme-severity ARDS cases where recovery chances were otherwise good, and should be applied only at specialized centres(176, 177).

Systemic steroid treatment has been debated and investigated in many studies with mixed findings regarding general ARDS. In the case of COVID-19-associated ARDS(178) and community-acquired pneumonia(179), steroids seem to confer a mortality benefit. For ARDS cases of other causes, there may be benefit in moderate to severe ARDS if steroids are administered in the early course of the disease, although the optimal dose and timing is unclear(177, 180). For steroids administered only after more than 2 weeks, there may be an association with harm(181).

Neuromuscular blocking agents have been tried in studies with contradictory results(182, 183). In a study with beneficial effects, treatment with cisatracurium was given for 48 h during the early phase of severe ARDS(182). One proposed mechanism of benefit would be reduced VILI due to reduced ventilator-patient dyssynchrony and decreased inflammation in lungs and systemically(182).

Inhaled nitric oxide and inhaled nebulized prostacyclin selectively dilates capillaries in contact with ventilated alveoli, thereby preferentially letting blood flow to areas where gas exchange is possible(184, 185). Both treatments have been shown to increase oxygenation but lack demonstrated survival benefit or improvement in patient-centred outcomes(185). For inhaled nitric oxide, there may be a signal for harm with increased renal impairment(184).

Restrictive fluid therapy seems to improve number of ventilator-free days compared to liberal fluid therapy(186).

Antimicrobial or anti-viral therapy should be administered as indicated for diagnosed or presumed current infections. There is no added value to prophylactic antibiotic treatment of ARDS patients without a specific infection, and guidelines do not support the use of prophylactic antibiotics(167, 177, 187).

Many other direct pharmacological treatments have been tested with neutral, inconclusive, or negative results. None has shown benefit, despite preceding encouraging results from animal studies. The tested agents include surfactant for adults with ARDS(188-190), β 2-agonists(191), statins(192, 193), ASA(194), ibuprofen(195), nutritional supplements and antioxidants(196, 197). As mentioned in the section on oxylipins, sEH inhibition attenuated lung injury in mice receiving LPS(84), but this concept has not been investigated in larger animals or humans.

Animal models

There is no experimental animal model with universal applicability to human ARDS. All experimental models lack at least some aspect of clinical ARDS. Proposed criteria for ARDS models suggest that at least three of the following four domains should be present if a model should be considered relevant: histologic lung injury with tissue damage, alveolar-capillary barrier disruption, inflammation and physiological dysfunction(198).

Mice are commonly used in ARDS research. Methods of lung injury induction include intratracheal instillation of LPS or acid, prolonged hyperoxia, high tidal volume ventilation, caecal ligation + puncture, intravenous LPS and surfactant removal combined with injurious ventilation(199, 200). Mice are readily accessible and easy to work with, allowing for large sample sizes. They are also available in many transgenic variants, allowing for mechanistic studies of selected subsystems(199). Disadvantages of mice models include considerable anatomical and immunological differences compared to humans, and difficulties to apply intensive care methods considered for humans due to their small size(199, 200). Finally, several therapies that have shown benefit in mice models have failed to generate positive results in clinical trials, demonstrating that mouse models do not fully replicate human ARDS(199, 201).

Rats are also used in ARDS studies. The lung injury-induction methods used in mice may be used in rats. Additionally, due to their larger size, rats can be subjected to oleic acid injection or haemorrhagic shock model combined with sepsis. Rats are also more easily mechanically ventilated than mice(202). They also can be observed with more advanced monitoring and more sampling(203). Disadvantages are similar to those for mice, with the addition of higher cost for rats(202).

Large animals used in experimental models (pigs, sheep and primates) have physiology more similar to humans(204). They are well suited for studies using human interventions and for example ventilatory strategies(205). Large animal models are generally limited by high cost and ethical (societal preference) considerations (204). Primates are not used for ARDS research due to the ethical difficulties and extreme costs.

Pigs are commonly used with different established lung injury models; surfactant depletion followed by injurious ventilation, LPS infusion, intrabronchial instillation of pathogens or intravenous oleic acid

injection(205). Depending on model of choice, inflammatory aspects may be more or less prominent(206, 207). Pigs have anatomical and physiological similarities to humans that enables the application of ARDS criteria and the use of therapeutic techniques used in man. Sheep are also commonly used in ARDS research, with lung injury models including intravenous LPS, intratracheal acid instillation and inhalational smoke injury(205-207). Advantages and disadvantages are similar to those in pigs.

Aims

The main goals of this project were to improve understanding of pathway metabolism of bioactive lipids in inflammation coupled to acute lung injury, to identify lung injury biomarker patterns that could help clinicians identify injurious mechanical ventilation and to test if soluble epoxide hydrolase inhibition can attenuate lung injury development in a large animal model.

To those ends, the included original papers have the following specific aims:

- Paper I To test if (and which) oxylipin levels in bronchoalveolar lavage fluid, BALF, react in response to lung injury and if that response is detectable in plasma.
- Paper II To test if (and which) extracellular vesicles characteristics in BALF samples change in response to lung injury and if the same is detectable in plasma.
- Paper III To assess if plasma oxylipin levels change during the first day of mechanical ventilation in the ICU.
- Paper IV To establish a new pig model of long-term venous access and to optimize venipuncture technique in this model.
- Paper V To test whether sEH inhibition in a large animal lung injury model can attenuate development of lung injury.

Finally, previously unpublished work in this thesis aims to establish pharmacokinetic parameters of the sEH inhibitor trans-4-(4-(3-(4-Trifluoromethoxy-phenyl)-ureido)-cyclohexyloxy)-benzoic acid, t-TUCB, previously not tested in pigs.

Materials and methods

Ethical considerations

The animal models in Papers I, II and V utilized animals anesthetized at the beginning of the experiments and later euthanized without waking up. The discomfort experienced by the animals in these experiments is thus considered minimal.

Paper IV and the unpublished work on an sEH inhibitor included pigs that were anesthetized for the establishment of permanent venous access, but then were awakened and moving freely in pens. Although great care was taken to use adequate pain relief and to monitor the animal well-being, there was a small risk of discomfort or pain and also adverse effects by a pharmacological agent not previously tested in pigs. Animal well-being was assessed using appearance and behaviour assessments each day, by the research facility staff and co-authors. There was also partly restricted access to other animals during the four-week study period. With all aspects considered, this experiment was deemed to produce a small degree of discomfort for the animals. The animals included were limited to a small subject number (n=4).

Paper III utilized biobank samples and data from a previously conducted observational ICU study(208). That study was deemed to be ethically uncomplicated as blood samples were drawn from indwelling arterial catheters and patient care was not affected by the study. The present study was performed without a request for additional study participant consent, as judged appropriate by the Swedish ethical review process. Investigators in the present study did not have access to a code key or personal information beyond age and sex of the study participants.

Approval for animal experiments was granted by Umeå University Animal Experimental Ethics Review Committee, documents A43-12, A24-13 and 31-12910/12). In Paper III, permission to include human subject and samples was granted by the Ethical Review Board in Linköping, Sweden (2010/427-31 and 2018/16-32).

Animals

All animals used in the studies were juvenile Yorkshire x Swedish landrace pigs, bred for commercial and research purposes at

Forslundagymnasiet, an upper secondary public school with agricultural focus and regulated animal breeding in Umeå, Sweden. Animals weighed between 25 and 50 kg.

In the University research animal facility, animals were kept pairwise in 8 m² pens with straw and free access to water. The animals were fed a commercially available pig diet twice daily except for the morning before induction of anaesthesia. Lighted and dark pen periods were 12:12 h, and room temperature was kept at 20±1°C.

For the acute/terminal experiments (Papers I, II and V), animals were delivered to the facility and allowed to be acclimatized 1-3 days before the experiment. Animals included in the longer-term study on pharmacokinetics (Paper IV and the previously unpublished pharmacokinetic data) were also acclimatized pairwise in pens after delivery to the research facility. After insertion of long-term venous catheters under anaesthesia, these animals were allowed to recover from anaesthesia in individual pens and were housed in their individual pens throughout the remainder of the experimental period. The animals were allowed visual, auditory, olfactory, and to a small degree tactile, contact with other individuals through cage bars separating the pens. They were trained daily by a handler to accept handling of the central venous catheter to allow both blood sampling and study drug injections. Daily weight gain during the study period was on average 732 g. After completion of the terminal/acute study, anesthetized animals were euthanized by intravenous potassium chloride. Awake animals were anesthetized with intravenous high dose intravenous ketamine before the potassium injection.

Experimental preparation

All animal experiments started with induction of general anaesthesia. Premedication was administered in the pen with an intramuscular injection of ketamine 10 mg/kg, xylazine 2.2 mg/kg and atropine 0.05 mg/kg. The animals were then transported to the laboratory, and an auricular vein was cannulated for intravenous induction of anaesthesia.

Pigs anesthetized to receive tunnelled central venous catheters were anesthetized with 2 mg/kg propofol bolus followed by intravenous infusion of propofol 6-10 mg/kg/h and remifentanyl 0.2-0.4 µg/kg/min. The choice of anaesthetics was done with focus on fast post-operative recovery. Upon induction of anaesthesia, these animals also received a

single dose of prophylactic intramuscular cefovecin 8 mg/kg. During anaesthesia, animals were orotracheally intubated using a standard direct laryngoscope with a size 4 Miller blade in the prone position. Mechanical ventilation was performed with volume control ventilation, tidal volume 8 ml/kg, PEEP 5, I:E 1:2 and respiratory rate set to achieve normocapnia estimated from end-tidal carbon dioxide concentration. Local infiltration around the catheter implantation site with 20 ml of bupivacaine 2.5 mg/ml with adrenaline + 5 µg/ml was administered for postoperative analgesia. After discontinuing the anaesthetic drugs, the animals were extubated and given supplemental oxygen as needed for the first few minutes to achieve arterial oxygen saturation of at least 96%. The animals were allowed a 3–6-day recovery period in individual pens before start of pharmacokinetic experiments.

Animals included in studies in Papers I and II were anesthetized with intravenous pentobarbital 10 mg/kg and subsequent anaesthesia was maintained with intravenous infusion of 20 µg/kg/h fentanyl, 0.3 mg/kg/h midazolam and 5 mg/kg/h pentobarbital, a combination that was standard procedure in our lab at the time. Orotracheal intubation was performed as described above and animals were initially ventilated with volume control ventilation, tidal volume 8 ml/kg, PEEP 5, I:E 1:2, fraction of inspired oxygen 0.4 and respiratory rate set to achieve normocapnia. External warming with an electric pad was used if core temperature dropped below 38°C. A central venous catheter was percutaneously inserted and an arterial catheter were placed after a cut-down procedure of the neck, both under sterile conditions. Ringer's acetate was administered as maintenance fluid with 4-5 ml/kg/h and 250 ml boluses of hydroxyethyl starch solution were administered if hypovolemia was suspected.

Animals in the Paper V study were anesthetized with an intravenous bolus dose of 2 mg/kg ketamine and 0.3 mg/kg midazolam, followed by orotracheal intubation as described above and maintenance of anaesthesia with continuous infusion of ketamine 5 mg/kg/h, midazolam 0.3 mg/kg/h, and fentanyl 10-25 µg/kg/h. Intramuscular injections of xylazine 2.3 mg/kg were administered as needed when anaesthesia was deemed to need deepening. The anaesthetics were chosen to minimize circulatory side effects. After neck dissection, the exposed carotid artery was cannulated, and the external jugular vein was used for insertion of a pulmonary artery catheter. A urinary catheter was placed surgically after mini-laparotomy. All surgical procedures were performed under sterile conditions. Ringer's acetate was administered at 5 ml/kg/h and extra boluses of 20 ml/kg of Ringer's acetate were

administered whenever hypovolemia was suspected. Peripheral vascular resistance was maintained using noradrenaline as needed up to 1 $\mu\text{g}/\text{kg}/\text{min}$. If augmentation of cardiac output was deemed necessary, infusion of adrenaline could be added up to 1 $\mu\text{g}/\text{kg}/\text{min}$.

Research participants, human

Paper III used a prospectively collected cohort of cases with indwelling arterial cannulas admitted primarily to the ICU of Östersund Hospital, Östersund, Sweden, with samples collected between 1 February 2012 and 31 January 2013(208). Subjects, or their next of kin, agreed to participate in an observational study which included daily collection of a blood sample. Verbal consent by patents or next of kin was accepted by the ethical review board in view of the observational nature of the study(208). All subjects received standard care as needed for their respective condition. From the original study cohort of 278 subjects, 147 cases with complete data records and samples were identified. Of these, 25 cases were intubated during their ICU stay and were thus included in the analysis. Another 26 cases within this screening cohort were matched for age and sex, and included in the analysis as comparison cases in this observational study. The matched controls were the participants with matching sex and closes age match. When there were multiple age matches among potential controls, the subject with study serial number closest after the index case was selected.

Protocol

Paper I

All animals were subjected to surfactant removal by saline lavage. After preoxygenation with 100% O₂, 30 ml/kg of 38°C 0.9% sodium chloride (NaCl) solution was instilled into the trachea through the tracheal tube. Immediately after administration of the whole volume, the fluid was allowed to drain passively over several seconds. This was repeated to a total of four times with short recovery periods between the administrations to allow the animals' oxygen saturation to return to at least 96%.

After lung lavage, the animals were randomized by simple lot to either low tidal volume ventilation (LTV) or to high tidal volume ventilation (HTV). After the lung lavage procedure, animals in the LTV group were ventilated with 8 ml/kg tidal volume, PEEP 8, FiO₂ set to achieve normoxemia and respiratory rate set to achieve normocapnia. The HTV

group was ventilated with 20 ml/kg tidal volume, PEEP 0, FiO₂ 1.0 and respiratory rate 20/min. Dead space was increased with extra tubing as needed to achieve normocapnia.

Samples of blood and BALF were collected at baseline before the lung lavage and 1h, 2h, 4h and 6h after the start of ventilation according to protocol and randomization. BALF was collected by wedging a flexible bronchoscope into a segment bronchus with subsequent instillation of 50 ml 0.9% NaCl solution followed by gentle suctioning of the instilled fluid. This procedure was performed three times, and the total recovered fluid volume was noted before centrifuging the BALF 15 minutes at 400 g and 4°C. The supernatant was frozen to -70°C in aliquots and the cell pellets resuspended in phosphate buffer solution for later cell counts. Blood was drawn from the arterial catheter into standard EDTA tubes. After centrifuging for 10 minutes at 2000 g and 4°C, the plasma was recovered and frozen to -70°C.

Exhaled breath condensate

A cooling tube to condensate exhaled air was manufactured by bending an 8 cm long standard 14 mm diameter copper tube twice to 90 degrees, thus creating a u-shaped tube. The bent portion of the tube was then placed in iced water, with a total of 60 cm of the tube immersed. The ends of the tube were fitted with rubber adaptors designed for use with ventilator tubing. During exhaled breath condensate, EBC, collection, the collection device was inserted in the expiratory tubing of the ventilator to lead the exhaled air through the cooling tube for ten minutes. The collection device was then detached and the produced EBC was poured from the copper tube into Eppendorf tubes. The tracheal tube was clamped to retain PEEP whenever the EBC tube was connected or disconnected. The samples were immediately frozen to -70°C.

After spontaneous death or euthanasia, lung biopsies were collected from upper and lower lobes of both lungs and placed in formaldehyde before later histological evaluation.

Paper II

Paper II is based on samples from the same subjects as Paper I, and the study protocol was identical to Paper I with the exception that blood was collected in citrate tubes and the centrifuged at 2000 g for 20 minutes at room temperature before the plasma was recovered and frozen at -70°C.

Paper III

For study participants receiving an arterial line after being admitted to the participating ICU, blood sampling was performed as soon as possible after admission, 06.00 the following morning and 06.00 the day after that. Furthermore, for those being intubated, a new blood sample was collected as soon as possible after intubation and again 06.00 the following morning and 06.00 the day after that. If intubation preceded any of the samples following admission, these samples were excluded from the analysis in favour of the samples related to the intubation. All samples were collected through the indwelling arterial line into standard EDTA tubes. Within 30 minutes of sampling, the tubes were spun at 2000 g and the resulting plasma immediately frozen at -70°C.

Paper IV

Tunnelled long-term central venous catheters were placed in anesthetized animals. After surgical scrub and preparation of a sterile field and the animal lying in a lateral position and head tilted 10° down, classic Seldinger technique was used to first puncture and then place a guidewire in the external jugular vein. A 5 mm cut was made in the skin adjacent to the guide wire and a 4 Fr dilatator was inserted over the wire. Another 5 mm skin incision was made over the dorsal aspect of the neck near the midline. A catheter with subcutaneous cuff was then tunnelled to the dorsal exit point. After exchanging the first dilatator for a large bore dilatator, the introducing stylet of the dilatator was removed with the guide wire. The catheter was cut to appropriate length and inserted through the remaining introducer sheath that was subsequently removed. The skin was sutured at the wounds dressed. A purpose-made covering cloth with central Velcro opening was sutured to the skin to cover the external part of the catheter.

Large pigs (weighing 47-50 kg) were placed in the lateral position, and the upwards-facing external jugular vein was punctured with landmark technique. In random order, both a standard 18 Ga needle followed by immediate insertion of a 0.97 mm guidewire and a micropuncture 21 Ga needle followed by insertion of a 0.46 mm guide wire used to facilitate insertion of a small-bore dilatator before change to the larger 0.97 mm guide wire were used. Both external jugular veins were used in this fashion in all animals (except one where one vein proved impossible to identify). Time to proper 0.97 mm wire placement was noted for all techniques.

Six small pigs (weighing 25-32 kg) included in the study in Papers I and II lying in dorsal recumbency had the external jugular vein punctured with a 21 Ga needle, followed by a 0.46 mm guide wire that was exchanged to a 0.97 mm guide wire through a dilatator / introducer sheath. Time from skin puncture to proper placement of the 0.97 mm guide wire was noted.

Paper V

One pilot animal received an infusion of 1-adamantanyl-3-(5-(2-(ethylethoxy)ethoxy)pentyl)urea, AEPU, at 0.1 mg/kg/h for 255 minutes. Blood samples were collected 5 minutes before start of infusion and the immediately after start of infusion and after 5, 35, 65, 120, 185, 240, 255, 270, 285, 300 and 330 minutes. At each sampling time, blood was drawn through the arterial catheter into standard EDTA tubes. From these tubes, aliquots of 10 µl EDTA-treated blood was set on filter paper for later analysis according to a previously published protocol(209).

In the main study, two pigs were included in parallel each day. AEPU and placebo infusions were prepared by an investigator not taking part in the rest of the experiment. The animals were pairwise assigned to either group and placebo and AEPU infusions were started immediately after induction of anaesthesia and intubation. After a two-hour period when the animals were prepared with the experimental setup, LPS treatment was started with a 0.1 mg/kg bolus administered over 30 minutes followed by an infusion of 0.01 mg/kg/h that was administered over the rest of the experiment. Animals were monitored for physiological parameters and oxygenation, and samples were serially collected to measure AEPU blood concentrations as well as oxylipin levels. Samples were collected at baseline (before LPS), after 6 h of LPS infusion and after 9 hours, just before euthanasia. Bilateral lung biopsies were collected postmortem.

LPS was chosen to induce the experimental lung injury as it was hypothesized that an inflammatory stimulus would be possible to block with pharmacological modulation of the inflammatory process. Also, the previously used VILI model was deemed to be too severe to allow any pharmacological treatment to be effective.

t-TUCB pharmacokinetics

Animals used in Paper IV were equipped with long term central venous double lumen catheters and then allowed a 3–6-day recovery period after the procedure. Each of the catheter lumens was dedicated to either

injection or sampling and clearly marked accordingly. All samples were drawn, and injections performed, after careful aspiration and disposal of the fluid retained in the catheter. After sampling or injection, the catheter lumen was heparinized with heparin solution exactly matched to the internal diameter of the lumen.

After collection of baseline samples, 0.1 mg/kg t-TUCB dissolved in dimethyl sulfoxide (DMSO) to a concentration of 10 mg/ml, was administered by intravenous injection in all animals. Exactly one week later, the animals received a 1 mg/kg intravenous dose. One week after that, a third intravenous dose of 2 mg/kg t-TUCB was administered. Finally, one week after the third dose the animals were given an oral dose of 1 mg/kg t-TUCB hidden inside a pastry.

Blood samples were collected immediately before each dose and three minutes after each intravenous dose. Samples were then again collected after approximately 30, 60, 120, 240 and 480 minutes and after 1, 2, 3 and 4 days. Different lumens of the indwelling catheters were used for injection and for sampling. The animals were euthanized by intravenous administration of potassium chloride under general anaesthesia after the final samples were secured.

For determination of blood concentration of the study drug, 10 µl blood was immediately transferred to an Eppendorf tube containing 50 µl of distilled water before short mixing on a Vortex machine. 200 µl of ethyl acetate was then added before vigorous mixing for 1 minute on a vortex machine. The samples were then immediately frozen to -80 °C. The same procedure was then repeated for each sample collected at different time points according to protocol for later measurement of t-TUCB concentration in blood according to a previously described protocol(210, 211).

Methodological considerations

In Paper I and II, the overall aim was identification of biomarkers of VILI. Thus, an experimental model where the lung injury was induced by injurious ventilation was chosen. The pretreatment with saline lavage was deemed necessary to make the animals' lungs susceptible to the injurious effects of ventilation and the lavage was administered to both groups to specifically study the effects of ventilation, although the model could be affected by high inspiratory fraction of oxygen in the high tidal volume group.

In Paper V, a lung injury model based on an inflammatory insult was chosen as this was hypothesized to be more likely to be attenuated by anti-inflammatory treatment than the very severe VILI model previously used. Also, the previously published positive effects of sEH inhibition came from a rodent LPS lung injury model(84) and Paper V aimed to reproduce those results in a large animal model. The anaesthesia protocol in Paper V was refined with the intent of limiting circulatory side effects in the model with severe septic features.

Paper III used biobank samples previously collected by a collaborating research group in a previously published study(208). This biobank contained samples from a large number of subjects but not all of them were complete after analysis for the initial study. A limited laboratory capacity necessitated selection of a smaller number of subjects than the original cohort for participation in this study. As the focus here was primarily concerned with mechanical ventilation and acute lung injury, all intubated cases with complete sets of samples in the biobank were selected together with controls matched for age and sex.

Paper IV was the result of methodological preparations to perform the previously unpublished study on t-TUCB. A different inhibitor (AEPU) was chosen as the results from the t-TUCB study did not yield reliable pharmacological parameters for the study drug. The efforts to optimize a long-term catheterization model in pigs were, however, deemed worthy of publication as previously published models of long-term cannulation of swine were based on more invasive surgical cut down techniques.

The pharmacokinetic study of t-TUCB and Paper V were projects completed in collaboration with Hammock Laboratory at University of California, Davis. Initially, t-TUCB was chosen from Hammock Laboratory's large database of small molecule sEH inhibitors as data from other species implied that the substance could be dosed intravenously with a half-life suitable for convenient dosing(211, 212). As we were not aware of any sEH inhibitor with known pharmacokinetic properties in pigs, AEPU was chosen after confirmation that the substance inhibits recombinant pig sEH largely on the notion that an inhibitor suitable for continuous infusion could be easily dosed under the conditions of this experiment.

Analyses

Oxylipins in plasma, BALF and EBC were quantified using a previously published protocol(213, 214). On the day of analysis, the frozen samples were thawed at room temperature. Solid-phase extraction cartridges (Waters Oasis HLB) were pre-conditioned with ethyl acetate, methanol, and aqueous methanol containing 0.1% acetic acid. Individual samples were loaded onto the cartridges with added internal standards and antioxidants. The cartridges were then washed, dried under vacuum and eluted into polypropylene tubes containing glycerol as a trapping agent. Another drying process evaporated the solvent, and the remaining residues were reconstituted in methanol. A recovery standard was added prior to analysis. Oxylipin separation and quantification were performed using ultra-performance liquid chromatography coupled to tandem mass spectrometry (UPLC-MS/MS). Chromatographic separation was optimized using a time-based gradient of different solvents. The mass spectrometer operated in negative ion mode, and peak integration was carried out manually using MassHunter software.

EVs in plasma and BALF were quantified by flow cytometry. EV-enriched pellets were obtained from all samples by high-speed centrifugation, first at 2000 RCF for 20 minutes and for most of the supernatant also at 20 800 RCF for 45 minutes. The EV-enriched pellet obtained was then resuspended in phosphate buffer and again recentrifuged at 20 800 RCF for 45 minutes. The resulting pellet was subsequently resuspended in plasma. 20 μ l of the pellet was incubated with fluorescently labeled markers for investigated antigens. EVs were analyzed using a Beckman Gallios flow cytometer. Size gating was established using Megamix calibration beads (BioCytex) with diameters of 0.5 μ m, 0.9 μ m, and 3.0 μ m. EVs were defined as particles less than 1.0 μ m in diameter and positive for lactadherin. Control antibodies without reaction to porcine antigens were included as negative controls, along with fluorescence minus one controls. Results were presented as EVs/l.

Statistics

All details are described in the individual papers. In Papers I, III and V, only oxylipin metabolites quantified in at least 80% of samples were included in statistical analysis. Principal component analysis, PCA, was used to exclude batch effects and OPLS-DA was used to evaluate group differences with effects from multiple inputs (data not shown as the multivariate methods failed to identify batch effects or significant group

differences). Observations below limit of detection (LOD) were treated as missing in group comparisons. In EBC, the limit in detection frequency for inclusion in analysis was lowered to detection in at least 50% of samples due to the exploratory nature of this compartment. When multiple comparisons were performed, correction for this was done using the false discovery rate, FDR, set to 10%(215). In all papers, distributions of biomarker observations were assessed graphically and by Shapiro-Wilk tests to determine if they approximated a normal distribution. Comparisons of two group means were analyzed with Student's T-test for normally distributed continuous data. Group comparisons between two groups with continuous data without a normal distribution were compared with Mann-Whitney-U. Fisher's exact test was used for comparisons of nominal data in two groups. In Paper I, group comparisons over time were made with mixed linear models after transformation of data according to the optimal transformation identified by a Box-Cox analysis. In Paper III, log transformation preceded Student's T-test comparisons. Correlation of measurements was evaluated between different compartments in Papers I and II using Spearman's ρ . In Paper II, a two-way ANOVA for repeated measures compared EVs between groups over time. This was done after performing a one-way ANOVA for each variable and treatment group to detect changes over the serial measurements. For pharmacokinetic calculations, area under the curve, AUC, for individual animals were calculated in R 4.4.1 using the trapez method: library pracma, command `line auc <- trapz(time_values, concentration_values)`. For calculation of the elimination rate constant k , the terminal elimination phase was identified from a semilogarithmic plot of concentration vs time with the assumption that a straight line identified the terminal elimination phase. Log-transformed concentrations were included in a linear regression to determine the slope of the curve, giving k . Half-life was calculated from k via the formula $t^{1/2} = \ln(2) / k$. Clearance (CL) was calculated from dose/AUC. Volume of distribution, VD, was calculated from CL/ k . Statistical significance was considered when $p < 0.05$.

Results

Paper I

15 animals were included in the study, 9 in the HTV group and 6 in the LTV group. 3 animals in the HTV group died before collection of the 6 h samples, and one of those died before the 4 h samples were collected. Animals in the HTV group received higher tidal volumes, more oxygen and were notably more affected with a severely reduced P/F ratio and higher histological lung injury scores. Table 1 summarizes the characteristics of the two study groups. After 2 hours, neutrophil accumulation was evident in BALF (Figure 2).

Table 1. Study groups. Data presented as median (interquartile range). Group comparisons were made using Mann-Whitney-U test. LTV – low tidal ventilation. HTV – high tidal ventilation. Histological lung injury score is graded as 0 = no lung injury, 1 = mild lung injury, 2 = moderate lung injury and 3 = severe lung injury.

Variables	LTV n=6	HTV n=9	p
Weight (kg)	35.5 (28 - 50)	32.5 (30 - 37)	0.78
Tidal volume (ml)	280 (228 - 400)	680 (600 - 747)	<0.001
Respiratory rate (breaths/min)	30 (26 - 38)	20 (20 - 20)	0.003
Fluid administration (ml/kg/h)	7.7 (4.4 - 8.2)	10.0 (9 - 12.0)	0.026
Peak insp. pressure (cmH₂O)	22 (20 - 23)	45(41 - 47)	<0.001
Last compliance (ml/cmH₂O)	14.3 (7.0 - 21.7)	14.9 (9.2 - 20.6)	0.60
FiO₂	0.35 (0.29 - 0.40)	1.0 (1.0 - 1.0)	<0.001
Worst P/F ratio (kPa)	46 (34 - 52)	9.7 (7 - 19)	0.008
Lung injury score	0.125 (0 - 0.44)	2.75 (2.5 - 2.75)	0.044

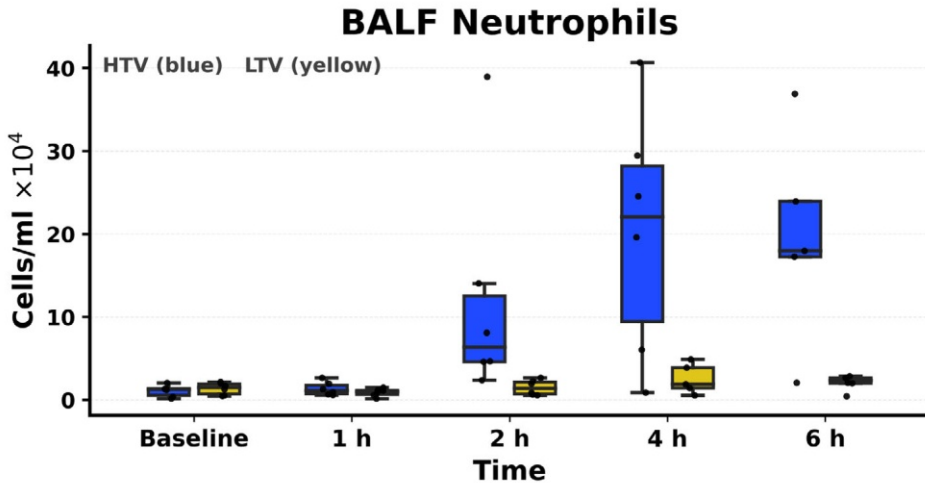


Figure 2. Bronchoalveolar lavage fluid neutrophils. A significant increase in number of neutrophils in the high tidal volume ventilation (HTV) group is evident after 2 hours. BALF. Neutrophils did not increase in the low tidal volume ventilation (LTV) group.

Oxylipins in bronchoalveolar lavage fluid and plasma

2 BALF samples were lost during the extraction process and were subsequently excluded. Of the investigated oxylipins, 37 metabolites were detected and quantified in at least one of the samples in both BALF and plasma, none of which was deemed to have a normal distribution. In BALF, 20 metabolites were quantified in more than 80% of the samples and thus included in further analysis. In plasma, 24 metabolites reached the 80 % quantification limit.

From the COX metabolic pathway, 4 AA metabolites met the 80% inclusion criterion in BALF (Figure 3), and 3 metabolites did so in plasma (Figure 4). In BALF, $\text{PGF}_{2\alpha}$, PGE_2 and PGD_2 could be transformed into an approximate normal distribution and subsequently formally analysed. In plasma, successful transformation and further analysis were possible for all three metabolites detected in more than 80% of samples (TXB_2 , $\text{PGF}_{2\alpha}$, and PGE_2).

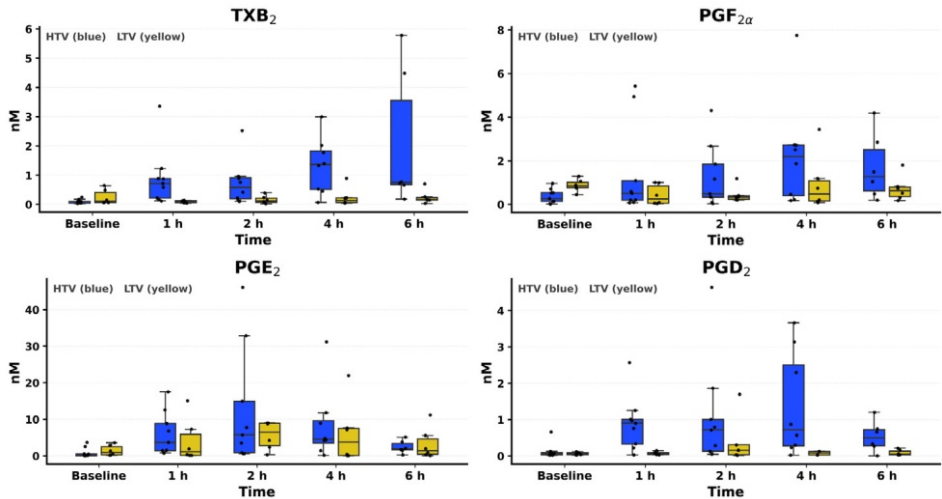


Figure 3. Cyclooxygenase-derived arachidonic acid metabolites in bronchoalveolar lavage fluid. Observations from the group with high tidal volume ventilation (HTV) is shown in blue and low tidal ventilation (LTV) in yellow.

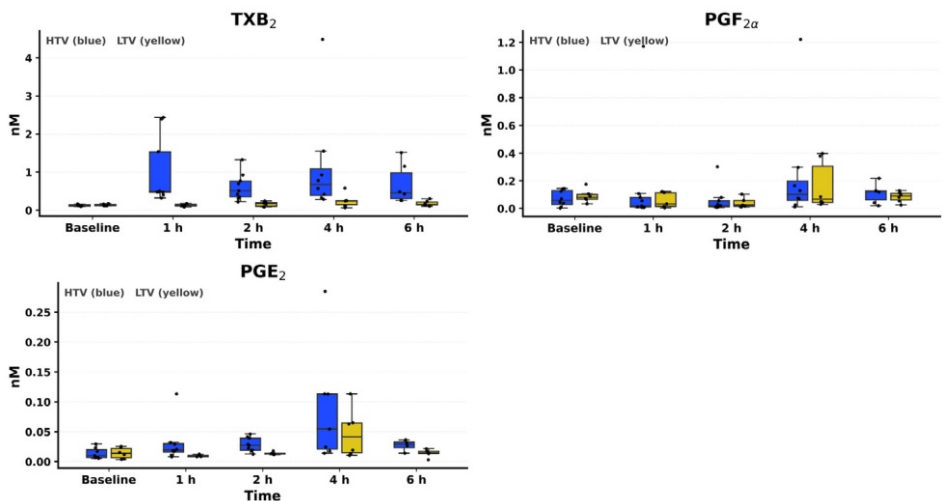


Figure 4. Cyclooxygenase-derived arachidonic acid metabolites in plasma. Observations from the group with high tidal volume ventilation (HTV) is shown in blue and low tidal ventilation (LTV) in yellow.

Two sEH-derived diols from CYP metabolism of AA were detected in more than 80% of BALF samples (Figure 5). One of the diols, 11,12-DiHETrE, was successfully transformed into an acceptable normal distribution. In plasma, 5 metabolites were detected in more than 80% of samples (Figure 6). These were one epoxide, 5,6-EpETrE, and 3 sEH-derived diols, 8,9-DiHETrE, 11,12-DiHETrE and 14,15-DiHETrE, (none

of which corresponded to the epoxide) as well as one alcohol, 20-HETE. All five plasma metabolites could be transformed into a normal distribution and included into further analysis.

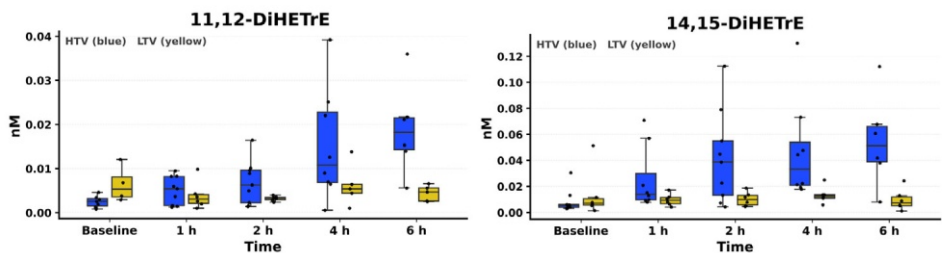


Figure 5. Cytochrome P 450-derived arachidonic acid metabolites in bronchoalveolar lavage fluid. Observations from the group with high tidal volume ventilation (HTV) is shown in blue and low tidal ventilation (LTV) in yellow.

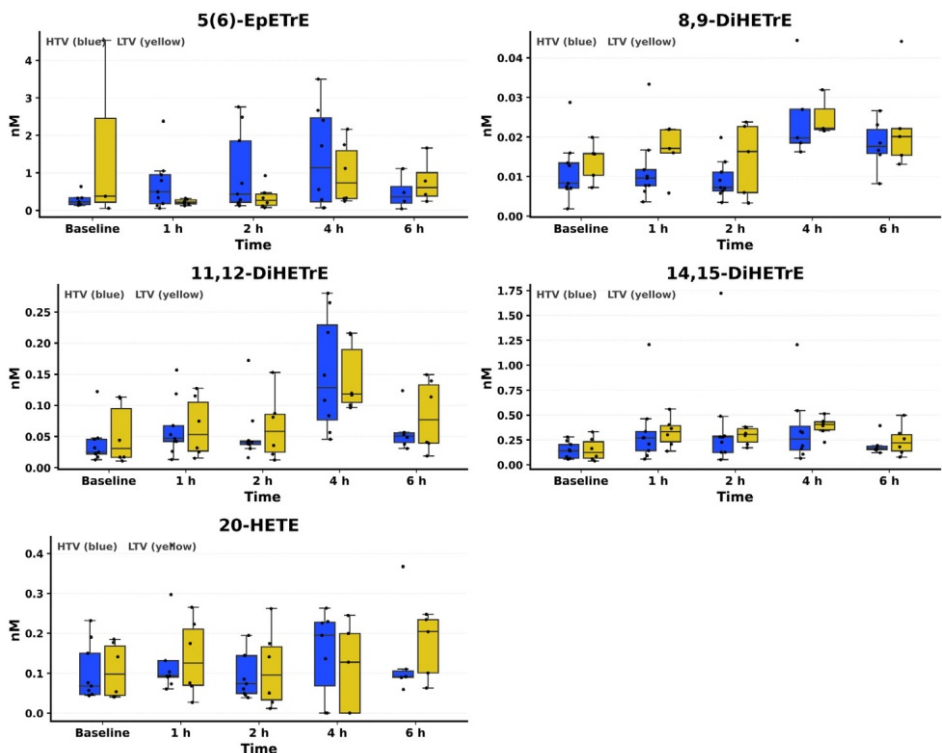


Figure 6. Cytochrome P 450-derived arachidonic acid metabolites in plasma. Observations from the group with high tidal volume ventilation (HTV) is shown in blue and low tidal ventilation (LTV) in yellow.

Metabolites of AA from the LOX pathway were also detected. In BALF, 5 different of these metabolites had a detection frequency of more than 80% (Figure 7) and in plasma 6 metabolites were sufficiently quantified (Figure 8). Of these, 2 in BALF (11-HETE and 15-HETE) as well as 4 in plasma (5-HETE, 11-HETE, 15-HETE and 15-oxo-EETE) could be transformed into a normal distribution allowing further analysis.

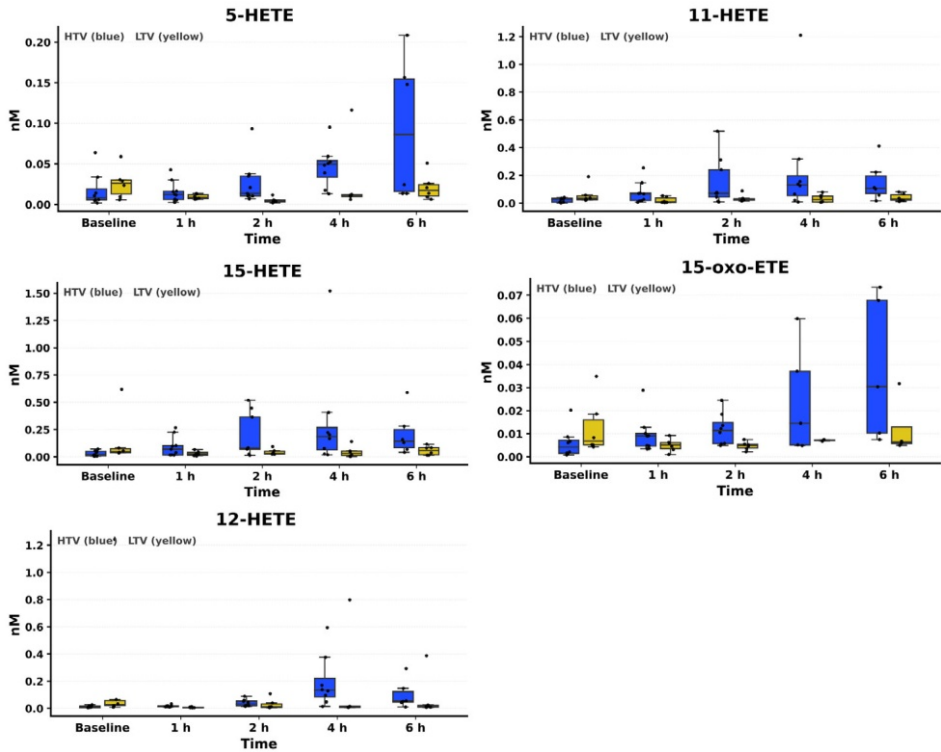


Figure 7. Lipoxigenase-derived arachidonic acid metabolites in bronchoalveolar lavage fluid. Observations from the group with high tidal volume ventilation (HTV) is shown in blue and low tidal volume ventilation (LTV) in yellow.

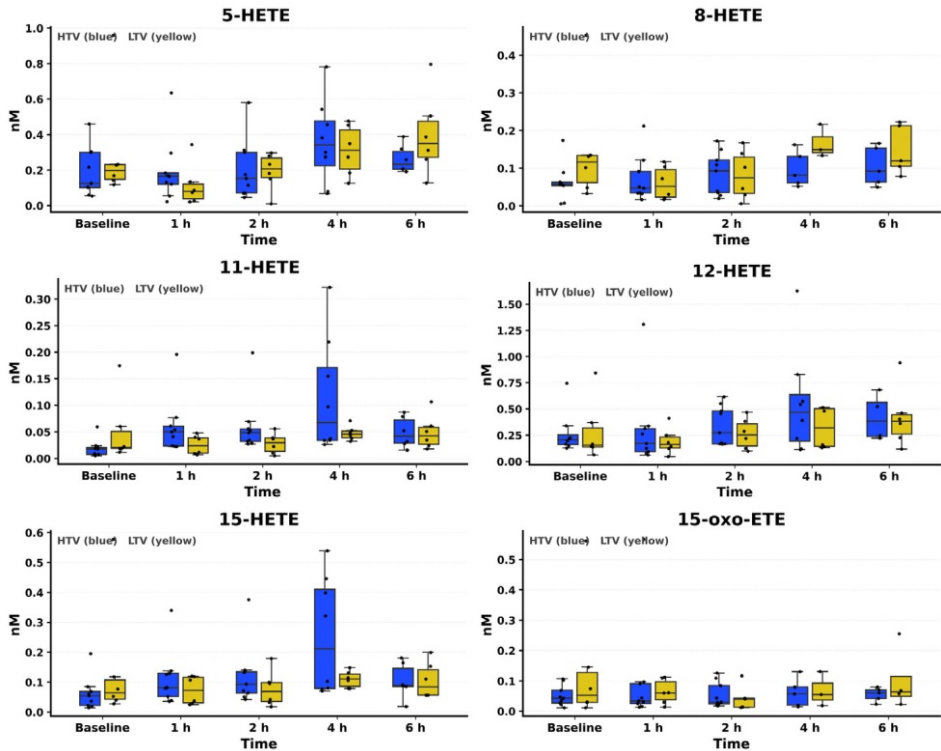


Figure 8. Lipoxigenase-derived arachidonic acid metabolites in plasma. Observations from the group with high tidal volume ventilation (HTV) is shown in blue and low tidal ventilation (LTV) in yellow.

In both BALF (Figure 9) and plasma (Figure 10), two CYP-produced LA epoxides and their corresponding diols, were detected in more than 80% of samples. In BALF, only the two diols 9,10-DiHOME and 12,13-DiHOME could be transformed into a normal distribution, while all four metabolites in plasma (9(10)-EpOME, 12(13)-EpOME, 9,10-DiHOME and 12,13-DiHOME) reached normality after transformation.

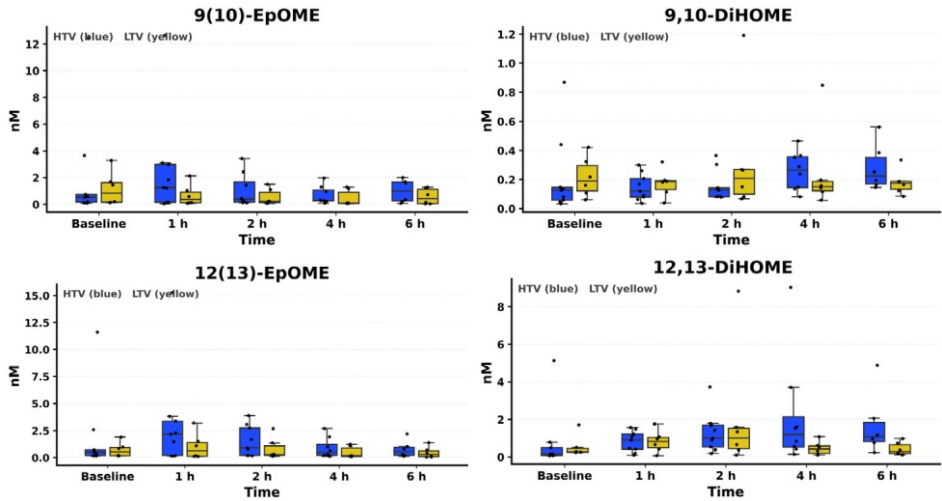


Figure 9. Cytochrome P 450-derived linoleic acid metabolites in bronchoalveolar lavage fluid. Observations from the group with high tidal volume ventilation (HTV) is shown in blue and low tidal ventilation (LTV) in yellow.

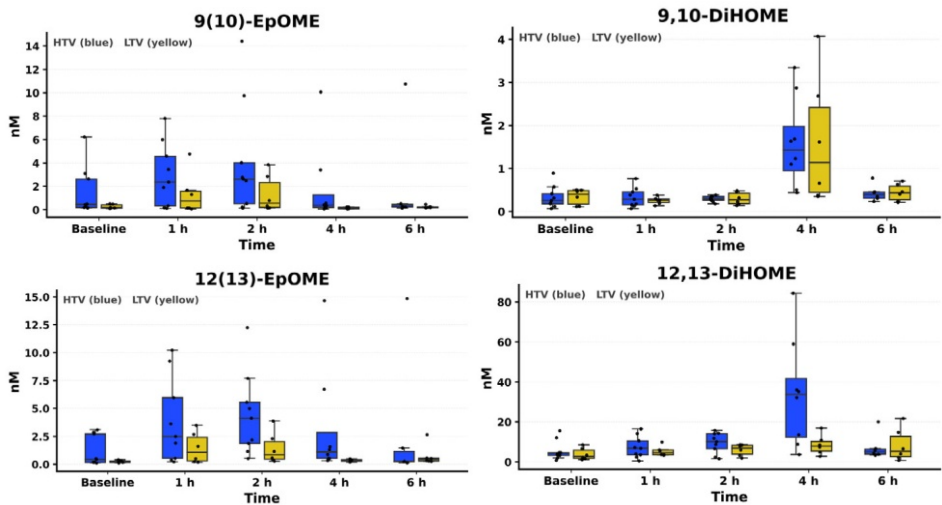


Figure 10. Cytochrome P 450-derived linoleic acid metabolites in plasma. Observations from the group with high tidal volume ventilation (HTV) is shown in blue and low tidal ventilation (LTV) in yellow.

Products from LOX metabolism of LA were detected in more than 80% in all cases in all five investigated cases in both BALF (Figure 11) and plasma (Figure 12). Of these, 9,10,13-TriHOME, 9-HODE and 13-HODE in BALF could be transformed into a normal distribution, as well as 9,10,13-TriHOME, 9,12,13-TriHOME, 9-HODE, 13-HODE and 13-oxo-ODE in plasma.

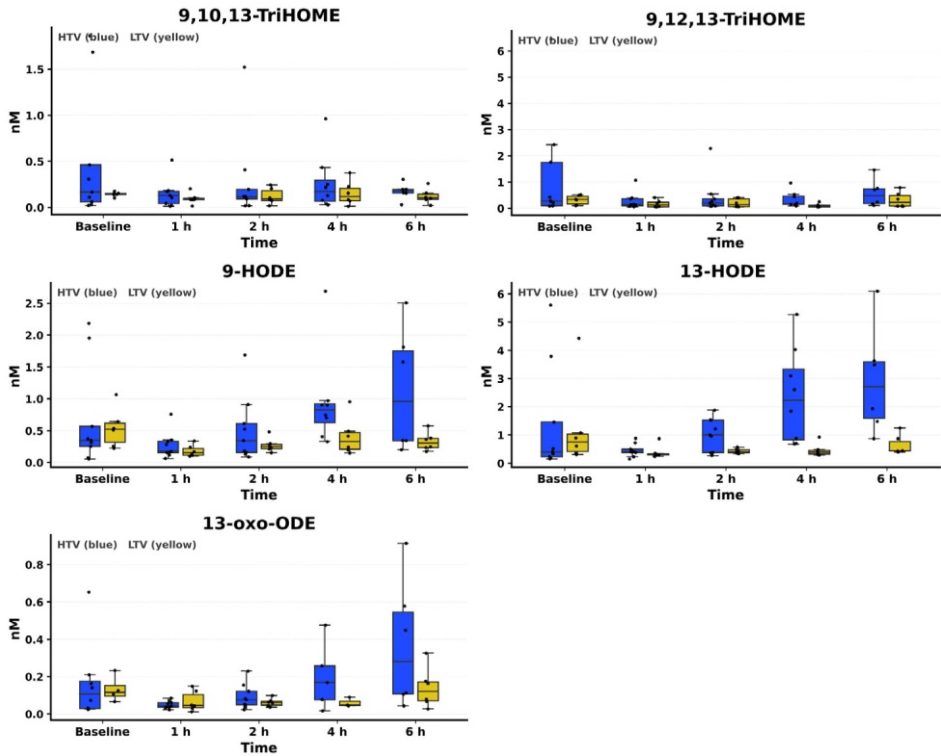


Figure 11. Lipoxigenase-derived linoleic acid metabolites in bronchoalveolar lavage fluid. Observations from the group with high tidal volume ventilation (HTV) is shown in blue and low tidal ventilation (LTV) in yellow.

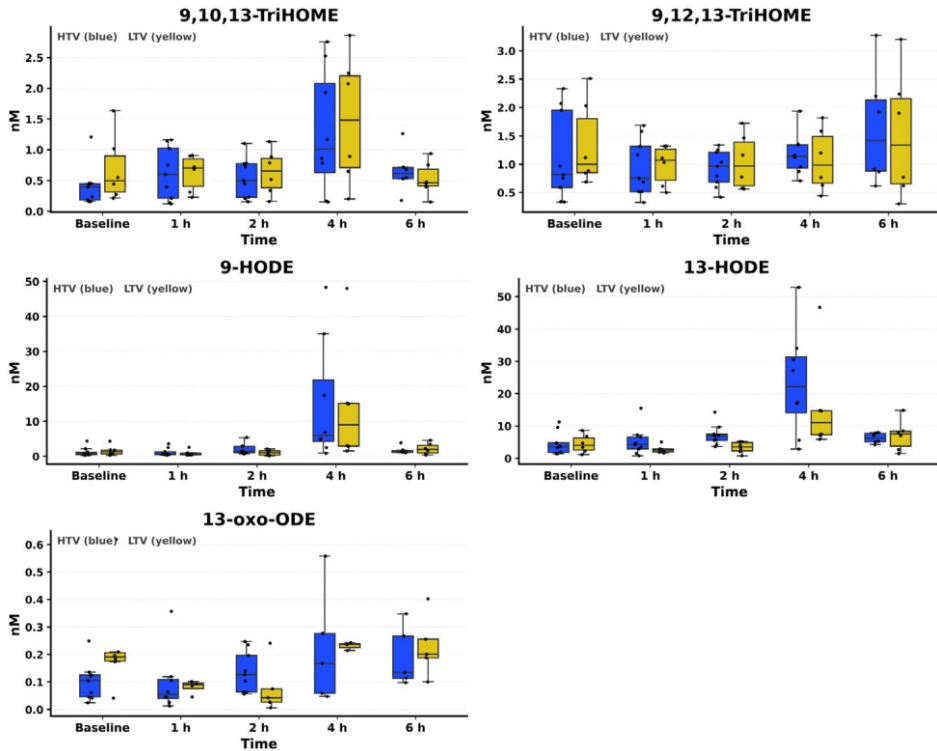


Figure 12. Lipoxigenase-derived linoleic acid metabolites in plasma. Observations from the group with high tidal volume ventilation (HTV) is shown in blue and low tidal ventilation (LTV) in yellow.

One LOX-produced DGLA metabolite was detected in more than 80% of samples in plasma (Figure 13), but not in BALF. No investigated LOX metabolite of DHA or EPA origin was detected in at least 80% of samples.

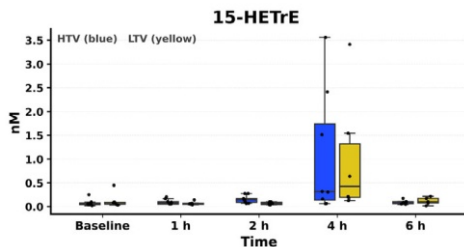


Figure 13. Lipoxigenase-derived dihome- γ -linolenic acid metabolite in plasma. Observations from the group with high tidal volume ventilation (HTV) is shown in blue and low tidal ventilation (LTV) in yellow.

In total, 11 BALF oxylipin were included in mixed model analysis of group-time interactions. Of these, $\text{PGF}_{2\alpha}$ was lower in the HTV group at baseline. 10% FDR was calculated to be <0.0514 for BALF comparisons. Nine metabolites ($\text{PGF}_{2\alpha}$, PGD_2 , PGE_2 , 11-HETE, 15-HETE, 11,12-DiHETrE, 12,13-DiHOME, 9-HODE and 13-HODE) exhibited significant interactions between time and group and all of these showed elevated levels in the HTV group.

From the plasma samples, a total of 21 metabolites met the criteria for formal analysis after transformation. There were no differences in baseline levels of any of these plasma metabolites. For the plasma metabolites, 10% FDR gave a significance level of $p < 0.012$. 4 metabolites had significant interactions between time and group: TXB_2 , PGE_2 , 11-HETE and 15-HETE.

Simple group comparisons of untransformed observations of all metabolites are shown in a heatmap in Figure 14. 19 of the investigated oxylipins were detected in more than 80% of observations in both BALF and plasma. Spearman correlations of these metabolites are presented in Table 2.

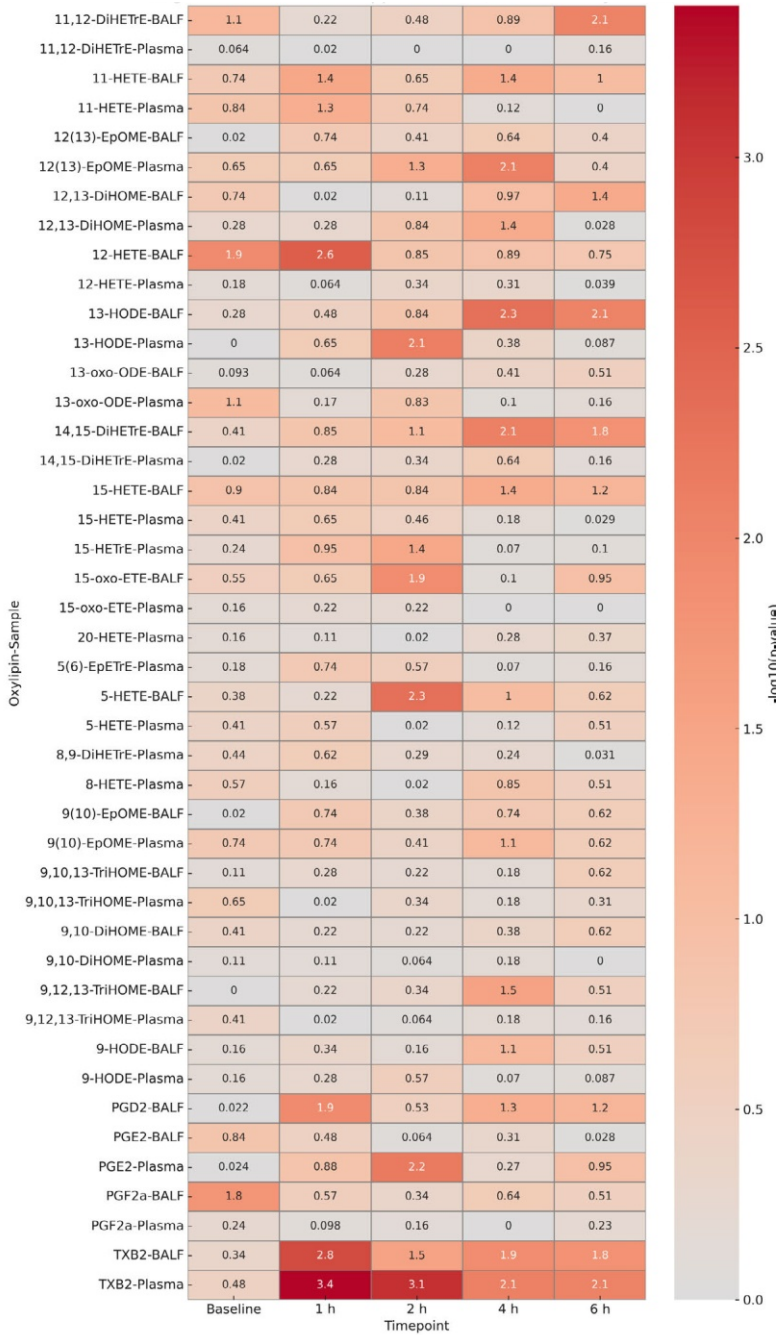


Figure 14. Heatmap of significance testing. Significance levels of group are presented with log values for all variables with detection frequency > 80%. Comparisons were made with Mann Whitney U tests.

Table 2. Correlations between compartments. Correlations between observations in bronchoalveolar lavage fluid and plasma were calculated using Spearman's ρ .

Oxylipin	Spearman ρ	p-value	n
TXB ₂	0.77	<0.0001	70
9(10)-EpOME	0.60	<0.0001	70
12(13)-EpOME	0.58	<0.0001	71
PGF _{2α}	0.52	<0.0001	68
9,12,13-TriHOME	0.51	<0.0001	71
9,10,13-TriHOME	0.44	0.0001	71
11-HETE	0.41	0.0003	71
12,13-DiHOME	0.41	0.0004	71
9-HODE	0.36	0.002	71
15-HETE	0.34	0.003	71
13-HODE	0.34	0.004	71
14,15-DiHETrE	0.32	0.006	70
11,12-DiHETrE	0.28	0.02	65
13-oxo-ODE	0.19	0.16	56
5-HETE	0.17	0.16	69
15-oxo-ETE	0.11	0.44	57
PGE ₂	0.08	0.54	60
12-HETE	0.02	0.86	66
9,10-DiHOME	-0.02	0.85	71

Oxylipins in exhaled breath condensate

The method for EBC collection was developed during the course of experiments, and EBC was thus only collected from the last 9 subjects. 4 of these subjects were in the HTV group and 5 subjects were in the LTV group. 2 EBC samples were lost during the extraction process and were subsequently excluded. 24 oxylipins met the 50% detection frequency limit (Figure 15).

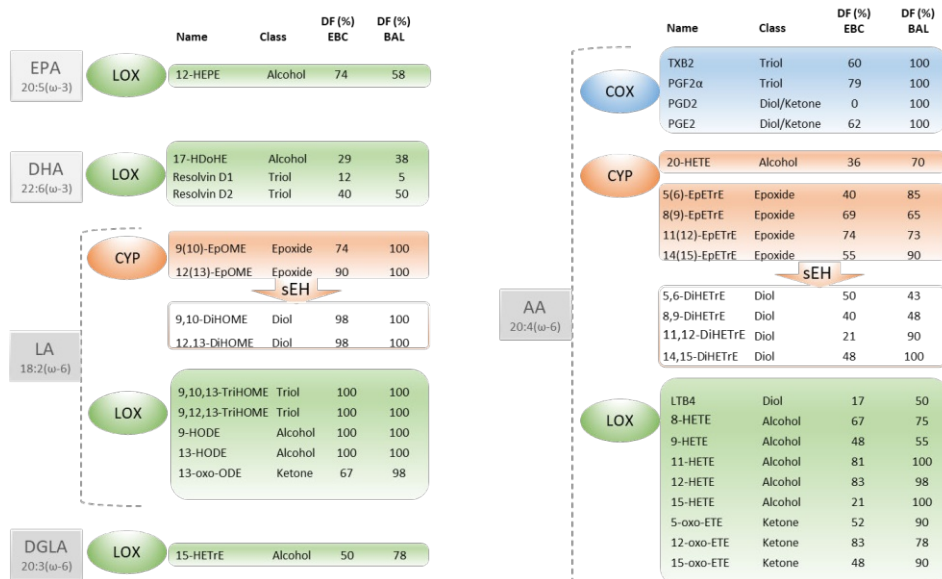


Figure 15. Overview of investigated oxylipins in samples with EBC measurements. Fatty acid precursors are shown in grey boxes: ω -3 eicosapentaenoic acid (EPA) and docosahexaenoic acid (DHA), as well as ω -6 linoleic acid (LA), dihomo- γ -linolenic acid (DGLA), and arachidonic acid (AA). Detection frequency (DF) is shown for exhaled breath condensate (EBC) and bronchoalveolar lavage fluid (BALF) in the same samples for comparison. Of these 37 substances, 24 had DF of at least 50% in EBC. LOX – lipoxygenase, CYP – cytochrome P450, sEH – soluble epoxide hydrolase, COX – cyclooxygenase.

No formal group comparisons were made on EBC observations due to the limited number of individual subjects in each group. Correlation analysis of correlation between observations in BALF and EBC were performed metabolites with detection frequency of at least 50% in EBC (Table 3). Individual EBC observations of the 6 metabolites with significant positive BALF-EBC correlation are plotted in Figure 16. No correction for multiple comparisons was performed regarding these correlations.

Table 3. Correlations between airway samples. Correlations between observations in bronchoalveolar lavage fluid and exhaled breath condensate were calculated using Spearman's ρ .

Oxylipin	Spearman ρ	p-value	n
9,10,13-TriHOME	0.715	<0.0001	42
9,12,13-TriHOME	0.516	0.0005	42
12-oxo-ETE	0.479	0.012	27
8(9)-EpETrE	0.432	0.094	16
11(12)- EpETrE	0.411	0.033	27
12(13)-EpOME	0.399	0.013	38
12,13-DiHOME	0.357	0.022	41
PGF _{2α}	0.2	0.27	33
5-oxo-ETE	0.132	0.67	13
PGE2	0.13	0.53	26
TXB2	0.12	0.57	25
11-HETE	0.102	0.57	34
9(10)-EpOME	0.102	0.59	31
13-HODE	0.055	0.73	42
9-HODE	0.04	0.81	42
12-HETE	0.006	0.97	33
8-HETE	-0.007	0.98	19
13-oxo-ODE	-0.024	0.91	25
15-HETrE	-0.093	0.72	17
12-HEPE	-0.209	0.41	18
14(15)- EpETrE	-0.22	0.35	20
5-HETE	-0.395	0.034	29
9,10-DiHOME	-0.429	0.005	41

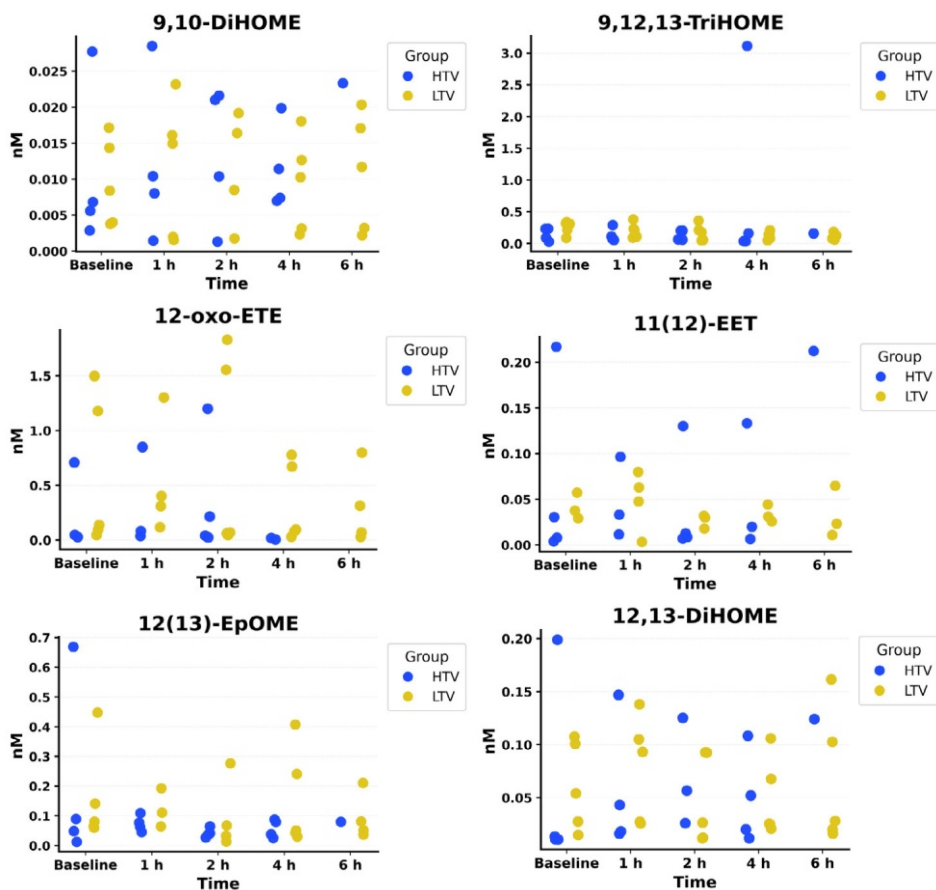


Figure 16. Oxylipins in exhaled breath condensate, EBC. Individual observations of the six metabolites with significant positive Spearman correlation between EBC and bronchoalveolar lavage fluid. Observations from the group with high tidal volume ventilation (HTV) are shown in blue and low tidal ventilation (LTV) in yellow.

Paper II

As the paper utilized the same research subjects as in Paper I, all characteristics of study groups are identical with the results presented under Paper I.

BALF EVs

In BALF, SYTO 13 increased significantly over time in the HTV group ($p=0.004$) and compared to the LTV group ($p=0.02$) (Figure 17). SYTO 13 + HMGB1 also increased in the HTV group ($p=0.001$) and compared to the LTV group ($p=0.002$) (Figure 18). The remaining subpopulations of EVs are presented in Figure 19.

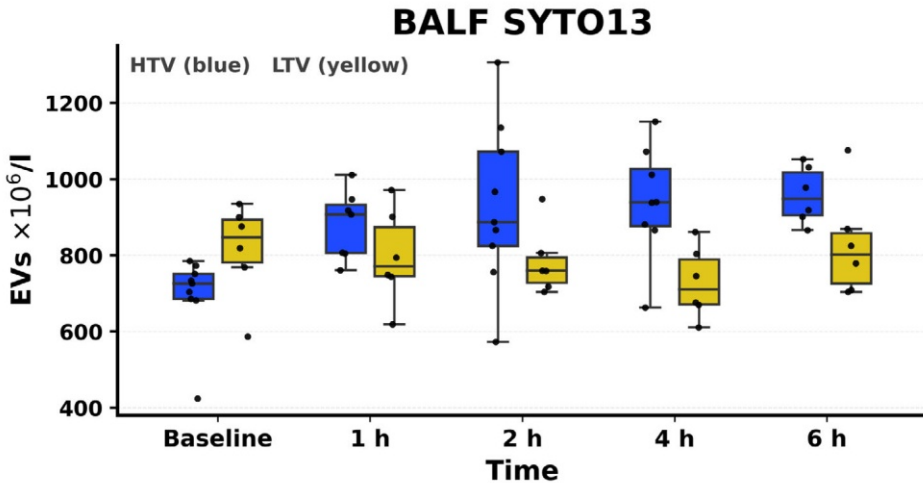


Figure 17. SYTO 13 positive EVs in BALF. Observations from the group with high tidal volume ventilation (HTV) is shown in blue and low tidal ventilation (LTV) in yellow. HTV EVs increased over time ($p=0.004$) and compared to the LTV group ($p=0.02$).

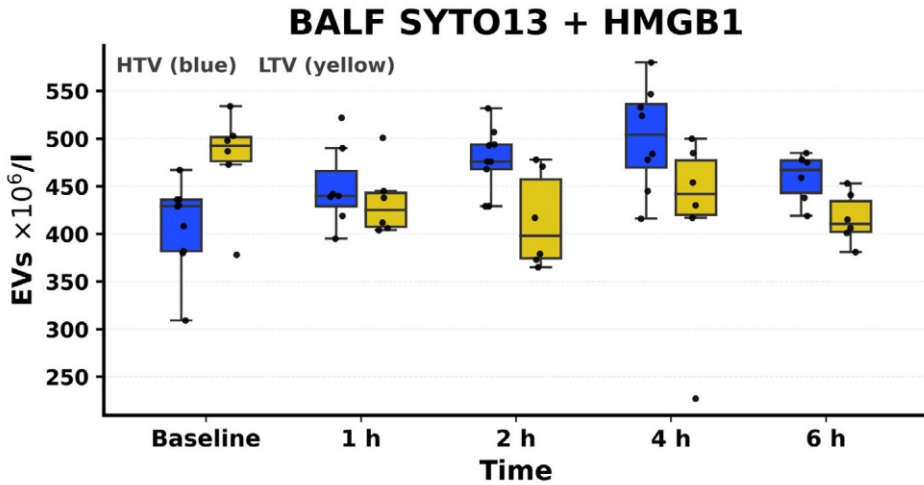


Figure 18. SYTO 13 positive EVs also expressing HMGB1 in BALF.
 Observations from the group with high tidal volume ventilation (HTV) is shown in blue and low tidal ventilation (LTV) in yellow. HTV EVs increased over time ($p=0.002$) and compared to the LTV group ($p=0.002$).

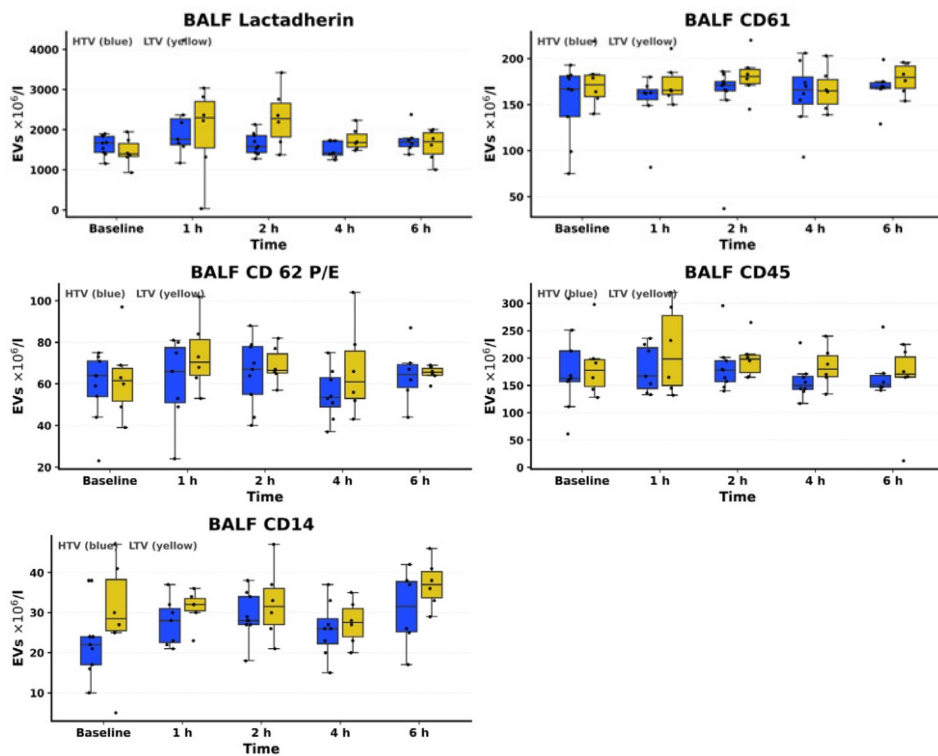


Figure 19. BALF EVs.

	Group	p^1	p^2
Lactadherin	LTV	0.23	
	HTV	0.13	0.23
Lactadherin + CD61	LTV	0.84	
	HTV	0.93	0.92
Lactadherin + CD62 P/E	LTV	0.80	
	HTV	0.72	0.85
Lactadherin + CD45	LTV	0.61	
	HTV	0.86	0.87
Lactadherin + CD14	LTV	0.39	
	HTV	0.35	0.94

Observations from the group with high tidal volume ventilation (HTV) is shown in blue and low tidal ventilation (LTV) in yellow. P^1 indicates result of a one-way ANOVA for each group and variable over time. P^2 indicates 2-way ANOVA result for treatment group and all time points.

Plasma EVs

SYTO 13 positive EVs are displayed in Figure 20 and Lactadherin positive EVs in Figure 21. None of the EVs in plasma significantly correlated to their corresponding observation in BALF (Table 4).

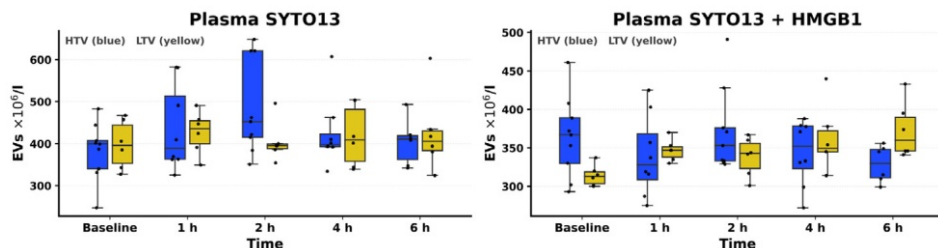


Figure 20. Plasma EVs containing SYTO 13.

	Group	p^1	p^2
SYTO 13	LTV	0.92	
	HTV	0.17	0.46
SYTO 13 + HMGB1	LTV	0.02	
	HTV	0.40	0.03

Observations from the group with high tidal volume ventilation (HTV) is shown in blue and low tidal ventilation (LTV) in yellow. P^1 indicates result of a one-way ANOVA for each group and variable over time. P^2 indicates 2-way ANOVA result for treatment group and all time points.

Table 4. Correlations of EVs in different compartments. Correlations between observations in bronchoalveolar lavage fluid and plasma were calculated using Spearman's ρ .

EV population	Spearman ρ	p-value	n
Lactadherin + CD14	0,099	0,42	69
Lactadherin + CD62 P/E	-0,080	0,51	69
SYTO 13	0,068	0,58	69
Lactadherin + CD45	0,057	0,64	69
Lactadherin +CD61	0,051	0,68	69
Lactadherin	0,033	0,79	69
SYTO 13 + HMGB1	0,027	0,82	69

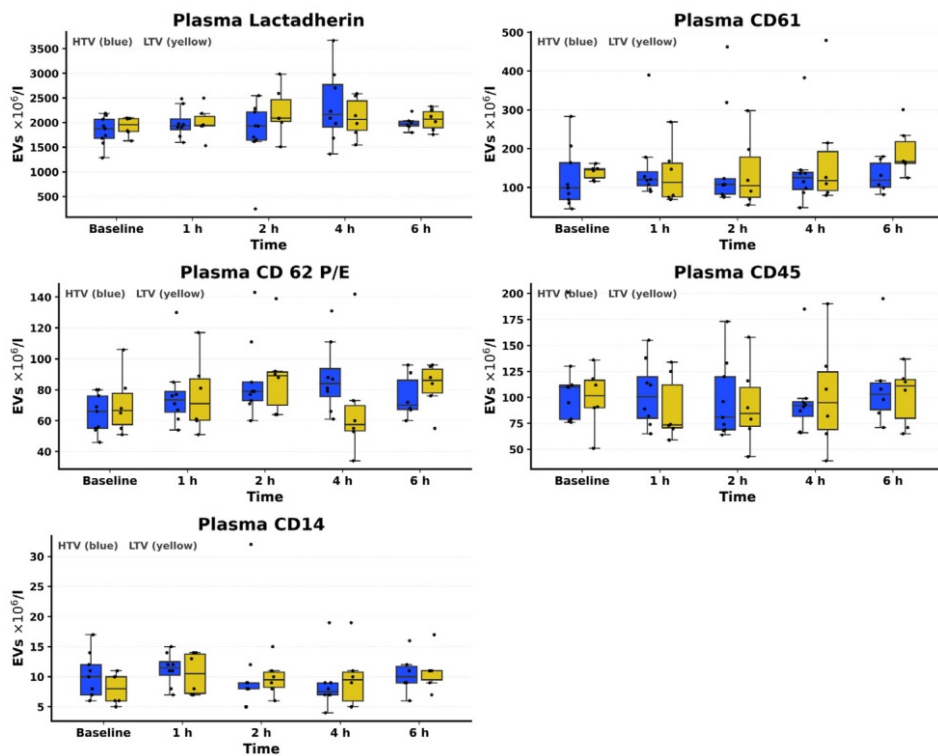


Figure 21. Plasma EVs positive for lactadherin.

	Group	p^1	p^2
Lactadherin	LTV	0.23	
	HTV	0.13	0.23
Lactadherin + CD61	LTV	0.84	
	HTV	0.93	0.92
Lactadherin + CD62 P/E	LTV	0.80	
	HTV	0.72	0.85
Lactadherin + CD45	LTV	0.61	
	HTV	0.86	0.87
Lactadherin + CD14	LTV	0.39	
	HTV	0.35	0.94

Observations from the group with high tidal volume ventilation (HTV) is shown in blue and low tidal ventilation (LTV) in yellow. P^1 indicates result of a one-way ANOVA for each group and variable over time. P^2 indicates 2-way ANOVA result for treatment group and all time points.

Paper III

Of 589 consecutive patients admitted to intensive care in Östersund Hospital, Sweden between 1 February 2012 and 31 January 2013, samples were collected in 278 cases. Of these cases, 147 were eligible for inclusion in the oxylipin study. A total of 22 men and 3 women with mixed diagnoses were intubated and had identifiable intact samples in the study biobank. Another 26 subjects, matched for age and sex but never intubated during the study, were selected from the cohort as controls (Figure 22).

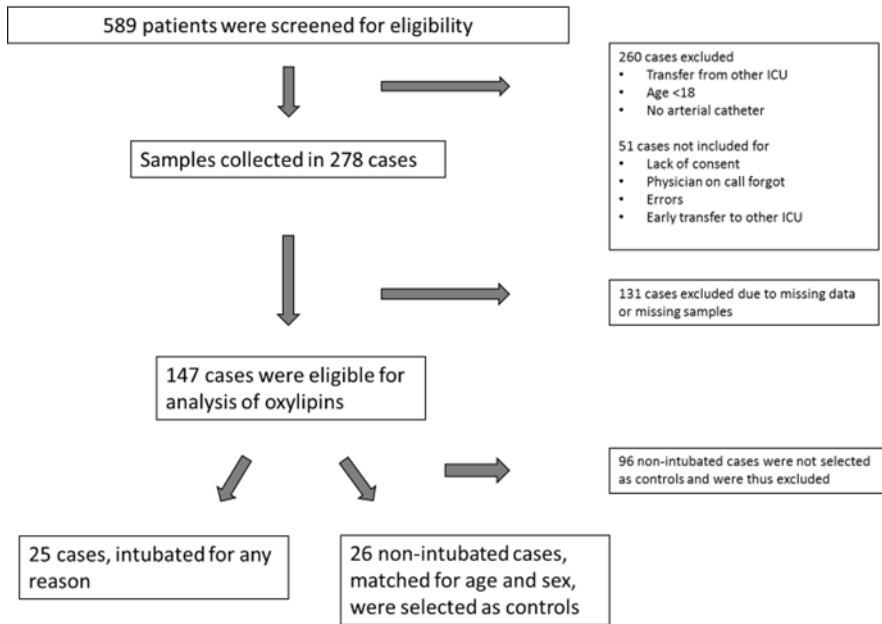


Figure 22. Included and excluded cases. ICU – intensive care unit.

Intubated cases had higher Simplified acute physiology score (SAPS) 3 on admission, higher ICU and 30-day mortality, longer ICU stay and higher maximal sequential organ failure assessment (SOFA) score compared to those that never were intubated. Notably, there were more men than women in the intubated group, which continued with the matched non-intubated group. Characteristics of the study groups are outlined in Table 5.

Table 5. Characteristics of study groups, matched for age and sex.

Categorical variable proportions were compared with Fisher's exact test. Continuous variables were compared with Mann-Whitney U test. SAPS – simplified acute physiology score. ICU – intensive care unit. SOFA – sequential organ failure assessment. LOS – length of stay. CRP – C-reactive protein. GI – gastrointestinal.

Variable	Intubated	Not intubated	p
N	25	26	
Sex (male/female)	22/3	23/3	
Age	75 (67-78)	74 (66-79)	0.94
SAPS 3 score	74 (66-81)	57 (44-64)	<0.001
ICU mortality	10 (40%)	1 (4%)	0.002
30-day mortality	14 (56%)	4 (15%)	0.003
Max SOFA score	11 (9-13)	6 (4-7)	<0.001
ICU LOS	9 (7-13)	2 (1-3)	<0.001
CRP	55 (10-162)	50 (2-123)	0.56
Main diagnosis			
Sepsis	8 (32%)	9 (35%)	0.75
Trauma	2 (8%)	3 (12%)	0.45
Cardiac arrest	6 (24%)	0 (0%)	0.004
Intoxication	0 (0%)	1 (4%)	N/A
GI bleeding	1 (4%)	0 (0%)	N/A
Other surgical	3 (12%)	4 (15%)	0.67
Other medical	5 (20%)	9 (35%)	0.06

Oxylipins during the first day of mechanical ventilation

In this study, the oxylipin panel included analysis of 67 different metabolites, 57 of which were detected in the study subjects. 23 oxylipins met the preset limit of 80% of observations above limit of quantification, LOQ, in samples collected from intubated patients and were included in formal analysis in Paper III. One metabolite, 12(13)-EpOME, was detected above LOQ in 84% of the observations but was accidentally omitted from analysis in the paper. Another 7 metabolites had at least 80% of observations above limit of detection, LOD, but with uncertain values for observations below LOQ.

After up to 24 h of mechanical ventilation, no oxylipin increased compared to baseline values at intubation. 10% FDR was calculated at

$\alpha=0.001$. 12-HETE was significantly lower on the first day after intubation than before, going from median 1.3 to median 0.61 ($p<0.001$) and thus meeting the criteria for statistical significance (Table 6). All other metabolites with 80% of observations above LOQ were numerically lower on the day after intubation than at the time of intubation, although none other than 12-HETE were significantly lower (Table 6).

Another 7 metabolites were quantified above LOD in at least 80% of observations, although several of the observations were below LOQ, rendering at least 20% of observations below LOQ or undetectable (Table 7).

Oxylipins in sepsis

Sepsis was the most common main diagnosis in both intubated and non-intubated cases (Table 5). When compared to non-septic patients, the group with sepsis did not differ in age, SAPS 3, SOFA score, mortality or LOS. CRP was higher in the septic group (Table 8).

When samples from both intubated and non-intubated cases were analysed, 59 different oxylipins could be detected (Figure 23). Of these, 32 were above LOD in at least 80% of observations and included in group analysis (Tables 9 – 14). Log transformed values were compared with independent samples T-test between groups on admission and with paired T-test between first and second samples. FDR 10% was calculated to yield a significant difference when $p\leq 0.04$. On admission, no oxylipin was higher in the sepsis group than in the non-septic group. 13 different oxylipins were lower in the septic group; 15,16-DiHODE and 9-HOTrE from ALA, 9(10)-EpOME and 13-HODE from LA, 19,20-DiHDPE from DHA, 17,18-DiHETE and 12-HEPE from EPA, 15-HETrE from DGLA and 11,12-DiHETrE, 14,15-DiHETrE, 5-HETE, 12-HETE and 15-HETE from AA. 25 metabolites in the control group and 6 in the sepsis group were lower on the second sample after admission compared to the first. No oxylipin increased between the first and second samples (Tables 9 – 14). Although CRP on admission was higher in the septic group than the non-septic group, none of the investigated oxylipins lower in the septic group had a significant negative correlation to CRP.

Table 6. Oxylipins at intubation and the day after. Oxylipins with Hedges' *g* were successfully log transformed and analyzed with paired Student's *t* test. Oxylipins without reported Hedges' *g* were analyzed with Wilcoxon signed-rank test. After 10% FDR, statistical significance was considered at $p < 0.001$.

Oxylipin	Time 1 median nM (IQR)	Time 2 median nM (IQR)	Hedges' <i>g</i> (95% CI)	<i>p</i>
9,10-DiHOME	0.97 (0.42-1.7)	0.88 (0.39-1.44)	0.12 (-0.16-0.4)	0.39
12,13-DiHOME	1.51 (0.86-2.52)	1.1 (0.61-1.67)	0.32 (-0.02-0.65)	0.06
9,10-DiHODE	0.1 (0.04-0.16)	0.08 (0.02-0.18)	0.19 (-0.16-0.53)	0.27
12,13-DiHODE	0.06 (0.04-0.16)	0.03 (0.02-0.08)	N/A	0.02
15,16-DiHODE	11.39 (6.74-19.93)	9.56 (5.58-13.24)	0.26 (-0.03-0.55)	0.06
11,12-DiHETrE	0.29 (0.2-0.38)	0.22 (0.16-0.35)	0.2 (-0.02-0.42)	0.07
14,15-DiHETrE	0.3 (0.19-0.37)	0.21 (0.17-0.31)	0.27 (-0.01-0.55)	0.05
17,18-DiHETE	0.25 (0.2-0.4)	0.24 (0.18-0.32)	0.2 (-0.04-0.44)	0.08
13,14-DiHDPE	0.08 (0.06-0.1)	0.06 (0.04-0.08)	0.36 (0.05-0.67)	0.02
16,17-DiHDPE	0.08 (0.06-0.12)	0.07 (0.06-0.09)	0.26 (-0.02-0.55)	0.06
19,20-DiHDPE	0.68 (0.44-1.14)	0.53 (0.47-0.95)	0.18 (-0.09-0.46)	0.17
9-HODE	2.80 (2.20-4.74)	2.40 (1.71-3.50)	0.3 (-0.08-0.67)	0.11
13-HODE	8.84 (6.98-13.02)	8.16 (5.71-10.52)	0.27 (-0.07-0.61)	0.11
13-HOTrE	0.62 (0.19-1.06)	0.45 (0.16-0.66)	N/A	0.14
5-HETE	0.21 (0.18-0.35)	0.19 (0.12-0.31)	0.34 (-0.05-0.73)	0.08
11-HETE	0.13 (0.1-0.15)	0.11 (0.07-0.14)	0.5 (0.06-0.95)	0.02
12-HETE	1.33 (0.96-1.7)	0.61 (0.45-1.08)	0.98 (0.43-1.52)	<0.001
15-HETE	0.34 (0.2-0.49)	0.29 (0.15-0.42)	0.24 (-0.02-0.51)	0.06
15-HETrE	0.15 (0.11-0.19)	0.13 (0.1-0.19)	0.08 (-0.26-0.42)	0.63
EKODE	1.38 (0.98-2.19)	1.11 (0.77-2.1)	0.26 (0.02-0.49)	0.03
12(13)-EpODE	0.1 (0.06-0.15)	0.08 (0.03-0.12)	N/A	0.07
15(16)-EpODE	1.30 (0.7-1.58)	0.88 (0.57-1.48)	0.32 (-0.08-0.72)	0.10
19(20)-EpDPE	0.08 (0.04-0.16)	0.06 (0.03-0.08)	N/A	0.11
12(13)-EpOME	0.60 (0.45-1.00)	0.38 (0.26-0.87)	0.34 (-0.05-0.73)	0.09

Table 7. Oxylipins at intubation and the day after with more than 20% of observations between limit of detection and limit of quantification. Samples were collected at intubation (Timepoint 1) and 06.00 the following morning (Timepoint 2) in 25 cases at both timepoints. Oxylipins without reported Hedges' g were analyzed with Wilcoxon signed-rank test. Oxylipins with reported Hedges' g had a normal distribution after log transformation and were analyzed with paired Student's t test. No correction for multiple tests was performed due to the exploratory nature of the investigation.

Oxylipin	Timepoint 1 median nM (IQR)	Timepoint 2 median nM (IQR)	Hedges' g (95% CI)	p
11,12-DiHETE	0.36 (0.25–0.66)	0.37 (0.27–0.60)	-0.07 (-0.56–0.43)	0.79
14,15-DiHETE	0.09 (0.05–0.12)	0.07 (0.04–0.12)	-0.03 (-0.41–0.36)	0.90
9-HOTrE	0.48 (0.22–0.88)	0.39 (0.13–0.79)	0.30 (-0.18–0.78)	0.22
20-HETE	0.12 (0.11–0.15)	0.09 (0.07–0.12)	0.43 (0.03–0.82)	0.04
5-HEPE	0.09 (0.05–0.13)	0.10 (0.06–0.12)	N/A	0.07
12-HEPE	0.13 (0.08–0.17)	0.03 (0.01–0.05)	N/A	<0.001
9(10)-EpOME	0.57 (0.48–1.61)	0.61 (0.37–1.41)	N/A	0.08

Table 8. Characteristics of septic and non-septic cases. SAPS – simplified acute physiology score. ICU – intensive care unit. SOFA – sequential organ failure assessment. LOS – length of stay. CRP – C-reactive protein. Categorical variables were compared with Fisher's exact test. Continuous variables were compared with Mann-Whitney U test.

Variable	Sepsis (n=17)	Not sepsis (n=34)	p
Sex (male/female)	15/2	30/4	1.0
Age	75 (67-80)	72 (67-78)	0.47
SAPS 3 score	66 (61-70)	63 (47-77)	0.23
ICU mortality	3 (18%)	8 (24%)	0.73
30-day mortality	5 (29%)	13 (38%)	0.76
Max SOFA score	9 (7-12)	7 (5-11)	0.21
ICU LOS	5 (2-8)	3 (2-4)	0.33
CRP	127 (56-177)	25 (1-73)	0.002

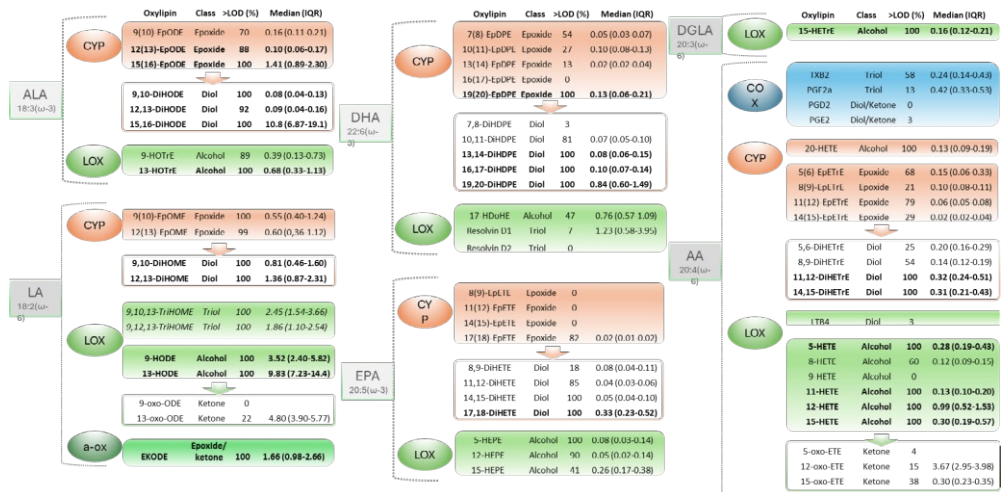


Figure 23. Grouped values of all observations during first and second sample of oxylipins in all cases. Bold numbers show metabolites included in analysis. Italics are used for uncertain observations not included in analysis due to analytical problems.

Table 9. Alpha-linoleic acid metabolites. Data presented as median (IQR). p^\dagger is derived from group comparison of 1st and 2nd samples using a paired Student's T-test on log transformed data. p^\bullet is derived from comparison of first samples among sepsis patients vs non-septic patients using an independent samples T-test. After 10% FDR, statistical significance was considered at $p < 0.04$.

Oxylipin	Group	1 st Sample	2nd Sample	p^\dagger	p^\bullet
12(13)-EpODE	Sepsis	0.09 (0.08-0.15)	0.09 (0.04-0.12)	0.41	0.3
	Control	0.12 (0.06-0.18)	0.08 (0.04-0.12)	0.009	
15(16)-EpODE	Sepsis	1.43 (1.18-1.96)	1.18 (0.89-1.46)	0.25	0.28
	Control	2.12 (1.31-2.57)	1.01 (0.59-1.56)	0.001	
9,10-DiHODE	Sepsis	0.06 (0.04-0.09)	0.06 (0.04-0.33)	0.44	0.21
	Control	0.10 (0.05-0.13)	0.07 (0.02-0.14)	0.35	
12,13-DiHODE	Sepsis	0.10 (0.04-0.11)	0.08 (0.05-0.12)	0.41	0.53
	Control	0.11 (0.05-0.18)	0.05 (0.02-0.13)	0.01	
15,16-DiHODE	Sepsis	11.65 (6.72-14.51)	7.12 (6.25-12.55)	0.11	0.03
	Control	18.05 (10.38-26.5)	9.68 (6.33-18.99)	0.002	
9-HOTrE	Sepsis	0.25 (0.16-0.49)	0.13 (0.05-0.18)	0.03	0.009
	Control	0.53 (0.31-0.84)	0.57 (0.12-1.14)	0.08	
13-HOTrE	Sepsis	0.82 (0.59-1.04)	0.73 (0.35-1.06)	0.69	0.63
	Control	0.82 (0.40-1.35)	0.47 (0.24-0.85)	0.01	

Table 10. Linoleic acid metabolites. Data presented as median (IQR). p^\dagger is derived from group comparison of 1st and 2nd samples using a paired Student's T-test on log transformed data. p^\bullet is derived from comparison of first samples among sepsis patients vs non-septic patients using an independent samples T-test. After 10% FDR, statistical significance was considered at $p < 0.04$.

Oxylipin	Group	1st Sample	2nd Sample	p^\dagger	p^\bullet
9(10)-EpOME	Sepsis	0.48 (0.43-0.73)	0.44 (0.37-0.57)	0.84	0.01
	Control	0.71 (0.54-1.51)	1.28 (0.44-2.06)	0.15	
12(13)-EpOME	Sepsis	0.56 (0.37-0.8)	0.44 (0.34-0.68)	0.87	0.15
	Control	0.76 (0.46-1.12)	0.57 (0.29-1.47)	0.18	
9,10-DiHOME	Sepsis	0.72 (0.51-1.01)	0.69 (0.35-1.67)	0.33	0.18
	Control	1.17 (0.63-1.62)	0.78 (0.4-1.44)	0.06	
12,13-DiHOME	Sepsis	1.13 (0.92-1.58)	1.02 (0.70-1.52)	0.27	0.08
	Control	1.63 (1.19-2.63)	1.17 (0.59-2.26)	0.02	
9-HODE	Sepsis	3.81 (3.01-5.47)	2.8 (2.31-3.33)	0.01	0.11
	Control	5.58 (3.07-7.80)	3.34 (2.29-5.06)	0.006	
13-HODE	Sepsis	8.25 (6.42-13.81)	6.98 (5.59-9.77)	0.09	0.02
	Control	13.66 (8.84-17.05)	8.87 (7.55-11.95)	0.009	
EKODE	Sepsis	2.03 (1.34-3.65)	1.80 (1.32-2.50)	0.19	0.74
	Control	1.93 (1.37-3.65)	1.02 (0.79-2.13)	<0.001	

Table 11. Docosahexaenoic acid metabolites. Data presented as median (IQR). p^\dagger is derived from group comparison of 1st and 2nd samples using a paired Student's T-test on log transformed data. p^\bullet is derived from comparison of first samples among sepsis patients vs non-septic patients using an independent samples T-test. After 10% FDR, statistical significance was considered at $p < 0.04$.

Oxylipin	Group	1st Sample	2nd Sample	p^\dagger	p^\bullet
19(20)-EpDPE	Sepsis	0.12 (0.05-0.14)	0.15 (0.09-0.19)	0.49	0.23
	Control	0.16 (0.08-0.27)	0.08 (0.04-0.20)	0.001	
13,14-DiHDPE	Sepsis	0.08 (0.07-0.13)	0.07 (0.05-0.11)	0.25	0.07
	Control	0.12 (0.08-0.18)	0.08 (0.06-0.11)	0.002	
16,17-DiHDPE	Sepsis	0.11 (0.08-0.14)	0.08 (0.06-0.09)	0.004	0.16
	Control	0.13 (0.09-0.18)	0.09 (0.07-0.13)	0.001	
19,20-DiHDPE	Sepsis	0.81 (0.65-1.02)	0.62 (0.45-0.71)	0.04	0.04
	Control	1.41 (0.70-1.74)	0.90 (0.57-1.23)	<0.001	

Table 12. Eicosapentaenoic acid metabolites. Data presented as median (IQR). p^\dagger is derived from group comparison of 1st and 2nd samples using a paired Student's T-test on log transformed data. p^\bullet is derived from comparison of first samples among sepsis patients vs non-septic patients using an independent samples T-test. After 10% FDR, statistical significance was considered at $p < 0.04$.

Oxylipin	Group	1st Sample	2nd Sample	p^\dagger	p^\bullet
17(18)-EpETE	Sepsis	0.01 (0.01-0.02)	0.01 (0.01-0.01)	0.11	0.09
	Control	0.02 (0.01-0.03)	0.01 (0.01-0.02)	0.008	
11,12-DiHETE	Sepsis	0.04 (0.03-0.05)	0.04 (0.03-0.05)	0.32	0.09
	Control	0.05 (0.04-0.07)	0.04 (0.03-0.06)	0.05	
14,15-DiHETE	Sepsis	0.06 (0.04-0.09)	0.04 (0.04-0.07)	0.1	0.08
	Control	0.08 (0.05-0.15)	0.07 (0.04-0.13)	0.06	
17,18-DiHETE	Sepsis	0.31 (0.22-0.39)	0.23 (0.17-0.33)	0.007	0.01
	Control	0.48 (0.34-0.63)	0.32 (0.22-0.42)	0.001	
5-HEPE	Sepsis	0.10 (0.06-0.15)	0.09 (0.06-0.15)	0.36	0.52
	Control	0.13 (0.06-0.20)	0.11 (0.05-0.14)	0.007	
12-HEPE	Sepsis	0.04 (0.03-0.14)	0.05 (0.01-0.15)	0.88	0.02
	Control	0.11 (0.05-0.18)	0.04 (0.01-0.12)	<0.001	

Table 13. Dihomo- γ -linolenic acid metabolites. Data presented as median (IQR). p^\dagger is derived from group comparison of 1st and 2nd samples using a paired Student's T-test on log transformed data. p^\bullet is derived from comparison of first samples among sepsis patients vs non-septic patients using an independent samples T-test. After 10% FDR, statistical significance was considered at $p < 0.04$.

Oxylipin	Group	1st Sample	2nd Sample	p^\dagger	p^\bullet
15-HETrE	Sepsis	0.15 (0.11-0.17)	0.13 (0.12-0.14)	0.33	0.03
	Control	0.19 (0.16-0.27)	0.16 (0.12-0.21)	0.007	

Table 14. Arachidonic acid metabolites. Data presented as median (IQR). p^\dagger is derived from group comparison of 1st and 2nd samples using a paired Student's T-test on log transformed data. p^\bullet is derived from comparison of first samples among sepsis patients vs non-septic patients using an independent samples T-test. After 10% FDR, statistical significance was considered at $p < 0.04$.

Oxylipin	Group	1st Sample	2nd Sample	p^\dagger	p^\bullet
20-HETE	Sepsis	0.13 (0.09-0.20)	0.12 (0.06-0.14)	0.61	0.19
	Control	0.17 (0.11-0.24)	0.12 (0.09-0.20)	<0.001	
11,12-DiHETrE	Sepsis	0.29 (0.2-0.43)	0.26 (0.20-0.34)	0.08	0.02
	Control	0.44 (0.28-0.61)	0.30 (0.24-0.48)	0.002	
14,15-DiHETrE	Sepsis	0.31 (0.19-0.40)	0.23 (0.19-0.27)	0.04	0.00 9
	Control	0.41 (0.30-0.57)	0.31 (0.21-0.41)	0.001	
5-HETE	Sepsis	0.26 (0.19-0.40)	0.24 (0.19-0.30)	0.1	0.03
	Control	0.41 (0.23-0.58)	0.25 (0.18-0.41)	0.01	
11-HETE	Sepsis	0.13 (0.08-0.20)	0.13 (0.11-0.17)	0.72	0.15
	Control	0.14 (0.11-0.20)	0.12 (0.08-0.17)	0.01	
12-HETE	Sepsis	0.83 (0.50-1.14)	0.83 (0.41-1.72)	0.29	0.00 4
	Control	1.31 (0.96-1.70)	0.81 (0.46-1.38)	0.01	
15-HETE	Sepsis	0.21 (0.16-0.31)	0.22 (0.19-0.28)	0.07	0.01
	Control	0.42 (0.24-0.62)	0.36 (0.19-0.65)	0.012	

Paper IV

A central vein was successfully cannulated in all four animals included in the study. The dual lumen central venous catheters were tunneled to an entry point on the back of the animals' necks, and all catheters remained protected by the external sewn-on covering during the 4-week study period. Details of the procedure are reported in Paper IV. No animal showed signs of a catheter infection or thrombosis during the study period.

All catheters remained functional for injections and blood samplings during the four-week study period. Use of a single lumen of one catheter was discontinued during the last study week as that lumen had been accidentally rendered unsterile.

Catheter insertion times

In pigs weighing 24-30 kg, full catheter insertion took more than one hour in the two animals where the primary venipuncture was done with a standard 18 Ga needle. The most time-consuming step was placement of the guidewire. In another two animals where a 21 Ga needle was used for venipuncture, the guidewire was placed in under 15 minutes and the whole procedure completed in less than 30 minutes.

In pigs weighing 50 kg, time to placement of a 0.97 mm guide wire in an external jugular vein was on average 128 s (range 38 – 275 s, n=7) when venipuncture was performed with a 21 Ga microintroducer set and 69 s (range 38 – 98 s, n=7) when an 18 Ga needle was used. This difference was not statistically significant ($p=0.128$). In pigs weighing 25-32 kg, a 0.97 mm guide wire was successfully placed in the external jugular vein in all animals using the 21 Ga micropuncture needle (n=6). The procedure took on average 6.5 min (range 3 to 15 min).

Paper V

From 23 screened sEH inhibitors, AEPU was chosen for further studies based on its low melting point, high water solubility, and low pig IC_{50} . Because of very low liver microsomal stability, a short half-life and a need for continuous infusion during treatment were predicted.

A 0.1 mg/kg/h infusion of AEPU in a single animal resulted in a rise of plasma AEPU concentration for the first 120 minutes. In steady state, this infusion resulted in a plasma concentration of approximately 200 nM, with only minor alterations over time. After discontinuation of the infusion, AEPU concentrations decreased quickly in plasma and the substance was completely eliminated within 15 minutes.

A total of 20 animals were randomized to participate in the lung injury experiment, 10 animals in each group. One animal in the control group died from pneumothorax before start of placebo infusion, leaving a total of 19 animals in the final analysis. There were no statistically significant differences between the two groups in any of the recorded variables at baseline (Table 15).

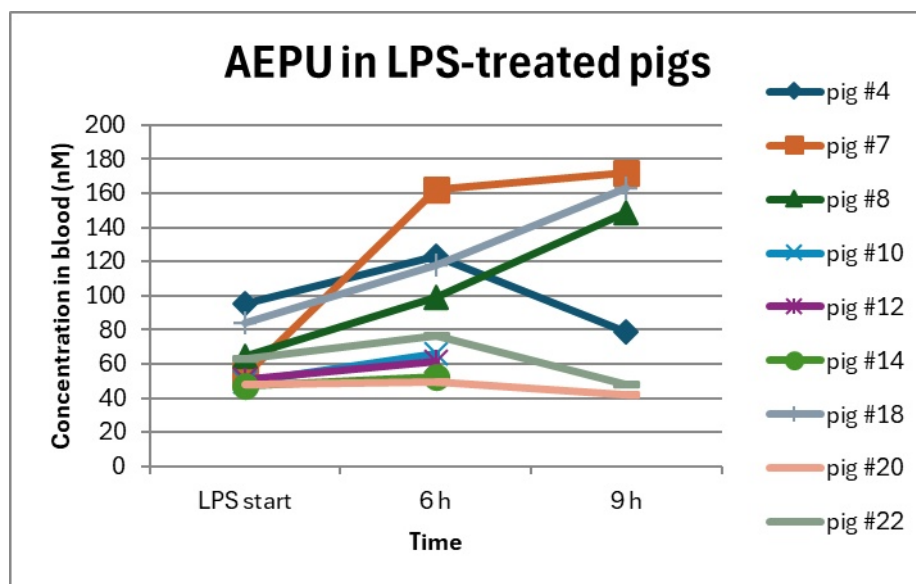


Figure 24. AEPU concentrations in blood. Measurements of blood AEPU concentrations in individual animals receiving active treatment.

During the experiments, all animals in the AEPU-treated group had stable or increasing blood concentrations of the study drug. The lowest concentration observed was 47 nM, with the majority of observations considerably higher (Figure 24). AEPU was not detected in any of the samples from animals in the placebo group (data not shown).

After LPS administration, all animals except one in each group showed signs of severe cardiopulmonary compromise. There were no differences between the groups regarding any parameters relating to lung injury, circulatory effects, or any other measured clinical parameter (Table 16). Among the oxylipins measured in plasma, the ratio of 12(13)-EpOME/12,13- DiHOME was increased after six hours in the AEPU group ($p=0.026$). There were no other significant differences in epoxide/diol ratios between the groups.

Table 15. Study group characteristics at baseline. Data presented as median (IQR). Continuous variables were compared with independent samples *t*-test or Mann Whitney U test, as appropriate. Nominal variables were compared using Fischer's exact test. Abbreviations: AEPU – 1-adamantanyl-3-(5-(2-(ethylethoxy)ethoxy)pentyl)urea, PaCO₂ – partial pressure of carbon dioxide in arterial blood, P/F – ratio of arterial partial pressure of oxygen to fraction of inspired oxygen, MPAP – mean pulmonary artery pressure, MAP – mean arterial pressure, PCWP – pulmonary capillary wedge pressure, SVR – systemic vascular resistance, CVP – central venous pressure, PIP – peak inspiratory pressure, SvO₂ – saturation of oxygen in venous blood.

	AEPU (n=10)	Control (n=9)	p
Weight (kg)	30 (29 - 31)	29 (28–37)	0.60
% Male	70	78	0.63
Hemoglobin (g/L)	91 (90 - 96)	94 (93–95)	0.74
Creatinine (µmol/L)	71 (62–71)	71 (71–80)	0.32
Bilirubin (µmol/L)	5.1 (3.4 - 5.1)	5.1 (5.1 - 5.1)	0.50
Temperature (°C)	38.6 (38.1 - 39.1)	38.9 (38.6 - 39.7)	0.13
pH	7.46 (7.44 - 7.48)	7.44 (7.41 - 7.44)	0.16
PaCO ₂ (kPa)	4.9 (4.7 - 5.1)	4.6 (4.5 - 5.0)	0.80
P/F (kPa)	72 (68 - 73)	69 (65 - 71)	0.16
MPAP (mmHg)	25 (24 - 28)	25 (20 - 26)	0.25
MAP (mmHg)	91 (74 - 108)	83 (81 - 84)	0.66
PCWP (mmHg)	17 (15–18)	15 (14 - 17)	0.24
SVR (dynes*sec/cm ⁵)	1506 (1154 - 1718)	1624 (1045 - 1742)	0.94
PVR (dynes*sec/cm ⁵)	171 (157 - 207)	165 (163 - 267)	1.00
CVP (mmHg)	15 (14 - 17)	16 (15 - 18)	0.73
PIP (cmH ₂ O)	25 (24 - 25)	25 (24 - 26)	0.45
Compliance (ml/cmH ₂ O)	11.2 (10.9 - 11.5)	10.8 (10.4 - 13.3)	0.36
SvO ₂ (%)	71 (66 - 74)	72 (62 - 72)	0.55

Table 16. Study group characteristics at the end of experiments. Data presented as median (IQR). Continuous variables were compared with independent samples t-test or Mann Whitney U test, as appropriate. Nominal variables were compared using Fischer's exact test. Abbreviations: AEPu, 1-adamantanyl-3-(5-(2-(ethylethoxy)ethoxy)pentyl)urea; PaCO₂, partial pressure of carbon dioxide in arterial blood; P/F, ratio of arterial partial pressure of oxygen to fraction of inspired oxygen; MPAP, mean pulmonary artery pressure; MAP, mean arterial pressure; PCWP, pulmonary capillary wedge pressure; SVR, systemic vascular resistance; PVR, pulmonary vascular resistance; CVP, central venous pressure; PIP, peak inspiratory pressure; W/D, wet/dry; SvO₂, saturation of oxygen in venous blood.

	AEPu	Control	P
Premature death (%)	40	33	0.57
Total fluid given (ml)	5785 (5080 - 7210)	5090 (4180 - 6080)	0.44
Urine output (ml)	700 (320 - 1200)	825 (575 - 925)	0.89
Hemoglobin (g/L)	116 (107 - 128)	102 (99 - 118)	0.13
Creatinine (µmol/L)	133 (102 - 152)	133 (115 - 159)	0.48
Bilirubin (µmol/L)	11.1 (8.6 - 18.8)	8.6 (6.8 - 22.2)	0.66
Temperature (°C)	38.5 (38.0 - 40.1)	38.9 (38.9 - 40.1)	0.36
pH	7.16 (7.07 - 7.26)	7.25 (7.14 - 7.29)	0.32
PaCO ₂ (kPa)	5.8 (4.9 - 7.1)	5.8 (4.5 - 6.0)	0.45
P/F (kPa)	22 (11 - 42)	31 (28 - 47)	0.40
MPAP (mmHg)	46 (35 - 50)	42 (35 - 42)	0.46
MAP (mmHg)	66 (55 - 97)	78 (55 - 93)	0.91
PCWP (mmHg)	18 (16 - 21)	18 (16 - 20)	0.91
SVR (dynes*sec/cm ⁵)	1314 (1089 - 2375)	1230 (958 - 1457)	0.48
PVR (dynes*sec/cm ⁵)	643 (390 - 1057)	486 (345 - 827)	0.36
CVP (mmHg)	16 (15 - 17)	20 (16 - 24)	0.37
PIP (cmH ₂ O)	33 (29 - 37)	33 (29 - 37)	0.85
Compliance (ml/cmH ₂ O)	7.9 (7.3 - 9.7)	7.9 (7.0 - 10.7)	0.78
SvO ₂ (%)	55 (25 - 66)	55 (48 - 59)	0.59
W/D ratio	6.9 (6.0 - 9.0)	6.1 (5.3 - 6.5)	0.24
Histology injury score	2.7 (2 - 3)	2.6 (2 - 3)	0.65

Pharmacokinetic parameters of t-TUCB

Breach of protocol

For the last experimental cycle concerning the oral 1 mg/kg dose of t-TUCB, one of the animals had the sampling lumen of the catheter permanently clamped because of contamination and in one animal samples were suspected to be accidentally collected through the injection lumen. Because of this, all the results from the final oral dose were discarded from further analysis due to probable study drug contamination of the samples from the catheter.

Clinical observations

The animals were clinically not apparently affected by the 0.1 mg/ml dose. After the 1 mg/kg iv dose, all animals were heavily sedated for several hours. With the suspicion that sedation was induced by DMSO, t-TUCB concentration was increased four times for the last two doses to reduce the amount of administered DMSO. After the 2 mg /kg dose (with half the DMSO dose per kg), only light sedation occurred and was reversed after approximately one hour. No sedation occurred after the oral dose.

t-TUCB concentrations in blood

The 0.1 mg/kg dose yielded a maximal plasma concentration of an average of 1088 ng/ml three minutes after the injection. However, the pre-injection baseline value showed an average concentration of 374 ng/ml. At sampling 1 h after injection, blood levels had decreased below the initial baseline measurements.

The 1 mg/kg dose was preceded by baseline measurements similar to the measurements before the first dose (average 360 ng/ml). However, in several of the following measurements, blood levels were measured at levels several orders of magnitude larger than others, with no plausible pattern and extremely large spread. The maximum concentration measured was 4,6 million ng/ml 30 minutes after injection (which was 500 times higher than the measured concentration in blood 3 minutes after injection). There were large measured fluctuations over time with individual subjects having peak values as late as after 24 hours.

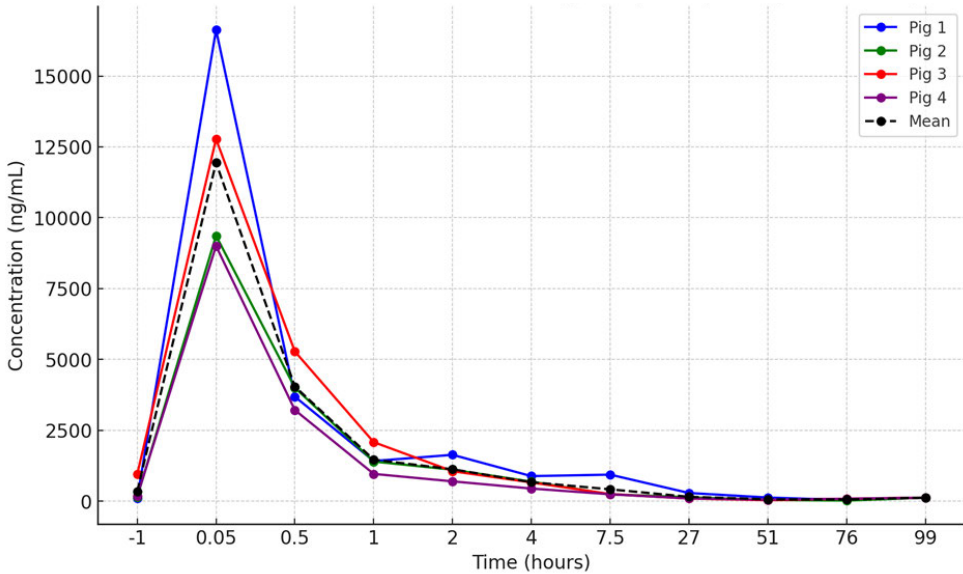


Figure 25. *t*-TUCB concentrations in blood. Individual measurements, and mean concentration, of *t*-TUCB in blood after intravenous injection of 2 mg/kg *t*-TUCB at time 0 hours.

Baseline values before the 2 mg/kg dose were similar to the previous baseline values (average 346 ng/ml). After injection, peak values were detected after 3 minutes (average 11943 ng/ml, range 9003 – 16628 ng/ml). Elimination was almost complete after 27 h (Figure 25).

From time and concentration measurements, AUC, *k*, $t_{1/2}$, CL and VD were all calculated individually and on average (Table 17). The semilogarithmic plot of concentration vs time revealed a terminal elimination phase between 2 and 27 hours (Figure 26).

Table 17. Pharmacokinetic parameters of t-TUCB. Calculated pharmacokinetic parameters for individual animals as well as mean. AUC – area under the curve, k – elimination rate constant, $t_{1/2}$ - half life, CL – clearance, VD – volume of distribution.

Pig	AUC (ng*h/ml)	k (1/h)	$t_{1/2}$ (h)	CL (l/h)	VD (l)
1	42758	0.061	11.4	1.85	30.3
2	38152	0.071	9.76	2.14	30.2
3	40522	0.087	8.01	2.04	23.5
4	44426	0.071	9.72	2.69	37.9
Mean	41464	0.072	9.72	2.18	30.5

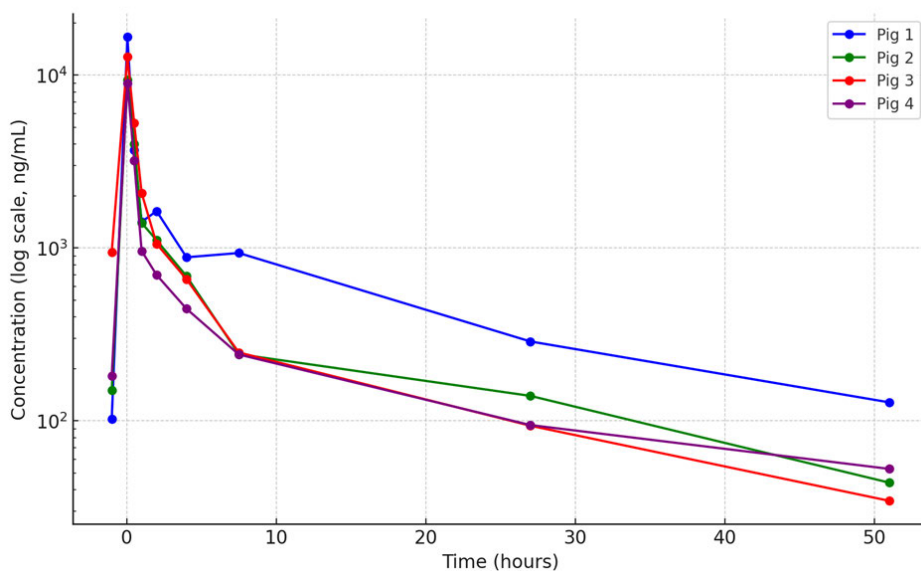


Figure 26. Log t-TUCB concentrations in blood. Log blood concentration over time after injection of 2 mg/kg t-TUCB. A straight line could be approximated from 2 hours, marking the terminal elimination phase.

Discussion

Oxylipins

In the experimental animal model of VILI presented here, nine different oxylipins in BALF and four in plasma were shown to increase over time in response to VILI. In contrast, oxylipin analysis in a cohort of intubated ICU patients showed that 12-HETE decreased during the first day of mechanical ventilation and no oxylipin increased during the same period. In a broader analysis of oxylipins in the cohort of intubated study participants together with non-intubated controls, several oxylipins were lower on admission in septic participants compared to non-septic comparators, and many oxylipins decreased during the first day of intensive care.

In the experimental animal study, the COX metabolites of AA PGD₂ and PGE₂ increased over time in the HTV group. The same response was seen in plasma TXB₂, whereas formal testing of interaction between group and time proved impossible for BALF TXB₂ due to skewed distribution. Nevertheless, Figure 3 clearly shows numerically higher BALF HTV levels that graphically also seem to increase over time. The COX AA metabolites are thus clearly associated with the development of lung injury, in line with previous work(216, 217). For comparison, none of the COX-derived AA metabolites had a detection frequency high enough to allow for formal testing in the plasma samples from the ICU cohort, and the possibility of COX AA metabolite expression could not be evaluated there.

In both BALF and plasma, the LOX metabolites of AA 11-HETE and 15-HETE increased over time in response to HTV, consistent with earlier reports of LOX metabolites being implicated in lung injury pathogenesis(216, 218-220). In contrast, the same metabolites were numerically lower after one day of mechanical ventilation compared to start of ventilation, although these differences were not statistically significant. Thus, the animal data suggests 11-HETE and 15-HETE increase in response to injurious ventilation, but this signal is not observed in study participants subjected to routine ICU mechanical ventilation. Among the investigated oxylipins, 12-HETE, another LOX metabolite of AA, was significantly lower after one day of mechanical ventilation compared to baseline. Also, in samples collected on admission to ICU, 15-HETE was significantly lower in study participants

with sepsis compared to those without sepsis, despite significant systemic inflammation evident from a considerable increase in CRP in the sepsis group. This confirms a previous report where 15-HETE was observed in lower levels at hospital admission in patients with COVID-19 disease compared to a cohort of healthy cases(221).

Among the AA derivatives, one CYP metabolite, further hydrolyzed by sEH, 11,12-DiHETrE, increased over time in the HTV group in BALF, but not in plasma. This could support the notion of sEH-metabolized diols being implicated in the lung injury development(222-225). In the human samples, this metabolite was lower on admission in patients with sepsis compared to those without, but there was no difference in 11,12-DiHETrE levels between baseline and after one day of mechanical ventilation. In sepsis, both 11,12-DiHETrE and 14,15-DiHETrE were significantly lower than in non-sepsis patients on admission to intensive care.

In the animal study BALF samples, another example of sEH products implicated in VILI is the CYP/sEH-produced diol 12,13-DiHOME. This metabolite of LA origin increased over time in the HTV group, as did two LA LOX metabolites, 9-HODE and 13-HODE. However, in the ICU samples, these signals were not evident after one day of mechanical ventilation. In the baseline samples, both the CYP epoxide 9(10)EpOME and the LOX product 13-HODE were lower in the sepsis group than in non-septic cases.

No ALA metabolite was part of the investigated panel in the animal study. Among the human samples, several ALA metabolites were detected but none of them changed significantly during the first day of mechanical ventilation. The CYP/sEH metabolite 15,16-DiHODE and the LOX metabolite 9-HOTrE were lower on admission in septic cases compared to those without sepsis.

All investigated LOX metabolites of DHA had low detection frequencies in the animal study as well as among the human samples. In the human study, the panel of investigated oxylipins was expanded with a number of DHA metabolites of the CYP pathway. Among these, baseline levels were similar in septic cases compared to non-septic controls and none of them clearly differed from baseline after one day of mechanical ventilation.

The animal study included one LOX metabolite of EPA that did not meet the DF criteria for further analysis. In the human study, the panel was expanded with 4 epoxide/diol pairs of sEH substrates and metabolites as

well as two more LOX metabolites. Of these substances, only the LOX metabolite 12-HEPE decreased after one day of mechanical ventilation. 17,18-DiHETE, a diol hydrolyzed by sEH in the CYP pathway, was lower at ICU admission in septic cases compared to non-septic controls.

One LOX metabolite of DGLA, 15-HETrE, was investigated in both studies. There was no difference between groups in this metabolite in the animal study, and there was no difference between baseline and samples collected after one day of mechanical ventilation. At baseline, septic human subjects did have significantly lower levels of 15-HETrE compared to controls.

Although a number of metabolites have been shown to positively correlate to inflammatory processes(67, 79, 226), a large number of the measured oxylipins in the ICU study were lower on admission in septic cases in our study, contradicting the higher CRP in this group. These findings are in contrast to our finding of several oxylipins with positive correlation to neutrophil inflammation in the VILI model but in line with reports of decreases in some oxylipins observed in relation to critical illness(227). An alternate mechanism of oxylipin depletion is metabolization by mitochondrial β -oxidation stimulated by LPS as suggested by a previous study(228). This is a possible mechanism for observed lower levels of some oxylipins detected in septic patients.

The animal study included a two hit VILI model aiming to study the evolution of biomarkers during the development of lung injury. The model was successful in separating groups regarding both histological lung injury and physiological parameters of gas exchange. The study design was, however, limited by a small number of independent observations. It should also be noted that the VILI effect in the model was extremely severe and may therefore not represent VILI developing over long periods of time in the ICU.

The ICU study's strengths included sampling in early critical illness combined with robust analysis and interpretation routine regarding comparisons of samples after initiation of mechanical ventilation for this set of oxylipins. Limitations in the study design include a small sampling size given some expected variability in these types of oxylipin results. From the larger cohort of biobank samples, only a relatively small number of intubated cases had complete sets of samples retained. Laboratory capacity denied analysis of oxylipins in samples from all 147 cases with complete sample sets, and thus the matched controls were selected to increase the sample size with minimal selection bias and still

retaining all intubated cases upon who the main study question was focused. It is, however, impossible to draw conclusions from comparisons between intubated cases and their matched controls as the groups are inherently different from start. An error in matching controls to intubated cases led to the control group being increased by one case. As no direct comparisons were made between the two groups other than the study group characteristics described in Table 5, the results are not likely to be significantly affected by the sampling error. Possible under-powering can mean that there can be false positive or false negative results, which would need a larger sample size to identify. Concerning case sampling with fewer women, this also followed in the matched controls. With the limited sampling of females, it was deemed not reliable to report oxylipin results specifically by sex – a much larger cohort would be needed.

No specific conclusions are drawn from group comparisons of EBC oxylipins due to low DF a relatively low number of observations. Several metabolites exhibited positive correlation between EBC and BALF levels, but these correlations should also be interpreted with caution as a large number of metabolites were analyzed in a relatively low number of samples. The main finding is that oxylipin analysis in EBC is possible but further verification of possible correlations to BALF levels is necessary before EBC oxylipin levels are used to draw biological conclusions.

Extracellular vesicles

In the experimental VILI model, EVs stained with SYTO 13 as well as EVs positive for both SYTO 13 and HMGB1 increased over time in BALF, but not in plasma. This supports the idea that EVs may serve as marker of VILI, but the signal may need to be sampled in BALF rather than the more accessible plasma.

SYTO 13 dye binds to nucleic acids but does not discriminate between DNA or RNA of different forms(141). Although the presence of nucleic acids in EVs is of unclear nature, HMGB1 is a known DAMP(229) and thus especially SYTO 13 positive EVs also positive for HMGB1 may be associated with tissue damage. This EV increase in relation to lung injury development is in line with previous reports of EVs being markers of ARDS(230, 231) and also of EVs participating in inflammatory signaling in the lung(232). We demonstrated a significant increase in EVs containing nucleic acids in parallel to a marked increase in neutrophils

in BALF, although the cellular origin of these EVs cannot be elucidated with this study design.

As this study utilized the same subjects as the study in Paper I, the above-mentioned merits of the model applies to this study as well. It is worth noting that the control group also received a lung injury of sorts from the surfactant depletion. Nevertheless, none of the measured EVs increased from baseline in the control group. The lack of group differences apart from SYTO 13 and SYTO 13 + HMGB1 is therefore unlikely to be a result of damage signal in the group without hyperinflation injury.

The lack of plasma increase of EVs in parallel to their evolution in BALF does not exclude a later increase in plasma EV levels as lung injury progresses. It is also possible that the level of EV elevation detected in BALF in this study is insufficient to cause significant release of EVs into the bloodstream. In either case, the results of this study suggest that early detection of impending lung injury may not be facilitated by analysis of EVs in plasma, at least not with the markers studied here.

Long-term catheterization of pigs

In Paper IV, we present a method of minimally invasive establishment of long-term venous access in pigs using techniques readily available in human health care. The access can be used for both injections and blood sampling. Small pigs may be easier to cannulate using commercially available kits for puncture of smaller vessels, while this step is not necessary in larger animals.

Previously published reports of long-term venous access in pigs utilize more invasive surgical techniques(233, 234). The lack of surgical trauma in this model obliterates the need for postoperative analgesics while simultaneously presumably eliminating most of the inflammatory response coupled to surgery. The presented technique is thus a considerable refinement of animal welfare, as individual subjects avoid unnecessary pain and recovery from surgery. The establishment of secure vascular access could also potentially reduce the number of animals that need to be included in studies as sampling and injections are allowed for with great precision in time.

In conclusion, the model presented here shows benefit to previously published models of long-term vascular access in pigs and could be

adopted as standard of care for pigs included in studies with need of long-term venous access.

Soluble epoxide hydrolase inhibitor pharmacokinetics

The aim of the pharmacokinetic study was to establish pharmacokinetic properties of t-TUCB in pigs derived from dosing at intravenous 0.1 mg/kg, 1 mg/kg, 2 mg/kg and oral 1 mg/kg. As all results except those from the 2 mg/kg dose were discarded due to methodological problems, these results can only be interpreted with great caution. 2 mg/kg of t-TUCB did give a high initial blood concentration with an estimated half-life of approximately 10 hours and blood concentrations above 10 times the IC₅₀ for the better part of the first day after injection.

These results can be used to guide future dose finding studies where t-TUCB could be tested for once or twice daily intravenous administration in pigs. The optimal intravenous dose cannot be discerned from this study, but the 2 mg/kg dose did give blood concentrations that probably are relevant for in vivo inhibition of sEH.

The pharmacokinetic properties in pigs of t-TUCB have not been previously described in publications indexed in Medline. Previous reports have focused on t-TUCB as a sEH inhibitor in other species(211, 235), and data in the current study are in line with previous findings from other species.

The present study utilized a long-term venous access in pigs that allowed easy and stress-free handling of the study subjects with the possibility of exactly timing blood sampling after injections, with avoiding sampling from the same lumen used for injections. Due to an incompletely characterized chemistry analytical error with measured base line levels of the study drug being unexplainably present before injection of the drug and with unrealistically high spread of observations in one of the dose series, the results cannot be interpreted confidently. All conclusions presented here are thus drawn from the 2 mg/kg dose with only 4 included subjects. Yet under these conditions, all 4 subjects show blood concentration curves with similar profiles and reasonable spread of observations.

To conclude, this study does not establish a dosing regimen of definitive pharmacokinetic properties of t-TUCB. It does, however, suggest that

t-TUCB may be administered in clinically relevant intervals in pigs and that further dosing studies could be conducted with doses near 2 mg/kg.

Soluble epoxide hydrolase inhibition in acute lung injury

The main finding of the lung injury study here was that inhibition of sEH did not – in contrast to previous rodent studies(84, 224) – attenuate lung injury development in a model of LPS-induced lung injury. There were signs of biologically relevant effects on the target enzyme(236), but clinical outcomes were unaffected by the treatment.

Although ARDS and acute lung injury are inflammatory conditions and despite promising animal data(237-239) for non-steroidal anti-inflammatory drugs, there are no trials showing benefit of NSAIDs in human lung injury. The concept of inflammatory modulation by sEH inhibition has shown positive effects in LPS-treated rodents(84), suggesting that sEH inhibition may be a pharmacological alternative in research on ARDS treatments(224). The present study does not support that hypothesis, although it is possible that other sEH inhibitors or treatment in different models of lung injury produce different outcomes.

Why the present study failed to show benefit of sEH inhibition is not clear. The model was consistently severe with a relatively high mortality rate. It is possible that the inflammation was too severe to allow a pharmacological benefit of sEH inhibition to show. On the other hand, severe inflammation and high mortality are clinically relevant aspects of this condition and a prerequisite for a meaningful need of a pharmacological agent.

The study protocol with pretreatment of study drug before exposure to the inflammatory stimulus should, in theory, produce optimal conditions for a treatment effect to be evident, although the study period of nine hours is short in this context.

There are limitations to the study. First, data on dosing and pharmacokinetics of sEH inhibitors and AEPUs in pigs have not been previously published. An *in vitro* assay of IC₅₀ was conducted as well as a pharmacokinetic pilot in a pig subject and blood AEPUs concentrations were monitored throughout the experiment. Measurements of epoxide/diol ratios after AEPUs treatment compared to controls were comparable to previously published reports in epoxide/diol ratios in

monkeys treated with sEH-inhibitors. Despite this, it is still possible that AEPU did not achieve sufficient target engagement to alter the physiological effects of the enzyme and that a higher dose or choice of a different inhibitor could have had a different outcome. It is also possible that pigs, for unknown reasons, are poor models of sEH inhibition.

In summary, this study does not support the hypothesis that sEH inhibition attenuates lung injury development in response to LPS, at least not under the conditions tested here.

Conclusions

Severe lung injury from high tidal ventilation in pigs is associated with changes in oxylipin levels in both bronchial lavage fluid and in plasma. Lavage fluid changes involved more oxylipins than those in plasma.

A large number of oxylipins may be detected in intensive care patients and changes in levels during serial measures can be associated with clinical conditions. Several of the oxylipins exhibit concentration decreases during the early course of critical illness and treatment. More investigation is needed to further delineate associations between levels of oxylipins and clinical status. Oxylipins may hold promise as prognostic biomarkers or potentially therapeutic targets.

Extracellular vesicles containing nucleic acids increase in bronchoalveolar lavage fluid, but not in plasma, in response to severe hyperinflation lung injury in the early phase.

Pigs included in long-term studies requiring venous access for repeated injections of blood samples may be cannulated using standards in line with human health care. Minimally invasive percutaneous cannulation is feasible and practical.

The sEH inhibitor t-TUCB could potentially be a pharmacokinetically relevant drug suitable for sEH inhibition studies in pigs. Future dose finding studies could use the data presented here to guide study design.

Treatment with the sEH inhibitor AEPU did not attenuate the development of lung injury in a pig model of LPS-induced lung injury, despite promising results of sEH inhibition in mice with LPS challenge.

Final remarks and future perspectives

This thesis is the result of a project that started as a resident physician's introductory research project with the general idea of looking for biomarker patterns in ARDS. The project quickly became a PhD project, but the way forward was anything but straight. Initially, we did experiments on blind collection of BALF samples with a simple airway exchange catheter rather than the more resource-demanding bronchoscope. In parallel, we tried looking at BALF mRNA for cytokine production with the idea that mRNA-expression should precede the cytokines themselves. When that did not work (the blood contaminating BALF in our lung injury model made our mRNA assay useless), we started looking into oxylipins and extracellular vesicles in lung injury. This prompted us to replace our lab's old oleic acid lung injury model with the present two-hit VILI model as we hesitated to investigate fatty acid metabolites in the lung after injecting big chunks of fat with the intention of clogging the pulmonary microvasculature with fat emboli. We also spent a considerable amount of effort on plans for a project looking on exhaled particles in ventilated patients. Unfortunately, we were never able to form a working collaboration with the inventor of the intended equipment. This led us from biomarker work to an interest in sEH inhibition and to plans for experiments with sEH inhibition in the context of lung injury. Our previous experience with the severe VILI model of lung injury led us to yet again develop a new local animal model to tailor our experimental needs. The lack of known pharmacokinetic properties in pigs of any sEH inhibitor forced us to begin this effort with a pharmacokinetic study, which failed spectacularly due to analytical problems. The efforts to set up a long-term model for pig studies of pharmacokinetics did however result in the method paper on vascular access in pigs. In summary, this all resulted in a thesis built on oxylipins, extracellular vesicles, venous access in pigs, pharmacokinetics and finally anti-inflammatory treatment in lung injury.

As often the case with research, more questions than we answered arise from the studies we performed. Can oxylipins or EVs in EBC serve as relevant biomarkers in ICU patients on mechanical ventilation? Can oxylipins or EVs in any compartment be used to differentiate between lung injury of different aetiology or severity? Can the data generated on dosing and pharmacokinetics on t-TUCB be verified? Could a higher dose of AEPU or a different sEH inhibitor have altered the results of the LPS experiment? Could AEPU affect lung injury in a model of less severe

injury? If this project would be to be repeated, EBC studies could be collected both in all experiments as well as in ICU subjects. Also, with unlimited resources and time, a new pharmacokinetic study of a sEH inhibitor in pigs together with oxylipin analysis of plasma samples and analysis of lung biopsies to ascertain target engagement both systemically and locally could lay the foundation for a new lung injury study. With clearer data on the efficacy of sEH inhibition in the model, the results could be interpreted with more confidence.

Currently, we have no firm plans for the continuation of this project, but there are many ideas. Possibly, a study on EVs in EBC and plasma in ICU patients could be a reasonable continuation given our clinics resources and specific staff competencies. Such an observational study has been loosely discussed and may be the next project we start. Personally, I hope to be able to combine my hospital work with both local projects and collaborative research. A broader take on respiratory care, both in intensive care and anaesthesiology, is well within the field I would like to continue to investigate.

References

1. Ashbaugh DG, Bigelow DB, Petty TL, Levine BE. Acute respiratory distress in adults. *Lancet*. 1967;290(7511):319-23.
2. Ranieri VM, Rubenfeld GD, Thompson BT, Ferguson ND, Caldwell E, Fan E, et al. Acute respiratory distress syndrome: the Berlin Definition. *JAMA*. 2012;307(23):2526-33.
3. Matthay MA, Arabi Y, Arroliga AC, Bernard G, Bersten AD, Brochard LJ, et al. A New Global Definition of Acute Respiratory Distress Syndrome. *Am J Respir Crit Care Med*. 2024;209(1):37-47.
4. Meduri GU, Headley S, Kohler G, Stentz F, Tolley E, Umberger R, et al. Persistent elevation of inflammatory cytokines predicts a poor outcome in ARDS. Plasma IL-1 beta and IL-6 levels are consistent and efficient predictors of outcome over time. *Chest*. 1995;107(4):1062-73.
5. Ranieri V, Suter P, Tortorella C, De Tullio R, Dayer J, Brienza A, et al. Effect of mechanical ventilation on inflammatory mediators in patients with acute respiratory distress syndrome: a randomized controlled trial. *JAMA*. 1999;282(1):54-61.
6. Bos LDJ, Ware LB. Acute respiratory distress syndrome: causes, pathophysiology, and phenotypes. *Lancet*. 2022;400(10358):1145-56.
7. Li W, Li D, Chen Y, Abudou H, Wang H, Cai J, et al. Classic Signaling Pathways in Alveolar Injury and Repair Involved in Sepsis-Induced ALI/ARDS: New Research Progress and Prospect. *Dis Markers*. 2022;2022:6362344.
8. Thille AW, Esteban A, Fernández-Segoviano P, Rodríguez JM, Aramburu JA, Peñuelas O, et al. Comparison of the Berlin definition for acute respiratory distress syndrome with autopsy. *Am J Respir Crit Care Med*. 2013;187(7):761-7.
9. Thille AW, Peñuelas O, Lorente JA, Fernández-Segoviano P, Rodríguez JM, Aramburu JA, et al. Predictors of diffuse alveolar damage in patients with acute respiratory distress syndrome: a retrospective analysis of clinical autopsies. *Crit Care*. 2017;21(1):254.
10. Umbrello M, Formenti P, Bolgiaghi L, Chiumello D. Current Concepts of ARDS: A Narrative Review. *Int J Mol Sci*. 2016;18(1).
11. Matthay MA, Zemans RL, Zimmerman GA, Arabi YM, Beitler JR, Mercat A, et al. Acute respiratory distress syndrome. *Nat Rev Dis Primers*. 2019;5(1):18.
12. Cardinal-Fernández P, Lorente JA, Ballén-Barragán A, Matute-Bello G. Acute Respiratory Distress Syndrome and Diffuse Alveolar Damage. New Insights on a Complex Relationship. *Ann Am Thorac Soc*. 2017;14(6):844-50.
13. Kao KC, Hu HC, Chang CH, Hung CY, Chiu LC, Li SH, et al. Diffuse alveolar damage associated mortality in selected acute

- respiratory distress syndrome patients with open lung biopsy. *Crit Care*. 2015;19(1):228.
14. Batah SS, Fabro AT. Pulmonary pathology of ARDS in COVID-19: A pathological review for clinicians. *Respir Med*. 2021;176:106239.
 15. Bernard G, Artigas A, Brigham K, Carlet J, Falke K, Hudson L, et al. Report of the American-European consensus conference on ARDS: definitions, mechanisms, relevant outcomes and clinical trial coordination. The Consensus Committee. *Intensive Care Med*. 1994;20(3):225-32.
 16. Long ME, Mallampalli RK, Horowitz JC. Pathogenesis of pneumonia and acute lung injury. *Clin Sci (Lond)*. 2022;136(10):747-69.
 17. Slutsky AS. Lung injury caused by mechanical ventilation. *Chest*. 1999;116(1 Suppl):9s-15s.
 18. Terragni PP, Rosboch G, Tealdi A, Corno E, Menaldo E, Davini O, et al. Tidal hyperinflation during low tidal volume ventilation in acute respiratory distress syndrome. *Am J Respir Crit Care Med*. 2007;175(2):160-6.
 19. Marini JJ. Evolving concepts for safer ventilation. *Crit Care*. 2019;23(Suppl 1):114.
 20. Medzhitov R. Inflammation 2010: new adventures of an old flame. *Cell*. 2010;140(6):771-6.
 21. Nathan C, Ding A. Nonresolving inflammation. *Cell*. 2010;140(6):871-82.
 22. Sugimoto MA, Sousa LP, Pinho V, Perretti M, Teixeira MM. Resolution of Inflammation: What Controls Its Onset? *Front Immunol*. 2016;7:160.
 23. Sheppe AEF, Edelmann MJ. Roles of Eicosanoids in Regulating Inflammation and Neutrophil Migration as an Innate Host Response to Bacterial Infections. *Infect Immun*. 2021;89(8):e0009521.
 24. Kaur BP, Secord E. Innate Immunity. *Immunol Allergy Clin North Am*. 2021;41(4):535-41.
 25. Wang K, Huang H, Zhan Q, Ding H, Li Y. Toll-like receptors in health and disease. *MedComm (2020)*. 2024;5(5):e549.
 26. Wicherska-Pawłowska K, Wróbel T, Rybka J. Toll-Like Receptors (TLRs), NOD-Like Receptors (NLRs), and RIG-I-Like Receptors (RLRs) in Innate Immunity. TLRs, NLRs, and RLRs Ligands as Immunotherapeutic Agents for Hematopoietic Diseases. *Int J Mol Sci*. 2021;22(24).
 27. Kurup SP, Tarleton RL. Perpetual expression of PAMPs necessary for optimal immune control and clearance of a persistent pathogen. *Nat Commun*. 2013;4:2616.
 28. Vance RE, Isberg RR, Portnoy DA. Patterns of pathogenesis: discrimination of pathogenic and nonpathogenic microbes by the innate immune system. *Cell Host Microbe*. 2009;6(1):10-21.

29. Chen R, Zou J, Chen J, Zhong X, Kang R, Tang D. Pattern recognition receptors: function, regulation and therapeutic potential. *Signal Transduct Target Ther.* 2025;10(1):216.
30. Rothschild DE, McDaniel DK, Ringel-Scaia VM, Allen IC. Modulating inflammation through the negative regulation of NF- κ B signaling. *J Leukoc Biol.* 2018.
31. Takeuchi O, Akira S. Pattern recognition receptors and inflammation. *Cell.* 2010;140(6):805-20.
32. Rayees S, Rochford I, Joshi JC, Joshi B, Banerjee S, Mehta D. Macrophage TLR4 and PAR2 Signaling: Role in Regulating Vascular Inflammatory Injury and Repair. *Front Immunol.* 2020;11:2091.
33. Medzhitov R. Origin and physiological roles of inflammation. *Nature.* 2008;454(7203):428-35.
34. Hu G, Malik AB, Minshall RD. Toll-like receptor 4 mediates neutrophil sequestration and lung injury induced by endotoxin and hyperinflation. *Crit Care Med.* 2010;38(1):194-201.
35. Sender V, Stamme C. Lung cell-specific modulation of LPS-induced TLR4 receptor and adaptor localization. *Commun Integr Biol.* 2014;7:e29053.
36. Root-Bernstein R. Innate Receptor Activation Patterns Involving TLR and NLR Synergisms in COVID-19, ALI/ARDS and Sepsis Cytokine Storms: A Review and Model Making Novel Predictions and Therapeutic Suggestions. *Int J Mol Sci.* 2021;22(4).
37. Lim EY, Lee SY, Shin HS, Kim GD. Reactive Oxygen Species and Strategies for Antioxidant Intervention in Acute Respiratory Distress Syndrome. *Antioxidants (Basel).* 2023;12(11).
38. Varadaradjalou S, Féger F, Thieblemont N, Hamouda NB, Pleau JM, Dy M, et al. Toll-like receptor 2 (TLR2) and TLR4 differentially activate human mast cells. *Eur J Immunol.* 2003;33(4):899-906.
39. Virk H, Arthur G, Bradding P. Mast cells and their activation in lung disease. *Transl Res.* 2016;174:60-76.
40. Mukai K, Tsai M, Saito H, Galli SJ. Mast cells as sources of cytokines, chemokines, and growth factors. *Immunol Rev.* 2018;282(1):121-50.
41. Chaplin DD. Overview of the immune response. *J Allergy Clin Immunol.* 2010;125(2 Suppl 2):S3-23.
42. Wang R, Lan C, Benlagha K, Camara NOS, Miller H, Kubo M, et al. The interaction of innate immune and adaptive immune system. *MedComm (2020).* 2024;5(10):e714.
43. Smith-Garvin JE, Koretzky GA, Jordan MS. T cell activation. *Annu Rev Immunol.* 2009;27:591-619.
44. Cyster JG, Allen CDC. B Cell Responses: Cell Interaction Dynamics and Decisions. *Cell.* 2019;177(3):524-40.

45. Polonsky M, Chain B, Friedman N. Clonal expansion under the microscope: studying lymphocyte activation and differentiation using live-cell imaging. *Immunol Cell Biol.* 2016;94(3):242-9.
46. O'Shea JJ, Paul WE. Mechanisms underlying lineage commitment and plasticity of helper CD4+ T cells. *Science.* 2010;327(5969):1098-102.
47. Murphy KM, Reiner SL. The lineage decisions of helper T cells. *Nat Rev Immunol.* 2002;2(12):933-44.
48. Ng CT, Fong LY, Abdullah MNH. Interferon-gamma (IFN- γ): Reviewing its mechanisms and signaling pathways on the regulation of endothelial barrier function. *Cytokine.* 2023;166:156208.
49. Gaffen SL. Structure and signalling in the IL-17 receptor family. *Nat Rev Immunol.* 2009;9(8):556-67.
50. Josefowicz SZ, Lu LF, Rudensky AY. Regulatory T cells: mechanisms of differentiation and function. *Annu Rev Immunol.* 2012;30:531-64.
51. El Kebir D, Filep JG. Modulation of Neutrophil Apoptosis and the Resolution of Inflammation through β 2 Integrins. *Front Immunol.* 2013;4:60.
52. Carlini V, Noonan DM, Abdalalem E, Goletti D, Sansone C, Calabrone L, et al. The multifaceted nature of IL-10: regulation, role in immunological homeostasis and its relevance to cancer, COVID-19 and post-COVID conditions. *Front Immunol.* 2023;14:1161067.
53. Serhan CN, Petasis NA. Resolvins and protectins in inflammation resolution. *Chem Rev.* 2011;111(10):5922-43.
54. Ivanov AI, Romanovsky AA. Prostaglandin E2 as a mediator of fever: synthesis and catabolism. *Front Biosci.* 2004;9:1977-93.
55. Strehl C, Ehlers L, Gaber T, Buttgerit F. Glucocorticoids-All-Rounders Tackling the Versatile Players of the Immune System. *Front Immunol.* 2019;10:1744.
56. Perretti M, D'Acquisto F. Annexin A1 and glucocorticoids as effectors of the resolution of inflammation. *Nat Rev Immunol.* 2009;9(1):62-70.
57. Kolmus K, Tavernier J, Gerlo S. β 2-Adrenergic receptors in immunity and inflammation: stressing NF- κ B. *Brain Behav Immun.* 2015;45:297-310.
58. Chhatar S, Lal G. Role of adrenergic receptor signalling in neuroimmune communication. *Curr Res Immunol.* 2021;2:202-17.
59. Tracey KJ. Physiology and immunology of the cholinergic antiinflammatory pathway. *J Clin Invest.* 2007;117(2):289-96.
60. Procaccini C, de Candia P, Russo C, De Rosa G, Lepore MT, Colamatteo A, et al. Caloric restriction for the immunometabolic control of human health. *Cardiovasc Res.* 2024;119(18):2787-800.

61. Meydani SN, Das SK, Pieper CF, Lewis MR, Klein S, Dixit VD, et al. Long-term moderate calorie restriction inhibits inflammation without impairing cell-mediated immunity: a randomized controlled trial in non-obese humans. *Aging (Albany NY)*. 2016;8(7):1416-31.
62. Zeyda M, Stulnig TM. Adipose tissue macrophages. *Immunol Lett*. 2007;112(2):61-7.
63. Ahmad R, Thomas R, Kochumon S, Sindhu S. Increased adipose tissue expression of IL-18R and its ligand IL-18 associates with inflammation and insulin resistance in obesity. *Immun Inflamm Dis*. 2017;5(3):318-35.
64. Hotamisligil GS. Inflammation and metabolic disorders. *Nature*. 2006;444(7121):860-7.
65. Visser M, Bouter LM, McQuillan GM, Wener MH, Harris TB. Elevated C-reactive protein levels in overweight and obese adults. *Jama*. 1999;282(22):2131-5.
66. Parchem K, Letsiou S, Petan T, Oskolkova O, Medina I, Kuda O, et al. Oxylipin profiling for clinical research: Current status and future perspectives. *Prog Lipid Res*. 2024;95:101276.
67. Dennis EA, Norris PC. Eicosanoid storm in infection and inflammation. *Nature reviews Immunology*. 2015;15(8).
68. Das UN. Essential Fatty Acids and Their Metabolites in the Pathobiology of Inflammation and Its Resolution. *Biomolecules*. 2021;11(12):1873.
69. Calder PC. Eicosanoids. *Essays Biochem*. 2020;64(3):423-41.
70. Bailey JM, Bryant RW, Whiting J, Salata K. Characterization of 11-HETE and 15-HETE, together with prostacyclin, as major products of the cyclooxygenase pathway in cultured rat aorta smooth muscle cells. *J Lipid Res*. 1983;24(11):1419-28.
71. Powell WS, Rokach J. Biosynthesis, biological effects, and receptors of hydroxyeicosatetraenoic acids (HETEs) and oxoeicosatetraenoic acids (oxo-ETEs) derived from arachidonic acid. *Biochim Biophys Acta*. 2015;1851(4):340-55.
72. Serhan CN. Lipoxins and aspirin-triggered 15-epi-lipoxins are the first lipid mediators of endogenous anti-inflammation and resolution. *Prostaglandins Leukot Essent Fatty Acids*. 2005;73(3-4):141-62.
73. Giménez-Bastida JA, Boeglin WE, Boutaud O, Malkowski MG, Schneider C. Residual cyclooxygenase activity of aspirin-acetylated COX-2 forms 15 R-prostaglandins that inhibit platelet aggregation. *Faseb j*. 2019;33(1):1033-41.
74. Calder PC. Omega-3 fatty acids and inflammatory processes: from molecules to man. *Biochem Soc Trans*. 2017;45(5):1105-15.
75. Patrignani P, Tacconelli S, Sciulli MG, Capone ML. New insights into COX-2 biology and inhibition. *Brain Res Brain Res Rev*. 2005;48(2):352-9.

76. Kuhn H, Banthiya S, van Leyen K. Mammalian lipoxygenases and their biological relevance. *Biochim Biophys Acta*. 2015;1851(4):308-30.
77. Ivanov I, Heydeck D, Hofheinz K, Roffeis J, O'Donnell VB, Kuhn H, et al. Molecular enzymology of lipoxygenases. *Arch Biochem Biophys*. 2010;503(2):161-74.
78. Murphy RC, Gijón MA. Biosynthesis and metabolism of leukotrienes. *Biochem J*. 2007;405(3):379-95.
79. Lundstrom SL, Balgoma D, Wheelock AM, Haeggstrom JZ, Dahlen SE, Wheelock CE. Lipid mediator profiling in pulmonary disease. *Curr Pharm Biotechnol*. 2011;12(7):1026-52.
80. Spector AA. Arachidonic acid cytochrome P450 epoxygenase pathway. *J Lipid Res*. 2009;50 Suppl:S52-6.
81. Imig J, Hammock B. Soluble epoxide hydrolase as a therapeutic target for cardiovascular diseases. *Nature reviews Drug discovery*. 2009;8(10).
82. Wang Y, Wagner K, Morisseau C, Hammock B. Inhibition of the Soluble Epoxide Hydrolase as an Analgesic Strategy: A Review of Preclinical Evidence. *Journal of pain research*. 2021;14:61-72.
83. Wagner KM, McReynolds CB, Schmidt WK, Hammock BD. Soluble epoxide hydrolase as a therapeutic target for pain, inflammatory and neurodegenerative diseases. *Pharmacol Ther*. 2017;180:62-76.
84. Zhou Y, Liu T, Duan JX, Li P, Sun GY, Liu YP, et al. Soluble Epoxide Hydrolase Inhibitor Attenuates Lipopolysaccharide-Induced Acute Lung Injury and Improves Survival in Mice. *Shock*. 2017;47(5):638-45.
85. Arango Duque G, Descoteaux A. Macrophage cytokines: involvement in immunity and infectious diseases. *Front Immunol*. 2014;5:491.
86. Fajgenbaum DC, June CH. Cytokine Storm. *N Engl J Med*. 2020;383(23):2255-73.
87. Thelemann C, Eren RO, Coutaz M, Brasseit J, Bouzourene H, Rosa M, et al. Interferon- γ induces expression of MHC class II on intestinal epithelial cells and protects mice from colitis. *PLoS One*. 2014;9(1):e86844.
88. Dinarello CA. Interleukin-1 in the pathogenesis and treatment of inflammatory diseases. *Blood*. 2011;117(14):3720-32.
89. Garlanda C, Di Ceglie I, Jaillon S. IL-1 family cytokines in inflammation and immunity. *Cell Mol Immunol*. 2025.
90. Kaur S, Bansal Y, Kumar R, Bansal G. A panoramic review of IL-6: Structure, pathophysiological roles and inhibitors. *Bioorg Med Chem*. 2020;28(5):115327.
91. Grebenciucova E, VanHaerents S. Interleukin 6: at the interface of human health and disease. *Front Immunol*. 2023;14:1255533.

92. Aliyu M, Zohora FT, Anka AU, Ali K, Maleknia S, Saffarioun M, et al. Interleukin-6 cytokine: An overview of the immune regulation, immune dysregulation, and therapeutic approach. *Int Immunopharmacol.* 2022;111:109130.
93. Vignali DA, Kuchroo VK. IL-12 family cytokines: immunological playmakers. *Nat Immunol.* 2012;13(8):722-8.
94. Cruikshank WW, Kornfeld H, Center DM. Interleukin-16. *J Leukoc Biol.* 2000;67(6):757-66.
95. Niewold TB, Lehman JS, Gunnarsson I, Meves A, Oke V. Role of interleukin-16 in human diseases: a novel potential therapeutic target. *Front Immunol.* 2025;16:1524026.
96. Hughes CE, Nibbs RJB. A guide to chemokines and their receptors. *Febs j.* 2018;285(16):2944-71.
97. Palomino DC, Marti LC. Chemokines and immunity. *Einstein (Sao Paulo).* 2015;13(3):469-73.
98. Thangam EB, Jemima EA, Singh H, Baig MS, Khan M, Mathias CB, et al. The Role of Histamine and Histamine Receptors in Mast Cell-Mediated Allergy and Inflammation: The Hunt for New Therapeutic Targets. *Front Immunol.* 2018;9:1873.
99. Lieberman P. The basics of histamine biology. *Ann Allergy Asthma Immunol.* 2011;106(2 Suppl):S2-5.
100. Berger M, Gray JA, Roth BL. The expanded biology of serotonin. *Annu Rev Med.* 2009;60:355-66.
101. Innes JK, Calder PC. Omega-6 fatty acids and inflammation. *Prostaglandins Leukot Essent Fatty Acids.* 2018;132:41-8.
102. Ricciotti E, FitzGerald GA. Prostaglandins and inflammation. *Arterioscler Thromb Vasc Biol.* 2011;31(5):986-1000.
103. Mitchell JA, Kirkby NS. Eicosanoids, prostacyclin and cyclooxygenase in the cardiovascular system. *Br J Pharmacol.* 2019;176(8):1038-50.
104. Peters-Golden M, Henderson WR, Jr. Leukotrienes. *N Engl J Med.* 2007;357(18):1841-54.
105. Montuschi P. Role of Leukotrienes and Leukotriene Modifiers in Asthma. *Pharmaceuticals (Basel).* 2010;3(6):1792-811.
106. Klos A, Tenner AJ, Johswich KO, Ager RR, Reis ES, Köhl J. The role of the anaphylatoxins in health and disease. *Mol Immunol.* 2009;46(14):2753-66.
107. Sarma JV, Ward PA. The complement system. *Cell Tissue Res.* 2011;343(1):227-35.
108. Guo RF, Ward PA. Role of C5a in inflammatory responses. *Annu Rev Immunol.* 2005;23:821-52.
109. Alfaro E, Díaz-García E, García-Tovar S, Zamarrón E, Mangas A, Galera R, et al. Impaired Kallikrein-Kinin System in COVID-19 Patients' Severity. *Front Immunol.* 2022;13:909342.

110. Marcianò G, Vocca C, Diraçoğlu D, Sevgin R, Gallelli L. Escin's Action on Bradykinin Pathway: Advantageous Clinical Properties for an Unknown Mechanism? *Antioxidants (Basel)*. 2024;13(9).
111. Saraiva M, Vieira P, O'Garra A. Biology and therapeutic potential of interleukin-10. *J Exp Med*. 2020;217(1).
112. Batlle E, Massagué J. Transforming Growth Factor- β Signaling in Immunity and Cancer. *Immunity*. 2019;50(4):924-40.
113. Tkacz K, Rolski F, Stefańska M, Węglarczyk K, Szatanek R, Siedlar M, et al. TGF- β Signalling Regulates Cytokine Production in Inflammatory Cardiac Macrophages during Experimental Autoimmune Myocarditis. *Int J Mol Sci*. 2024;25(11).
114. Vandevyver S, Dejager L, Tuckermann J, Libert C. New insights into the anti-inflammatory mechanisms of glucocorticoids: an emerging role for glucocorticoid-receptor-mediated transactivation. *Endocrinology*. 2013;154(3):993-1007.
115. Ehrchen JM, Roth J, Barczyk-Kahlert K. More Than Suppression: Glucocorticoid Action on Monocytes and Macrophages. *Front Immunol*. 2019;10:2028.
116. Arend WP, Malyak M, Guthridge CJ, Gabay C. Interleukin-1 receptor antagonist: role in biology. *Annu Rev Immunol*. 1998;16:27-55.
117. Liput KP, Lepczyński A, Ogłuszka M, Nawrocka A, Poławska E, Grzesiak A, et al. Effects of Dietary n-3 and n-6 Polyunsaturated Fatty Acids in Inflammation and Cancerogenesis. *Int J Mol Sci*. 2021;22(13).
118. Batiha GE, Al-Gareeb AI, Elekhawy E, Al-Kuraishy HM. Potential role of lipoxin in the management of COVID-19: a narrative review. *Inflammopharmacology*. 2022;30(6):1993-2001.
119. Barnig C, Lutzweiler G, Giannini M, Lejay A, Charles AL, Meyer A, et al. Resolution of Inflammation after Skeletal Muscle Ischemia-Reperfusion Injury: A Focus on the Lipid Mediators Lipoxins, Resolvins, Protectins and Maresins. *Antioxidants (Basel)*. 2022;11(6).
120. Ferreira I, Falcato F, Bandarra N, Rauter AP. Resolvins, Protectins, and Maresins: DHA-Derived Specialized Pro-Resolving Mediators, Biosynthetic Pathways, Synthetic Approaches, and Their Role in Inflammation. *Molecules*. 2022;27(5).
121. Pasquini S, Contri C, Borea PA, Vincenzi F, Varani K. Adenosine and Inflammation: Here, There and Everywhere. *Int J Mol Sci*. 2021;22(14).
122. Théry C, Witwer KW, Aikawa E, Alcaraz MJ, Anderson JD, Andriantsitohaina R, et al. Minimal information for studies of extracellular vesicles 2018 (MISEV2018): a position statement of the International Society for Extracellular Vesicles and update of the MISEV2014 guidelines. *J Extracell Vesicles*. 2018;7(1):1535750.

123. Doyle LM, Wang MZ. Overview of Extracellular Vesicles, Their Origin, Composition, Purpose, and Methods for Exosome Isolation and Analysis. *Cells*. 2019;8(7).
124. Yáñez-Mó M, Siljander PR, Andreu Z, Zavec AB, Borràs FE, Buzas EI, et al. Biological properties of extracellular vesicles and their physiological functions. *J Extracell Vesicles*. 2015;4:27066.
125. Jeppesen DK, Zhang Q, Coffey RJ. Extracellular vesicles and nanoparticles at a glance. *J Cell Sci*. 2024;137(23).
126. Buzas EI. The roles of extracellular vesicles in the immune system. *Nat Rev Immunol*. 2023;23(4):236-50.
127. Italiano JE, Jr., Mairuhu AT, Flaumenhaft R. Clinical relevance of microparticles from platelets and megakaryocytes. *Curr Opin Hematol*. 2010;17(6):578-84.
128. Fyfe J, Casari I, Manfredi M, Falasca M. Role of lipid signalling in extracellular vesicles-mediated cell-to-cell communication. *Cytokine Growth Factor Rev*. 2023;73:20-6.
129. Murao A, Aziz M, Wang H, Brenner M, Wang P. Release mechanisms of major DAMPs. *Apoptosis*. 2021;26(3-4):152-62.
130. Nieuwland R, Siljander PR. A beginner's guide to study extracellular vesicles in human blood plasma and serum. *Journal of extracellular vesicles*. 2024;13(1).
131. Shlomovitz I, Speir M, Gerlic M. Flipping the dogma - phosphatidylserine in non-apoptotic cell death. *Cell Commun Signal*. 2019;17(1):139.
132. Jing H, Wu X, Xiang M, Wang C, Novakovic VA, Shi J. Microparticle Phosphatidylserine Mediates Coagulation: Involvement in Tumor Progression and Metastasis. *Cancers (Basel)*. 2023;15(7).
133. Siljander PR. Platelet-derived microparticles - an updated perspective. *Thromb Res*. 2011;127 Suppl 2:S30-3.
134. Zarbock A, Polanowska-Grabowska RK, Ley K. Platelet-neutrophil-interactions: linking hemostasis and inflammation. *Blood Rev*. 2007;21(2):99-111.
135. André P. P-selectin in haemostasis. *Br J Haematol*. 2004;126(3):298-306.
136. Voukalis C, Shantsila E, Lip GYH. Microparticles and cardiovascular diseases. *Ann Med*. 2019;51(3-4):193-223.
137. Rheinländer A, Schraven B, Bommhardt U. CD45 in human physiology and clinical medicine. *Immunol Lett*. 2018;196:22-32.
138. Wang GH, Lu J, Ma KL, Zhang Y, Hu ZB, Chen PP, et al. The Release of Monocyte-Derived Tissue Factor-Positive Microparticles Contributes to a Hypercoagulable State in Idiopathic Membranous Nephropathy. *J Atheroscler Thromb*. 2019;26(6):538-46.
139. Mahida RY, Price J, Lugg ST, Li H, Parekh D, Scott A, et al. CD14-positive extracellular vesicles in bronchoalveolar lavage fluid as a

- new biomarker of acute respiratory distress syndrome. *Am J Physiol Lung Cell Mol Physiol.* 2022;322(4):L617-l24.
140. Tárnok A. SYTO dyes and histoproteins--myriad of applications. *Cytometry A.* 2008;73(6):477-9.
141. Ullal AJ, Pisetsky DS, Reich CF, 3rd. Use of SYTO 13, a fluorescent dye binding nucleic acids, for the detection of microparticles in in vitro systems. *Cytometry A.* 2010;77(3):294-301.
142. Mobarrez F, Antoniewicz L, Bosson JA, Kuhl J, Pisetsky DS, Lundbäck M. The effects of smoking on levels of endothelial progenitor cells and microparticles in the blood of healthy volunteers. *PLoS One.* 2014;9(2):e90314.
143. Bellani G, Laffey JG, Pham T, Fan E, Brochard L, Esteban A, et al. Epidemiology, Patterns of Care, and Mortality for Patients With Acute Respiratory Distress Syndrome in Intensive Care Units in 50 Countries. *Jama.* 2016;315(8):788-800.
144. Wick KD, Ware LB, Matthay MA. Acute respiratory distress syndrome. *Bmj.* 2024;387:e076612.
145. Pham T, Rubenfeld GD. Fifty Years of Research in ARDS. The Epidemiology of Acute Respiratory Distress Syndrome. A 50th Birthday Review. *Am J Respir Crit Care Med.* 2017;195(7):860-70.
146. Matthay MA, Ware LB, Zimmerman GA. The acute respiratory distress syndrome. *J Clin Invest.* 2012;122(8):2731-40.
147. Bromley SE, Shakery K, Vora P, Atabaki A, Reimer T, McDermott L, et al. Understanding Causes of Death in Patients With Acute Respiratory Distress Syndrome: A Narrative Review. *Crit Care Explor.* 2024;6(9):e1147.
148. Matthay MA, Zemans RL. The acute respiratory distress syndrome: pathogenesis and treatment. *Annu Rev Pathol.* 2011;6:147-63.
149. Huang X, Xiu H, Zhang S, Zhang G. The Role of Macrophages in the Pathogenesis of ALI/ARDS. *Mediators Inflamm.* 2018;2018:1264913.
150. Wang Z. The role of macrophages polarization in sepsis-induced acute lung injury. *Front Immunol.* 2023;14:1209438.
151. Grommes J, Soehnlein O. Contribution of neutrophils to acute lung injury. *Mol Med.* 2011;17(3-4):293-307.
152. Zhou X, Dai Q, Huang X. Neutrophils in acute lung injury. *Front Biosci (Landmark Ed).* 2012;17(6):2278-83.
153. Azoulay E, Zuber J, Bousfiha AA, Long Y, Tan Y, Luo S, et al. Complement system activation: bridging physiology, pathophysiology, and therapy. *Intensive Care Med.* 2024;50(11):1791-803.
154. Gattinoni L, Pesenti A, Avalli L, Rossi F, Bombino M. Pressure-volume curve of total respiratory system in acute respiratory failure. Computed tomographic scan study. *Am Rev Respir Dis.* 1987;136(3):730-6.

155. Gattinoni L, Pesenti A. The concept of "baby lung". *Intensive Care Med.* 2005;31(6):776-84.
156. Swenson KE, Swenson ER. Pathophysiology of Acute Respiratory Distress Syndrome and COVID-19 Lung Injury. *Crit Care Clin.* 2021;37(4):749-76.
157. Burnham EL, Janssen WJ, Riches DW, Moss M, Downey GP. The fibroproliferative response in acute respiratory distress syndrome: mechanisms and clinical significance. *Eur Respir J.* 2014;43(1):276-85.
158. Slutsky AS, Ranieri VM. Ventilator-induced lung injury. *N Engl J Med.* 2013;369(22):2126-36.
159. Dreyfuss D, Saumon G. Ventilator-induced lung injury: lessons from experimental studies. *Am J Respir Crit Care Med.* 1998;157(1):294-323.
160. Curley GF, Laffey JG, Zhang H, Slutsky AS. Biotrauma and Ventilator-Induced Lung Injury: Clinical Implications. *Chest.* 2016;150(5):1109-17.
161. Merola R, Vargas M, Battaglini D. Ventilator-Induced Lung Injury: The Unseen Challenge in Acute Respiratory Distress Syndrome Management. *J Clin Med.* 2025;14(11).
162. Brower RG, Matthay MA, Morris A, Schoenfeld D, Thompson BT, Wheeler A. Ventilation with lower tidal volumes as compared with traditional tidal volumes for acute lung injury and the acute respiratory distress syndrome. *N Engl J Med.* 2000;342(18):1301-8.
163. Amato MB, Meade MO, Slutsky AS, Brochard L, Costa EL, Schoenfeld DA, et al. Driving pressure and survival in the acute respiratory distress syndrome. *N Engl J Med.* 2015;372(8):747-55.
164. Bates JHT, Kaczka DW, Kollisch-Singule M, Nieman GF, Gaver DP, 3rd. Mechanical Power and Ventilator-induced Lung Injury: What Does Physics Have to Say? *Am J Respir Crit Care Med.* 2024;209(7):787-8.
165. Deshwal H, Elkhapery A, Ramanathan R, Nair D, Singh I, Sinha A, et al. Patient-Self Inflicted Lung Injury (P-SILI): An Insight into the Pathophysiology of Lung Injury and Management. *J Clin Med.* 2025;14(5).
166. Roca O, Telias I, Grieco DL. Bedside-available strategies to minimise P-SILI and VILI during ARDS. *Intensive Care Med.* 2024;50(4):597-601.
167. Fan E, Del Sorbo L, Goligher EC, Hodgson CL, Munshi L, Walkey AJ, et al. An Official American Thoracic Society/European Society of Intensive Care Medicine/Society of Critical Care Medicine Clinical Practice Guideline: Mechanical Ventilation in Adult Patients with Acute Respiratory Distress Syndrome. *Am J Respir Crit Care Med.* 2017;195(9):1253-63.

168. Pelosi P, Ball L, Barbas CSV, Bellomo R, Burns KEA, Einav S, et al. Personalized mechanical ventilation in acute respiratory distress syndrome. *Crit Care*. 2021;25(1):250.
169. Papazian L, Aubron C, Brochard L, Chiche JD, Combes A, Dreyfuss D, et al. Formal guidelines: management of acute respiratory distress syndrome. *Ann Intensive Care*. 2019;9(1):69.
170. Pozzi T, Collino F, Brusatori S, Romitti F, Busana M, Moerer O, et al. Specific Respiratory System Compliance in COVID-19 and Non-COVID-19 Acute Respiratory Distress Syndrome. *Am J Respir Crit Care Med*. 2023;208(3):328-30.
171. Brower RG, Lanken PN, MacIntyre N, Matthay MA, Morris A, Ancukiewicz M, et al. Higher versus lower positive end-expiratory pressures in patients with the acute respiratory distress syndrome. *N Engl J Med*. 2004;351(4):327-36.
172. Briel M, Meade M, Mercat A, Brower RG, Talmor D, Walter SD, et al. Higher vs lower positive end-expiratory pressure in patients with acute lung injury and acute respiratory distress syndrome: systematic review and meta-analysis. *Jama*. 2010;303(9):865-73.
173. Guérin C, Reignier J, Richard JC, Beuret P, Gacouin A, Boulain T, et al. Prone positioning in severe acute respiratory distress syndrome. *N Engl J Med*. 2013;368(23):2159-68.
174. Coppo A, Bellani G, Winterton D, Di Pierro M, Soria A, Faverio P, et al. Feasibility and physiological effects of prone positioning in non-intubated patients with acute respiratory failure due to COVID-19 (PRON-COVID): a prospective cohort study. *Lancet Respir Med*. 2020;8(8):765-74.
175. De Rosa S, Sella N, Bellani G, Foti G, Cortegiani A, Lorenzoni G, et al. Oxygenation improvement and duration of prone positioning are associated with ICU mortality in mechanically ventilated COVID-19 patients. *Ann Intensive Care*. 2025;15(1):20.
176. Combes A, Hajage D, Capellier G, Demoule A, Lavoué S, Guervilly C, et al. Extracorporeal Membrane Oxygenation for Severe Acute Respiratory Distress Syndrome. *N Engl J Med*. 2018;378(21):1965-75.
177. Qadir N, Sahetya S, Munshi L, Summers C, Abrams D, Beitler J, et al. An Update on Management of Adult Patients with Acute Respiratory Distress Syndrome: An Official American Thoracic Society Clinical Practice Guideline. *Am J Respir Crit Care Med*. 2024;209(1):24-36.
178. Zhao Y, Yao Z, Xu S, Yao L, Yu Z. Glucocorticoid therapy for acute respiratory distress syndrome: Current concepts. *J Intensive Med*. 2024;4(4):417-32.

179. Pirracchio R, Venkatesh B, Legrand M. Low-Dose Corticosteroids for Critically Ill Adults With Severe Pulmonary Infections: A Review. *Jama*. 2024;332(4):318-28.
180. Chang X, Li S, Fu Y, Dang H, Liu C. Safety and efficacy of corticosteroids in ARDS patients: a systematic review and meta-analysis of RCT data. *Respir Res*. 2022;23(1):301.
181. Steinberg KP, Hudson LD, Goodman RB, Hough CL, Lanken PN, Hyzy R, et al. Efficacy and safety of corticosteroids for persistent acute respiratory distress syndrome. *N Engl J Med*. 2006;354(16):1671-84.
182. Papazian L, Forel JM, Gacouin A, Penot-Ragon C, Perrin G, Loundou A, et al. Neuromuscular blockers in early acute respiratory distress syndrome. *N Engl J Med*. 2010;363(12):1107-16.
183. Moss M, Huang DT, Brower RG, Ferguson ND, Ginde AA, Gong MN, et al. Early Neuromuscular Blockade in the Acute Respiratory Distress Syndrome. *N Engl J Med*. 2019;380(21):1997-2008.
184. Gebistorf F, Karam O, Wetterslev J, Afshari A. Inhaled nitric oxide for acute respiratory distress syndrome (ARDS) in children and adults. *Cochrane Database Syst Rev*. 2016;2016(6):Cd002787.
185. Torbic H, Saini A, Harnegie MP, Sadana D, Duggal A. Inhaled Prostacyclins for Acute Respiratory Distress Syndrome: A Systematic Review and Meta-Analysis. *Crit Care Explor*. 2023;5(6):e0931.
186. Wiedemann HP, Wheeler AP, Bernard GR, Thompson BT, Hayden D, deBoisblanc B, et al. Comparison of two fluid-management strategies in acute lung injury. *N Engl J Med*. 2006;354(24):2564-75.
187. Luyt CE, Bouadma L, Morris AC, Dhanani JA, Kollef M, Lipman J, et al. Pulmonary infections complicating ARDS. *Intensive Care Med*. 2020;46(12):2168-83.
188. Dushianthan A, Grocott MPW, Murugan GS, Wilkinson TMA, Postle AD. Pulmonary Surfactant in Adult ARDS: Current Perspectives and Future Directions. *Diagnostics (Basel)*. 2023;13(18).
189. Spragg RG, Lewis JF, Walmrath HD, Johannigman J, Bellingan G, Laterre PF, et al. Effect of recombinant surfactant protein C-based surfactant on the acute respiratory distress syndrome. *N Engl J Med*. 2004;351(9):884-92.
190. Spragg RG, Taut FJ, Lewis JF, Schenk P, Ruppert C, Dean N, et al. Recombinant surfactant protein C-based surfactant for patients with severe direct lung injury. *Am J Respir Crit Care Med*. 2011;183(8):1055-61.
191. Gao Smith F, Perkins GD, Gates S, Young D, McAuley DF, Tunnicliffe W, et al. Effect of intravenous β -2 agonist treatment on clinical outcomes in acute respiratory distress syndrome (BALTI-2): a multicentre, randomised controlled trial. *Lancet*. 2012;379(9812):229-35.

192. McAuley DF, Laffey JG, O'Kane CM, Perkins GD, Mullan B, Trinder TJ, et al. Simvastatin in the acute respiratory distress syndrome. *N Engl J Med.* 2014;371(18):1695-703.
193. Gao XQ, Li YF, Jiang ZL. Impact of statins on ALI/ARDS: A meta-analysis. *Pulm Pharmacol Ther.* 2016;39:85-91.
194. Kor DJ, Carter RE, Park PK, Festic E, Banner-Goodspeed VM, Hinds R, et al. Effect of Aspirin on Development of ARDS in At-Risk Patients Presenting to the Emergency Department: The LIPS-A Randomized Clinical Trial. *Jama.* 2016;315(22):2406-14.
195. Bernard GR, Wheeler AP, Russell JA, Schein R, Summer WR, Steinberg KP, et al. The effects of ibuprofen on the physiology and survival of patients with sepsis. The Ibuprofen in Sepsis Study Group. *N Engl J Med.* 1997;336(13):912-8.
196. Rice TW, Wheeler AP, Thompson BT, deBoisblanc BP, Steingrub J, Rock P. Enteral omega-3 fatty acid, gamma-linolenic acid, and antioxidant supplementation in acute lung injury. *Jama.* 2011;306(14):1574-81.
197. Dushianthan A, Cusack R, Burgess VA, Grocott MP, Calder PC. Immunonutrition for acute respiratory distress syndrome (ARDS) in adults. *Cochrane Database Syst Rev.* 2019;1(1):Cd012041.
198. Kulkarni HS, Lee JS, Bastarache JA, Kuebler WM, Downey GP, Albaiceta GM, et al. Update on the Features and Measurements of Experimental Acute Lung Injury in Animals: An Official American Thoracic Society Workshop Report. *Am J Respir Cell Mol Biol.* 2022;66(2):e1-e14.
199. Aeffner F, Bolon B, Davis IC. Mouse Models of Acute Respiratory Distress Syndrome: A Review of Analytical Approaches, Pathologic Features, and Common Measurements. *Toxicol Pathol.* 2015;43(8):1074-92.
200. Matute-Bello G, Frevert CW, Martin TR. Animal models of acute lung injury. *Am J Physiol Lung Cell Mol Physiol.* 2008;295(3):L379-99.
201. Joelsson JP, Ingthorsson S, Kricker J, Gudjonsson T, Karason S. Ventilator-induced lung-injury in mouse models: Is there a trap? *Lab Anim Res.* 2021;37(1):30.
202. Joelsson JP, Karason S. Ventilator-induced lung injury in rat models: are they all equal in the race? *Lab Anim Res.* 2025;41(1):14.
203. Chimenti L, Morales-Quinteros L, Puig F, Camprubi-Rimblas M, Guillamat-Prats R, Gómez MN, et al. Comparison of direct and indirect models of early induced acute lung injury. *Intensive Care Med Exp.* 2020;8(Suppl 1):62.
204. Bastarache JA, Blackwell TS. Development of animal models for the acute respiratory distress syndrome. *Dis Model Mech.* 2009;2(5-6):218-23.

205. Wang HM, Bodenstern M, Markstaller K. Overview of the pathology of three widely used animal models of acute lung injury. *Eur Surg Res.* 2008;40(4):305-16.
206. Ballard-Croft C, Wang D, Sumpter LR, Zhou X, Zwischenberger JB. Large-animal models of acute respiratory distress syndrome. *Ann Thorac Surg.* 2012;93(4):1331-9.
207. Engel M, Nowacki RME, Jonker EM, Ophelders D, Nikiforou M, Kloosterboer N, et al. A comparison of four different models of acute respiratory distress syndrome in sheep. *Respir Res.* 2020;21(1):209.
208. Tydén J, Herwald H, Sjöberg F, Johansson J. Increased Plasma Levels of Heparin-Binding Protein on Admission to Intensive Care Are Associated with Respiratory and Circulatory Failure. *PloS one.* 2016;11(3):e0152035.
209. Liu JY, Tsai HJ, Morisseau C, Lango J, Hwang SH, Watanabe T, et al. In vitro and in vivo metabolism of N-adamantyl substituted urea-based soluble epoxide hydrolase inhibitors. *Biochem Pharmacol.* 2015;98(4):718-31.
210. Tsai HJ, Hwang SH, Morisseau C, Yang J, Jones PD, Kasagami T, et al. Pharmacokinetic screening of soluble epoxide hydrolase inhibitors in dogs. *Eur J Pharm Sci.* 2010;40(3):222-38.
211. Guedes AGP, Aristizabal F, Sole A, Adedeji A, Brosnan R, Knych H, et al. Pharmacokinetics and antinociceptive effects of the soluble epoxide hydrolase inhibitor t-TUCB in horses with experimentally induced radiocarpal synovitis. *J Vet Pharmacol Ther.* 2018;41(2):230-8.
212. Shihadih D, Harris T, Kodani S, Hwang S, Lee K, Mavangira V, et al. Selection of Potent Inhibitors of Soluble Epoxide Hydrolase for Usage in Veterinary Medicine. *Frontiers in veterinary science.* 2020;7.
213. Gouveia-Figueira S, Spath J, Zivkovic AM, Nording ML. Profiling the Oxylipin and Endocannabinoid Metabolome by UPLC-ESI-MS/MS in Human Plasma to Monitor Postprandial Inflammation. *PLoS One.* 2015;10(7):e0132042.
214. Gouveia-Figueira S, Karimpour M, Bosson J, Blomberg A, Unosson J, Pourazar J, et al. Mass spectrometry profiling of oxylipins, endocannabinoids, and N-acylethanolamines in human lung lavage fluids reveals responsiveness of prostaglandin E2 and associated lipid metabolites to biodiesel exhaust exposure. *Analytical and bioanalytical chemistry.* 2017;409(11).
215. Benjamini Y, Hochberg Y. Controlling the false discovery rate: a practical and powerful approach to multiple testing. *Journal of the Royal Statistical Society, Series B.* 1995;57(1):289-300.
216. Archambault AS, Zaid Y, Rakotoarivelo V, Turcotte C, Doré É, Dubuc I, et al. High levels of eicosanoids and docosanoids in the lungs of intubated COVID-19 patients. *Faseb j.* 2021;35(6):e21666.

217. Rivkind AI, Siegel JH, Guadalupi P, Littleton M. Sequential patterns of eicosanoid, platelet, and neutrophil interactions in the evolution of the fulminant post-traumatic adult respiratory distress syndrome. *Ann Surg.* 1989;210(3):355-72; discussion 72-3.
218. Caironi P, Ichinose F, Liu R, Jones RC, Bloch KD, Zapol WM. 5-Lipoxygenase deficiency prevents respiratory failure during ventilator-induced lung injury. *Am J Respir Crit Care Med.* 2005;172(3):334-43.
219. Karu N, Kindt A, Lamont L, van Gammeren AJ, Ermens AAM, Harms AC, et al. Plasma Oxylipins and Their Precursors Are Strongly Associated with COVID-19 Severity and with Immune Response Markers. *Metabolites.* 2022;12(7).
220. Zarbock A, Distasi MR, Smith E, Sanders JM, Kronke G, Harry BL, et al. Improved survival and reduced vascular permeability by eliminating or blocking 12/15-lipoxygenase in mouse models of acute lung injury (ALI). *J Immunol.* 2009;183(7):4715-22.
221. Castañé H, Iftimie S, Baiges-Gaya G, Rodríguez-Tomás E, Jiménez-Franco A, López-Azcona AF, et al. Machine learning and semi-targeted lipidomics identify distinct serum lipid signatures in hospitalized COVID-19-positive and COVID-19-negative patients. *Metabolism.* 2022;131:155197.
222. Tao W, Li PS, Yang LQ, Ma YB. Effects of a Soluble Epoxide Hydrolase Inhibitor on Lipopolysaccharide-Induced Acute Lung Injury in Mice. *PLoS One.* 2016;11(8):e0160359.
223. Liu LP, Li B, Shuai TK, Zhu L, Li YM. Deletion of soluble epoxide hydrolase attenuates mice Hyperoxic acute lung injury. *BMC Anesthesiol.* 2018;18(1):48.
224. Tao W, Xu G, Luo Y, Li PS. Inhibitors of soluble epoxide hydrolase on acute lung injury: a meta-analysis of preclinical studies. *Inflammopharmacology.* 2022;30(6):2027-33.
225. Guangsu D, Liang Z, Bin W, Lei L, Peiyu C. sEH activity is associated with mortality in patients with ARDS: a retrospective cohort study. *Biomark Med.* 2024;18(15-16):659-64.
226. Park GY, Christman JW. Involvement of cyclooxygenase-2 and prostaglandins in the molecular pathogenesis of inflammatory lung diseases. *Am J Physiol Lung Cell Mol Physiol.* 2006;290(5):L797-805.
227. Biagini D, Franzini M, Oliveri P, Lomonaco T, Ghimenti S, Bonini A, et al. MS-based targeted profiling of oxylipins in COVID-19: A new insight into inflammation regulation. *Free radical biology & medicine.* 2022;180:236-43.
228. Misheva M, Kotzamanis K, Davies LC, Tyrrell VJ, Rodrigues PRS, Benavides GA, et al. Oxylipin metabolism is controlled by mitochondrial β -oxidation during bacterial inflammation. *Nat Commun.* 2022;13(1):139.

229. Lotze MT, Tracey KJ. High-mobility group box 1 protein (HMGB1): nuclear weapon in the immune arsenal. *Nat Rev Immunol.* 2005;5(4):331-42.
230. Quan C, Wang M, Chen H, Zhang H. Extracellular vesicles in acute respiratory distress syndrome: Recent developments from bench to bedside. *Int Immunopharmacol.* 2021;100:108118.
231. Mahida R, Matsumoto S, Matthay M. Extracellular Vesicles: A New Frontier for Research in Acute Respiratory Distress Syndrome. *American journal of respiratory cell and molecular biology.* 2020;63(1).
232. Kadota T, Fujita Y, Araya J, Ochiya T, Kuwano K. Extracellular vesicle-mediated cellular crosstalk in lung repair, remodelling and regeneration. *Eur Respir Rev.* 2022;31(163).
233. Moritz MW, Dawe EJ, Holliday JF, Elliott S, Mattei JA, Thomas AL. Chronic central vein catheterization for intraoperative and long-term venous access in swine. *Lab Anim Sci.* 1989;39(2):153-5.
234. Lombardo C, Damiano G, Cassata G, Palumbo VD, Cacciabauda F, Spinelli G, et al. Surgical vascular access in the porcine model for long-term repeated blood sampling. *Acta Biomed.* 2010;81(2):101-3.
235. Wagner K, Inceoglu B, Dong H, Yang J, Hwang SH, Jones P, et al. Comparative efficacy of 3 soluble epoxide hydrolase inhibitors in rat neuropathic and inflammatory pain models. *Eur J Pharmacol.* 2013;700(1-3):93-101.
236. Ulu A, Appt S, Morisseau C, Hwang SH, Jones PD, Rose TE, et al. Pharmacokinetics and in vivo potency of soluble epoxide hydrolase inhibitors in cynomolgus monkeys. *Br J Pharmacol.* 2012;165(5):1401-12.
237. Kao RL, Huang W, Martin CM, Rui T. The effect of aerosolized indomethacin on lung inflammation and injury in a rat model of blunt chest trauma. *Can J Surg.* 2018;61(6):S208-s18.
238. Gnidec AG, Sibbald WJ, Cheung H, Metz CA. Ibuprofen reduces the progression of permeability edema in an animal model of hyperdynamic sepsis. *J Appl Physiol (1985).* 1988;65(3):1024-32.
239. Metz C, Sibbald WJ. Anti-inflammatory therapy for acute lung injury. A review of animal and clinical studies. *Chest.* 1991;100(4):1110-9.